Plates and shells: Asymptotic expansions and hierarchical models

Monique Dauge[1], Erwan Faou[2,] and Zohar Yosibash[3]

[1] *IRMAR, Université de Rennes1, Campus de Beaulieu, 35042 Rennes, France*
[2] *INRIA Rennes, Campus de Beaulieu, 35042 Rennes, France*
[3] *Dept. of Mechanical Engineering, Ben-Gurion University, Beer Sheva 84105, Israel*

ABSTRACT

Concerning thin structures such as plates and shells, the idea of reducing the equations of elasticity to two-dimensional models defined on the mid-surface seems relevant. Such a reduction was first performed thanks to kinematical hypotheses about the transformation of normal lines to the mid-surface. As nowadays, the asymptotic expansion of the displacement solution of the three-dimensional linear model is fully known at least for plates and clamped elliptic shells, we start from a description of these expansions in order to introduce the two-dimensional models known as hierarchical models: These models extend the classical models, and pre-suppose the displacement to be polynomial in the thickness variable, transverse to the mid-surface. Because of the singularly perturbed character of the elasticity problem as the thickness approaches zero, boundary- or internal layers may appear in the displacements and stresses, and so may numerical locking effects. The use of hierarchical models, discretized by higher degree polynomials (p-version of finite elements) may help to overcome these severe difficulties.

KEY WORDS:

1. INTRODUCTION

1.1. Structures

Plates and shells are characterized by *(i)* their mid-surface S, *(ii)* their thickness d. The plate or shell character is that d is *"small"* compared with the dimensions of S. In this respect, we qualify such structures as *thin domains*. In the case of plates, S is a domain of the plane, whereas in the case of shells, S is a surface embedded in the three-dimensional space. Of course, plates are shells with zero curvature. Nevertheless, considering plates as a particular class of shells in not so obvious: They always have been treated separately, for the reason that plates are simpler. We think, and hopefully demonstrate in this chapter, that eventually considering plates as shells sheds some light in the shell theory.

Other classes of thin domains do exist, such as rods, where two dimensions are small compared with the third one. We will not address them and quote for example Nazarov, 1999; Irago and Viaño, 1999. Real engineering structures are often union (or junction) of plates, rods, shells, etc... see Ciarlet (1988, 1997) and also Kozlov *et al.*, 1999; Agratov and Nazarov, 2000. We restrict our analysis to an isolated plate or shell. We assume moreover that the mid-surface S is smooth, orientable, and has a smooth boundary ∂S. The shell character includes the fact that the principal curvatures have the same order of magnitude as the dimensions of S. See Anicic and Léger, 1999 for a situation where a region with

Encyclopedia of Computational Mechanics. Edited by Erwin Stein, René de Borst and Thomas J.R. Hughes.

strong curvature (like $1/d$) is considered. The opposite situation is when the curvatures have the order of d: We are then in presence of shallow shells according to the terminology of Ciarlet and Paumier, 1986.

1.2. Domains and coordinates

In connection with our references, it is easier for us to consider d as the ***half-thickness*** of the structure. We denote our plate or shell by Ω^d. We keep the reference to the half-thickness in the notation because we are going to perform an ***asymptotic analysis*** for which we embed our structure in a whole family of structures $(\Omega^\varepsilon)_\varepsilon$, where the parameter ε tends to 0.

We denote the Cartesian coordinates of $\mathbb{R}^3$ by $\boldsymbol{x} = (x_1, x_2, x_3)$, a tangential system of coordinates on S by $\mathsf{x}_\top = (\mathsf{x}_\alpha)_{\alpha=1,2}$, a normal coordinate to S by x_3, with the convention that the mid-surface is parametrized by the equation $\mathsf{x}_3 = 0$. In the case of plates (x_α) are Cartesian coordinates in $\mathbb{R}^2$ and the domain Ω^d has the tensor product form

$$\Omega^d = S \times (-d, d).$$

In the case of shells, $\mathsf{x}_\top = (\mathsf{x}_\alpha)_{\alpha=1,2}$ denotes a local coordinate system on S, depending on the choice of a local chart in an atlas, and x_3 is the coordinate along a smooth unit normal field $\mathbf{n}$ to S in $\mathbb{R}^3$. Such a ***normal coordinate system***[1] $(\mathsf{x}_\top, \mathsf{x}_3)$ yields a smooth diffeomorphism between Ω^d and $S \times (-d, d)$. The ***lateral boundary*** Γ^d of Ω^d is characterized by $\mathsf{x}_\top \in \partial S$ and $\mathsf{x}_3 \in (-d, d)$ in coordinates $(\mathsf{x}_\top, \mathsf{x}_3)$.

1.3. Displacement, strain, stress and elastic energy

The displacement of the structure (deformation from the stress-free configuration) is denoted by $\mathbf{u}$, its Cartesian coordinates by (u_1, u_2, u_3), and its surface and transverse parts by $\mathbf{u}_\top = (\mathsf{u}_\alpha)$ and u_3 respectively. The transverse part u_3 is always an intrinsic function and the surface part $\mathbf{u}_\top$ defines a two-dimensional 1-form field on S, depending on x_3. The components (u_α) of $\mathbf{u}_\top$ depend on the choice of the local coordinate system $\mathsf{x}_\top$.

We choose to work in the framework of ***small deformations***[2]. Thus we use the strain tensor[3] $e = (e_{ij})$ given in Cartesian coordinates by

$$e_{ij}(\mathbf{u}) = \frac{1}{2}\Big(\frac{\partial u_i}{\partial x_j} + \frac{\partial u_j}{\partial x_i}\Big).$$

Unless stated otherwise, we assume the simplest possible behavior for the material of our structure, that is an ***isotropic material***. Thus, the elasticity tensor $A = (A^{ijkl})$ takes the form

$$A^{ijkl} = \lambda \delta^{ij}\delta^{kl} + \mu(\delta^{ik}\delta^{jl} + \delta^{il}\delta^{jk}),$$

with λ and μ the Lamé constants of the material and δ^{ij} the Kronecker symbol. We use Einstein's summation convention, and sum over double indices if they appear as subscripts and superscripts[4], e.g. $\sigma^{ij}\, e_{ij} \equiv \Sigma_{i,j=1}^3 \sigma^{ij}\, e_{ij}$. The constitutive equation is given by Hooke's law $\boldsymbol{\sigma} = A\boldsymbol{e}(\mathbf{u})$ linking the

[1] Also called S-coordinate system.
[2] See Ciarlet (1997, 2000) for more general non-linear models e.g. the von Kármán model.
[3] Linearized from the Green-St Venant strain tensor.
[4] Which is nothing but the contraction of tensors.

Encyclopedia of Computational Mechanics. Edited by Erwin Stein, René de Borst and Thomas J.R. Hughes.

stress tensor $\boldsymbol{\sigma}$ to the strain tensor $\boldsymbol{e}(\mathbf{u})$. Thus

$$\begin{aligned} \sigma^{ii} &= \lambda(e_{11}+e_{22}+e_{33}) + 2\mu e_{ii}, \quad i=1,2,3 \\ \sigma^{ij} &= 2\mu e_{ij} \quad \text{for} \quad i \neq j. \end{aligned} \tag{1}$$

The elastic bilinear form on a domain Ω is given by

$$a(\mathbf{u},\mathbf{u}') = \int_\Omega \boldsymbol{\sigma}(\mathbf{u}) : \boldsymbol{e}(\mathbf{u}')\, \mathrm{d}\boldsymbol{x} = \int_\Omega \sigma^{ij}(\mathbf{u})\, e_{ij}(\mathbf{u}')\, \mathrm{d}\boldsymbol{x}, \tag{2}$$

and the *elastic energy* of a displacement $\mathbf{u}$ is $\frac{1}{2}a(\mathbf{u},\mathbf{u})$. The *strain energy norm* of $\mathbf{u}$ is denoted by $\|\mathbf{u}\|_{E(\Omega)}$ and defined as $(\sum_{ij}\int_\Omega |e_{ij}(\mathbf{u})|^2\,\mathrm{d}\boldsymbol{x})^{1/2}$.

1.4. Families of problems

We will address two types of problems on our thin domain Ω^d: *(i)* Find the displacement $\mathbf{u}$ solution to the equilibrium equation $\mathbf{div}\,\boldsymbol{\sigma}(\mathbf{u}) = \mathbf{f}$ for a given load $\mathbf{f}$, *(ii)* Find the (smallest) vibration eigenmodes $(\Lambda, \mathbf{u})$ of the structure. For simplicity of exposition, we assume in general that the structure is clamped[5] along its lateral boundary Γ^d and will comment on other choices for lateral boundary conditions. On the remaining part of the boundary $\partial\Omega^d \backslash \Gamma^d$ ("top" and "bottom") traction free condition is assumed.

In order to investigate the influence of the thickness on the solutions and the discretization methods, we consider our (fixed physical) problem in Ω^d as part of a whole family of problems, depending on one parameter $\varepsilon \in (0, \varepsilon_0]$, the thickness. The definition of Ω^ε is obvious[6] by the formulae given in §1.2. For problem *(i)*, we choose the same right hand side $\mathbf{f}$ for all values of ε, which precisely means that we fix a smooth field $\mathbf{f}$ on Ω^{ε_0} and take $\mathbf{f}^\varepsilon := \mathbf{f}|_{\Omega^\varepsilon}$ for each ε.

Both problems *(i)* and *(ii)* can be set in variational form (principle of virtual work). Our three-dimensional variational space is the subspace $V(\Omega^\varepsilon)$ of the Sobolev space $H^1(\Omega^\varepsilon)^3$ characterized by the clamping condition $\mathbf{u}|_{\Gamma^\varepsilon} = 0$, and the bilinear form a (2) on $\Omega = \Omega^\varepsilon$, denoted by a^ε. The variational formulations are:

$$\textit{Find } \mathbf{u}^\varepsilon \in V(\Omega^\varepsilon) \textit{ such that} \qquad a^\varepsilon(\mathbf{u}^\varepsilon,\mathbf{u}') = \int_{\Omega^\varepsilon} \mathbf{f}^\varepsilon \cdot \mathbf{u}'\, \mathrm{d}\boldsymbol{x}, \quad \forall \mathbf{u}' \in V(\Omega^\varepsilon), \tag{3}$$

for the problem with external load, and

$$\begin{aligned} &\textit{Find } \mathbf{u}^\varepsilon \in V(\Omega^\varepsilon)\,,\, \mathbf{u}^\varepsilon \neq 0, \textit{ and } \Lambda^\varepsilon \in \mathbb{R} \textit{ such that} \\ &\qquad\qquad a^\varepsilon(\mathbf{u}^\varepsilon,\mathbf{u}') = \Lambda^\varepsilon \int_{\Omega^\varepsilon} \mathbf{u}^\varepsilon \cdot \mathbf{u}'\, \mathrm{d}\boldsymbol{x}, \quad \forall \mathbf{u}' \in V(\Omega^\varepsilon), \end{aligned} \tag{4}$$

for the eigen-mode problem. In engineering practice one is interested in the natural frequencies, $\omega^\varepsilon = \sqrt{\Lambda^\varepsilon}$. Of course, when considering our structure Ω^d, we are eventually only interested in $\varepsilon = d$. Taking the whole family $\varepsilon \in (0, \varepsilon_0]$ into account allows the investigation of the dependency with respect to the small parameter ε, in order to know if valid simplified models are available and how they can be discretized by finite elements.

---

[5] This condition is also called "condition of place".

[6] In fact, if the curvatures of S are "small", we may decide that Ω^d fits better in a family of shallow shells, see §4.4 later.

Encyclopedia of Computational Mechanics. Edited by Erwin Stein, René de Borst and Thomas J.R. Hughes.

1.5. Computational obstacles

Our aim is to study the possible discretizations for a reliable and efficient computation of the solutions $\mathbf{u}^d$ of problem (3) or (4) in our thin structure Ω^d. An option could be to consider Ω^d as a three-dimensional body and use 3D finite elements. In the standard version of finite elements (h-version) individual elements should not be stretched or distorted, which implies that all dimensions should be bounded by d. Even so, several layers of elements through the thickness may be necessary. Moreover the *a priori* error estimates may suffer from the behavior of the Korn inequality[7] on Ω^d.

An ideal alternative would simply be to get rid of the thickness variable and compute the solution of an "equivalent" problem on the mid-surface S. This is the aim of the *shell theory*. Many investigations were undertaken around 1960-70, and the main achievement is (still) the Koiter model, which is a multi-degree 3×3 elliptic system on S of half-orders $(1, 1, 2)$ with a singular dependence in d. But, as written in Koiter and Simmonds, 1973 *"Shell theory attempts the impossible: to provide a two-dimensional representation of an intrinsically three-dimensional phenomenon"*. Nevertheless, obtaining converging error estimates between the 3D solution $\mathbf{u}^d$ and a *reconstructed 3D displacement* $\mathbf{U}\mathbf{z}^d$ from the *deformation pattern* $\mathbf{z}^d$ solution of the Koiter model seems possible.

However, due to its 4-th order part, the Koiter model cannot be discretized by standard $\mathcal{C}^0$ finite elements. The Naghdi model, involving five unknowns on S, seems more suitable. Yet endless difficulties arise in the form of various locking effects, due to the singularly perturbed character of the problem.

With the twofold aim of improving the precision of the models and their approximability by finite elements, the idea of hierarchical models becomes natural: Roughly, it consists of an Ansatz of polynomial behavior in the thickness variable, with bounds on the degrees of the three components of the 3D displacement. The introduction of such models in variational form is due to Vogelius and Babuška, 1981a and Szabó and Sahrmann, 1988. Earlier beginnings in that direction can be found in Vekua (1955, 1965). The hierarchy (increasing the transverse degrees) of models obtained in that way can be discretized by the p-version of finite elements.

1.6. Plan of the chapter

In order to assess the validity of hierarchical models, we will compare them to asymptotic expansions of solutions $\mathbf{u}^\varepsilon$ when they are available: These expansions exhibit two or three different scales and boundary layer regions, which can or cannot be properly described by hierarchical models.

We first address plates, because much more is known for plates than for general shells. In §2 we describe the two-scale expansion of the solutions of (3) and (4): This expansion contains *(i)* a *regular part* each term of which is polynomial in the thickness variable x_3, *(ii)* a part mainly supported in a *boundary layer* around the lateral boundary Γ^ε. In §3, we introduce the hierarchical models as Galerkin projections on semi-discrete subspaces $V^{\mathbf{q}}(\Omega^\varepsilon)$ of $V(\Omega^\varepsilon)$ defined by assuming a polynomial behavior of degree $\mathbf{q} = (q_1, q_2, q_3)$ in x_3. The model of degree $(1, 1, 0)$ is the Reissner-Mindlin model and needs the introduction of a *reduced energy*. The $(1, 1, 2)$ model is the lowest degree model to use the same elastic energy (2) as the 3D model.

We address shells in §4 (asymptotic expansions and limiting models) and §5 (hierarchical models). After a short introduction of the metric and curvature tensors on the mid-surface, we first describe the

[7] The factor appearing in the Korn inequality behaves like d^{-1} for plates and partially clamped shells see Ciarlet *et al.*, 1996; Dauge and Faou, 2004

Encyclopedia of Computational Mechanics. Edited by Erwin Stein, René de Borst and Thomas J.R. Hughes.

three-scale expansion of the solutions of (3) on clamped elliptic shells: Two of these scales can be captured by hierarchical models. We then present and comment on the famous classification of shells as flexural or membrane. We also mention two distinct notions of shallow shells. We emphasize the universal role played by the Koiter model for the structure Ω^d, independently of any embedding of Ω^d in a family $(\Omega^\varepsilon)_\varepsilon$.

The last section is devoted to the discretization of the 3D problems and their 2D hierarchical projections, by p-version finite elements. The 3D thin elements (one layer of elements through the thickness) constitute a bridge between 3D and 2D discretizations. We address the issue of locking effects (shear and membrane locking) and the issue of capturing boundary layer terms. Increasing the degree p of approximation polynomials and using anisotropic meshes is a way towards solving these problems. We end this chapter by presenting a series of eigen-frequency computations on a few different families of shells and draw some "practical" conclusions.

2. MULTI-SCALE EXPANSIONS FOR PLATES

The question of an asymptotic expansion for solutions $\mathbf{u}^\varepsilon$ of problems (3) or (4) posed in a family of plates is difficult: One may think it is natural to expand $\mathbf{u}^\varepsilon$ either in polynomial functions in the thickness variable x_3, or in an asymptotic series in powers ε^k with regular coefficients $\mathbf{v}^k$ defined on the stretched plate $\Omega = S \times (-1, 1)$. In fact, for the class of loads considered here or for the eigen-mode problem, both those Ansätze are relevant, but they are unable to provide a correct description of the behavior of $\mathbf{u}^\varepsilon$ in the vicinity of the lateral boundary Γ^ε, where there is a boundary layer[8] of width $\sim \varepsilon$. And, worse, in the absence of knowledge of the boundary layer behavior, the determination of the terms $\mathbf{v}^k$ is impossible (except for $\mathbf{v}^0$).

The investigation of asymptotics as $\varepsilon \to 0$ was first performed by the construction of infinite *formal expansions*, see Friedrichs and Dressler, 1961; Gol'denveizer, 1962; Gregory and Wan, 1984. The principle of multi-scale asymptotic expansion is applied to thin domains in Maz'ya *et al.*, 1991. A two-term asymptotics is exhibited in Nazarov and Zorin, 1989. The whole asymptotic expansion is constructed in Dauge and Gruais (1996, 1998) and Dauge *et al.*, 1999/00.

The multi-scale expansions which we propose differ from the matching method in Il'in, 1992 where the solutions of singularly perturbed problems are fully described in rapid variables inside the boundary layer and slow variables outside the layer, both expansions being "matched" in an intermediate region. Our approach is closer to that of Vishik and Lyusternik, 1962 and Oleinik *et al.*, 1992.

2.1. Coordinates and symmetries

The mid-surface S is a smooth domain of the plane $\Pi \simeq \mathbb{R}^2$ and for $\varepsilon \in (0, \varepsilon_0)$ $\Omega^\varepsilon = S \times (-\varepsilon, \varepsilon)$ is the generic member of the family of plates. The plates are symmetric with respect to the plane Π. Since they are assumed to be made of an isotropic material, problems (3) or (4) commute with the symmetry $\mathfrak{S} : \mathbf{u} \mapsto (\mathbf{u}_\tau(\cdot, -\mathsf{x}_3),\ -\mathsf{u}_3(\cdot, -\mathsf{x}_3))$. The eigenspaces of $\mathfrak{S}$ are *membrane* and *bending*

[8] Except in the particular situation of a rectangular mid-surface with symmetry lateral boundary conditions (hard simple support or sliding edge), see Paumier, 1990.

Encyclopedia of Computational Mechanics. Edited by Erwin Stein, René de Borst and Thomas J.R. Hughes.

displacements[9], *cf* Friedrichs and Dressler, 1961:

$$\begin{aligned} \mathbf{u} \quad &\text{membrane iff} \quad \mathbf{u}_\top(\mathbf{x}_\top, +\mathsf{x}_3) = \mathbf{u}_\top(\mathbf{x}_\top, -\mathsf{x}_3) \ \text{ and } \ \mathsf{u}_3(\mathbf{x}_\top, +\mathsf{x}_3) = -\mathsf{u}_3(\mathbf{x}_\top, -\mathsf{x}_3) \\ \mathbf{u} \quad &\text{bending iff} \quad \mathbf{u}_\top(\mathbf{x}_\top, +\mathsf{x}_3) = -\mathbf{u}_\top(\mathbf{x}_\top, -\mathsf{x}_3) \ \text{ and } \ \mathsf{u}_3(\mathbf{x}_\top, +\mathsf{x}_3) = \mathsf{u}_3(\mathbf{x}_\top, -\mathsf{x}_3). \end{aligned} \tag{5}$$

Any general displacement $\mathbf{u}$ is the sum $\mathbf{u}_\mathsf{m} + \mathbf{u}_\mathsf{b}$ of a membrane and a bending part[10].

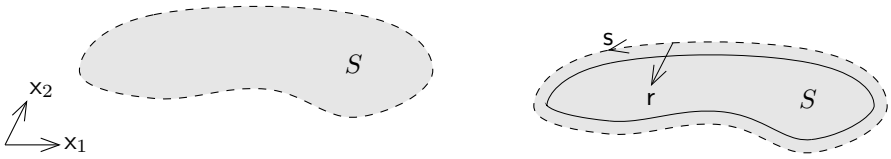

Figure 1. Cartesian and local coordinates on the mid-surface.

In addition to the coordinates $\mathbf{x}_\top$ in S, let r be the distance to ∂S in Π and s an arclength function on ∂S. In this way (r, s) defines a smooth coordinate system in a mid-plane tubular neighborhood $\mathcal{V}$ of ∂S. Let $\chi = \chi(\mathsf{r})$ be a smooth cut-off function with support in $\mathcal{V}$, equal to 1 in a smaller such neighborhood. It is used to substantiate boundary layer terms. The two following stretched (or rapid) variables appear in our expansions:

$$\mathsf{X}_3 = \frac{\mathsf{x}_3}{\varepsilon} \quad \text{and} \quad \mathsf{R} = \frac{\mathsf{r}}{\varepsilon}.$$

The stretched thickness variable X_3 belongs to $(-1, 1)$ and is present in all parts of our asymptotics, whereas the presence of R characterizes boundary layer terms.

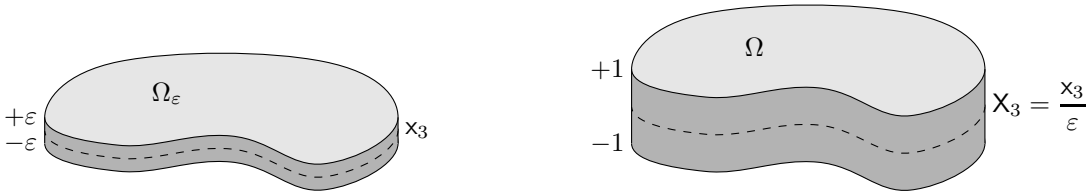

Figure 2. Thin plate and stretched plate.

2.2. Problem with external load

The solutions of the family of problems (3) have a two-scale asymptotic expansion in regular terms $\mathbf{v}^k$ and boundary layer terms $\mathbf{w}^k$, which we state as a theorem *cf* Dauge *et al.*, 1999/00; Dauge and

[9] Also called stretching and flexural displacements.
[10] According to formulae $\mathbf{u}_\mathsf{m} = \frac{1}{2}(\mathbf{u} + \mathfrak{S}\mathbf{u})$ and $\mathbf{u}_\mathsf{f} = \frac{1}{2}(\mathbf{u} - \mathfrak{S}\mathbf{u})$. They are also denoted by $\mathbf{u}^I$ and $\mathbf{u}^{II}$ in the literature.

Encyclopedia of Computational Mechanics. Edited by Erwin Stein, René de Borst and Thomas J.R. Hughes.

Schwab, 2002. Note that in contrast with the most part of those references, we work here with *natural displacements* (i.e. unscaled), which is more realistic from the mechanical and computational point of view, and allows an easier comparison with shells.

Theorem 2.1. *[Dauge et al., 1999/00] For the solutions of problem* (3)*, $\varepsilon \in (0, \varepsilon_0]$, there exist regular terms $\mathbf{v}^k = \mathbf{v}^k(\mathbf{x}_\tau, \mathsf{X}_3)$, $k \geq -2$, and boundary layer terms $\mathbf{w}^k = \mathbf{w}^k(\mathsf{R}, \mathsf{s}, \mathsf{X}_3)$, $k \geq 0$, such that*

$$\mathbf{u}^\varepsilon \simeq \varepsilon^{-2}\mathbf{v}^{-2} + \varepsilon^{-1}\mathbf{v}^{-1} + \varepsilon^0(\mathbf{v}^0 + \chi\mathbf{w}^0) + \varepsilon^1(\mathbf{v}^1 + \chi\mathbf{w}^1) + \dots \tag{6}$$

in the sense of asymptotic expansions: The following estimates hold

$$\|\mathbf{u}^\varepsilon - \sum_{k=-2}^{K} \varepsilon^k(\mathbf{v}^k + \chi\mathbf{w}^k)\|_{E(\Omega^\varepsilon)} \leq C_K(\mathbf{f})\,\varepsilon^{K+1/2}, \quad K = 0, 1, \dots,$$

where we have set $\mathbf{w}^{-2} = \mathbf{w}^{-1} = 0$ and the constant $C_K(\mathbf{f})$ is independent of $\varepsilon \in (0, \varepsilon_0]$.

2.2.1. Kirchhoff displacements and their deformation patterns. The first terms in the expansion of $\mathbf{u}^\varepsilon$ are Kirchhoff displacements, i.e. displacements of the form (with the surface gradient $\nabla_\tau = (\partial_1, \partial_2)$)

$$(\mathbf{x}_\tau, \mathsf{x}_3) \longmapsto \mathbf{v}(\mathbf{x}_\tau, \mathsf{x}_3) = \big(\boldsymbol{\zeta}_\tau(\mathbf{x}_\tau) - \mathsf{x}_3\nabla_\tau\zeta_3(\mathbf{x}_\tau), \zeta_3(\mathbf{x}_\tau)\big). \tag{7}$$

Here $\boldsymbol{\zeta}_\tau = (\zeta_\alpha)$ is a surface displacement and ζ_3 is a function on S. We call the three-component field $\boldsymbol{\zeta} := (\boldsymbol{\zeta}_\tau, \zeta_3)$ the *deformation pattern* of the KL displacement $\mathbf{v}$. Note that

$$\mathbf{v} \text{ bending iff } \boldsymbol{\zeta} = (\mathbf{0}, \zeta_3) \quad \text{and} \quad \mathbf{v} \text{ membrane iff } \boldsymbol{\zeta} = (\boldsymbol{\zeta}_\tau, 0).$$

In expansion (6) the first terms are Kirchhoff displacements. The next regular terms $\mathbf{v}^k$ are also generated by deformation patterns $\boldsymbol{\zeta}^k$ via higher degree formulae than in (7). We successively describe the $\mathbf{v}^k$, the $\boldsymbol{\zeta}^k$ and, finally, the boundary layer terms $\mathbf{w}^k$.

2.2.2. The four first regular terms. For the regular terms $\mathbf{v}^k$, $k = -2, -1, 0, 1$, there exist bending deformation patterns $\boldsymbol{\zeta}^{-2} = (\mathbf{0}, \zeta_3^{-2})$, $\boldsymbol{\zeta}^{-1} = (\mathbf{0}, \zeta_3^{-1})$, and full deformation patterns $\boldsymbol{\zeta}^0$, $\boldsymbol{\zeta}^1$ such that

$$\begin{aligned}
\mathbf{v}^{-2} &= (\mathbf{0},\ \zeta_3^{-2}) \\
\mathbf{v}^{-1} &= (-\mathsf{X}_3\nabla_\tau\zeta_3^{-2},\ \zeta_3^{-1}) \\
\mathbf{v}^{0} &= (\boldsymbol{\zeta}_\tau^0 - \mathsf{X}_3\nabla_\tau\zeta_3^{-1},\ \zeta_3^0) + (\mathbf{0},\ P_{\mathsf{b}}^2(\mathsf{X}_3)\Delta_\tau\zeta_3^{-2}) \\
\mathbf{v}^{1} &= (\boldsymbol{\zeta}_\tau^1 - \mathsf{X}_3\nabla_\tau\zeta_3^{0},\ \zeta_3^1) + (P_{\mathsf{b}}^3(\mathsf{X}_3)\nabla_\tau\Delta_\tau\zeta_3^{-2},\ P_{\mathsf{m}}^1(\mathsf{X}_3)\,\mathrm{div}\,\boldsymbol{\zeta}_\tau^0 + P_{\mathsf{b}}^2(\mathsf{X}_3)\Delta_\tau\zeta_3^{-1}).
\end{aligned} \tag{8}$$

In the above formulae, $\nabla_\tau = (\partial_1, \partial_2)$ is the surface gradient on S, $\Delta_\tau = \partial_1^2 + \partial_2^2$ is the surface Laplacian and $\mathrm{div}\,\boldsymbol{\zeta}_\tau$ is the surface divergence (i.e. $\mathrm{div}\,\boldsymbol{\zeta}_\tau = \partial_1\zeta_1 + \partial_2\zeta_2$). The functions P_{b}^ℓ and P_{m}^ℓ are polynomials of degree ℓ, whose coefficients depend on the Lamé constants according to:

$$\begin{gathered}
P_{\mathsf{m}}^1(\mathsf{X}_3) = -\,\frac{\lambda}{\lambda+2\mu}\,\mathsf{X}_3, \qquad P_{\mathsf{b}}^2(\mathsf{X}_3) = \frac{\lambda}{2\lambda+4\mu}\,\big(\mathsf{X}_3^2 - \frac{1}{3}\big), \\
P_{\mathsf{b}}^3(\mathsf{X}_3) = \frac{1}{6\lambda+12\mu}\,\big((3\lambda+4\mu)\,\mathsf{X}_3^3 - (11\lambda+12\mu)\,\mathsf{X}_3\big).
\end{gathered} \tag{9}$$

Note that the first blocks in $\sum_{k\geq -2}\varepsilon^k\mathbf{v}^k$ yield Kirchhoff displacements, whereas the second blocks have zero mean values through the thickness for each $\mathbf{x}_\tau \in S$.

Encyclopedia of Computational Mechanics. Edited by Erwin Stein, René de Borst and Thomas J.R. Hughes.

2.2.3. All regular terms with the help of formal series. We see from (8) that the formulae describing the successive $\mathbf{v}^k$ are *partly self-similar* and, also, that each $\mathbf{v}^k$ is enriched by a new term. That is why the whole regular term series $\sum_k \varepsilon^k \mathbf{v}^k$ can be efficiently described with the help of the *formal series product*.

A formal series is an infinite sequence $(a^0, a^1, \ldots, a^k, \ldots)$ of coefficients, which can be denoted in a symbolic way by $a[\varepsilon] = \sum_{k\geq 0} \varepsilon^k a^k$, and the product $a[\varepsilon]b[\varepsilon]$ of the two formal series $a[\varepsilon]$ and $b[\varepsilon]$ is the formal series $c[\varepsilon]$ with coefficients $c^\ell = \sum_{0\leq k\leq \ell} a^k b^{\ell-k}$. In other words

$$\text{The eq. } c[\varepsilon] = a[\varepsilon]b[\varepsilon] \quad \text{is equivalent to the series of eq.} \quad c^\ell = \sum\nolimits_{0\leq k\leq \ell} a^k b^{\ell-k}, \quad \forall \ell.$$

With this formalism we have the following identity *which extends formulae* (8):

$$\mathbf{v}[\varepsilon] = \mathbf{V}[\varepsilon]\boldsymbol{\zeta}[\varepsilon] + \mathbf{Q}[\varepsilon]\mathbf{f}[\varepsilon]. \tag{10}$$

(i) $\boldsymbol{\zeta}[\varepsilon]$ is the formal series of Kirchhoff deformation patterns $\sum_{k\geq -2} \varepsilon^k \boldsymbol{\zeta}^k$ *starting with* $k = -2$.
(ii) $\mathbf{V}[\varepsilon]$ has operator valued coefficients $\mathbf{V}^k$, $k \geq 0$, acting from $\mathcal{C}^\infty(\overline{S})^3$ into $\mathcal{C}^\infty(\overline{\Omega})^3$:

$$\begin{aligned}
\mathbf{V}^0\boldsymbol{\zeta} &= (\boldsymbol{\zeta}_\tau,\ \zeta_3)\\
\mathbf{V}^1\boldsymbol{\zeta} &= (-\mathsf{X}_3\nabla_\tau\zeta_3,\ P^1_{\mathsf{m}}(\mathsf{X}_3)\operatorname{div}\boldsymbol{\zeta}_\tau)\\
\mathbf{V}^2\boldsymbol{\zeta} &= (P^2_{\mathsf{m}}(\mathsf{X}_3)\nabla_\tau\operatorname{div}\boldsymbol{\zeta}_\tau,\ P^2_{\mathsf{b}}(\mathsf{X}_3)\Delta_\tau\zeta_3),\\
&\ldots\\
\mathbf{V}^{2j}\boldsymbol{\zeta} &= (P^{2j}_{\mathsf{m}}(\mathsf{X}_3)\nabla_\tau\Delta_\tau^{j-1}\operatorname{div}\boldsymbol{\zeta}_\tau,\ P^{2j}_{\mathsf{b}}(\mathsf{X}_3)\Delta_\tau^j\zeta_3),\\
\mathbf{V}^{2j+1}\boldsymbol{\zeta} &= (P^{2j+1}_{\mathsf{b}}(\mathsf{X}_3)\nabla_\tau\Delta_\tau^j\zeta_3,\ P^{2j+1}_{\mathsf{m}}(\mathsf{X}_3)\Delta_\tau^j\operatorname{div}\boldsymbol{\zeta}_\tau),
\end{aligned} \tag{11}$$

with P^ℓ_{b} and P^ℓ_{m} polynomials of degree ℓ (the first ones are given in (9)).
(iii) $\mathbf{f}[\varepsilon]$ is the Taylor series of $\mathbf{f}$ around the surface $\mathsf{x}_3 = 0$:

$$\mathbf{f}[\varepsilon] = \sum\nolimits_{k\geq 0} \varepsilon^k \mathbf{f}^k \quad \text{with} \quad \mathbf{f}^k(\mathbf{x}_\tau, \mathsf{X}_3) = \frac{\mathsf{X}_3^k}{k!}\frac{\partial^k \mathbf{f}}{\partial \mathsf{x}_3^k}\Big|_{\mathsf{x}_3=0}(\mathbf{x}_\tau). \tag{12}$$

(iv) $\mathbf{Q}[\varepsilon]$ has operator valued coefficients $\mathbf{Q}^k$ acting from $\mathcal{C}^\infty(\overline{\Omega})^3$ into itself. It starts[11] at $k = 2$:

$$\mathbf{Q}[\varepsilon] = \sum\nolimits_{k\geq 2} \varepsilon^k \mathbf{Q}^k. \tag{13}$$

Each $\mathbf{Q}^k$ is made of compositions of partial derivatives in the surface variables $\mathbf{x}_\tau$ with integral operators in the scaled transverse variable. Each of them acts in a particular way between *semi-polynomial spaces* $E^q(\Omega)$, $q \geq 0$, in the scaled domain Ω: We define for any integer q, $q \geq 0$

$$E^q(\Omega) = \big\{\mathbf{v} \in \mathcal{C}^\infty(\Omega)^3,\ \exists \mathbf{z}^n \in \mathcal{C}^\infty(\overline{S})^3,\ \mathbf{v}(\mathbf{x}_\tau, \mathsf{X}_3) = \sum_{n=0}^{q} \mathsf{X}_3^n \mathbf{z}^n(\mathbf{x}_\tau)\big\}. \tag{14}$$

Note that by (12), $\mathbf{f}^k$ belongs to $E^k(\Omega)$.

[11] We can see now that the four first equations given by equality (10) are $\mathbf{v}^{-2} = \mathbf{V}^0\boldsymbol{\zeta}^{-2}$, $\mathbf{v}^{-1} = \mathbf{V}^0\boldsymbol{\zeta}^{-1} + \mathbf{V}^1\boldsymbol{\zeta}^{-2}$, $\mathbf{v}^0 = \mathbf{V}^0\boldsymbol{\zeta}^0 + \mathbf{V}^1\boldsymbol{\zeta}^{-1} + \mathbf{V}^2\boldsymbol{\zeta}^{-2}$, $\mathbf{v}^1 = \mathbf{V}^0\boldsymbol{\zeta}^1 + \mathbf{V}^1\boldsymbol{\zeta}^0 + \mathbf{V}^2\boldsymbol{\zeta}^{-1} + \mathbf{V}^3\boldsymbol{\zeta}^{-2}$, which gives back (8).

Encyclopedia of Computational Mechanics. Edited by Erwin Stein, René de Borst and Thomas J.R. Hughes.

Besides, for any $k \geq 2$, $\mathbf{Q}^k$ acts from $E^q(\Omega)$ into $E^{q+k}(\Omega)$. The first term of the series $\mathbf{Q}[\varepsilon]\mathbf{f}[\varepsilon]$ is $\mathbf{Q}^2\mathbf{f}^0$ and we have:

$$\mathbf{Q}^2\mathbf{f}^0(\mathbf{x}_\tau, \mathsf{X}_3) = \Big(\mathbf{0},\ \frac{1-3\mathsf{X}_3^2}{6\lambda+12\mu}\,\mathsf{f}_3^0(\mathbf{x}_\tau)\Big).$$

As a consequence of formula (10), combined with the structure of each term, we find

Lemma 2.2. *[Dauge and Schwab, 2002] With the definition* (14) *for the semi-polynomial space* $E^q(\Omega)$*, for any* $k \geq -2$ *the regular term* $\mathbf{v}^k$ *belongs to* $E^{k+2}(\Omega)$.

2.2.4. Deformation patterns. From formula (8) extended by (10) we obtain explicit expressions for the regular parts $\mathbf{v}^k$ provided we know the deformation patterns $\boldsymbol{\zeta}^k$. The latter solves boundary value problems on the mid-surface S. Our multi-scale expansion approach gives back the well-known equations of plates (the Kirchhoff-Love model and the plane stress model) completed by a whole series of boundary value problems.

(i) The first bending generator ζ_3^{-2} solves the Kirchhoff-Love model

$$L_{\mathsf{b}}\zeta_3^{-2}(\mathbf{x}_\tau) = \mathsf{f}_3^0(\mathbf{x}_\tau),\ \ \mathbf{x}_\tau \in S \qquad \text{with} \qquad \zeta_3^{-2}\big|_{\partial S} = 0,\ \ \partial_{\mathbf{n}}\zeta_3^{-2}\big|_{\partial S} = 0 \tag{15}$$

where L_{b} is the fourth-order operator

$$L_{\mathsf{b}} := \frac{4\mu}{3}\frac{\lambda+\mu}{\lambda+2\mu}\,\Delta_\tau^2 = \frac{1}{3}(\widetilde{\lambda}+2\mu)\,\Delta_\tau^2 \tag{16}$$

and $\mathbf{n}$ the unit *interior* normal to ∂S. Here $\tilde{\lambda}$ is the "averaged" Lamé constant

$$\widetilde{\lambda} = \frac{2\lambda\mu}{\lambda+2\mu}\ . \tag{17}$$

(ii) The second bending generator ζ_3^{-1} is the solution of a similar problem

$$L_{\mathsf{b}}\zeta_3^{-1}(\mathbf{x}_\tau) = 0,\ \ \mathbf{x}_\tau \in S \qquad \text{with} \qquad \zeta_3^{-1}\big|_{\partial S} = 0,\ \ \partial_{\mathbf{n}}\zeta_3^{-1}\big|_{\partial S} = c^{\mathsf{b}}_{\lambda,\mu}\Delta_\tau\zeta_3^{-2}, \tag{18}$$

where $c^{\mathsf{b}}_{\lambda,\mu}$ is a positive constant depending on the Lamé coefficients.

(iii) The membrane part $\boldsymbol{\zeta}_\tau^0$ of the third deformation pattern solves the plane stress model

$$L_{\mathsf{m}}\boldsymbol{\zeta}_\tau^0(\mathbf{x}_\tau) = \mathbf{f}_\tau^0(\mathbf{x}_\tau),\ \ \mathbf{x}_\tau \in S \qquad \text{and} \qquad \boldsymbol{\zeta}_\tau^0|_{\partial S} = \mathbf{0} \tag{19}$$

where L_{m} is the second-order 2×2 system

$$\begin{pmatrix}\zeta_1\\ \zeta_2\end{pmatrix} \longmapsto -\begin{pmatrix}(\widetilde{\lambda}+2\mu)\partial_{11}+\mu\partial_{22} & (\widetilde{\lambda}+\mu)\partial_{12}\\ (\widetilde{\lambda}+\mu)\partial_{12} & \mu\partial_{11}+(\widetilde{\lambda}+2\mu)\partial_{22}\end{pmatrix}\begin{pmatrix}\zeta_1\\ \zeta_2\end{pmatrix}. \tag{20}$$

(iv) Here, again, the whole series of equations over the series of deformation patterns $\sum_{k\geq -2}\varepsilon^k\boldsymbol{\zeta}^k$ can be written in a global way using the formal series product, as *reduced equations on the mid-surface*:

$$\mathbf{L}[\varepsilon]\boldsymbol{\zeta}[\varepsilon] = \mathbf{R}[\varepsilon]\mathbf{f}[\varepsilon] \quad \text{in} \quad S \qquad \text{with} \qquad \mathbf{d}[\varepsilon]\boldsymbol{\zeta}[\varepsilon] = 0 \quad \text{on} \quad \partial S. \tag{21}$$

Here $\mathbf{L}[\varepsilon] = \mathbf{L}^0 + \varepsilon^2\mathbf{L}^2 + \varepsilon^4\mathbf{L}^4 + \ldots$, with

$$\mathbf{L}^0\boldsymbol{\zeta} = \begin{pmatrix}L_{\mathsf{m}} & 0\\ 0 & 0\end{pmatrix}\begin{pmatrix}\boldsymbol{\zeta}_\tau\\ \zeta_3\end{pmatrix}, \qquad \mathbf{L}^2\boldsymbol{\zeta} = \begin{pmatrix}L_{\mathsf{m}}^2 & 0\\ 0 & L_{\mathsf{b}}\end{pmatrix}\begin{pmatrix}\boldsymbol{\zeta}_\tau\\ \zeta_3\end{pmatrix}, \ldots \tag{22}$$

Encyclopedia of Computational Mechanics. Edited by Erwin Stein, René de Borst and Thomas J.R. Hughes.

where $L^2_{\mathsf{m}}\boldsymbol{\zeta}_\tau$ has the form $c\nabla_\tau\Delta_\tau \operatorname{div}\boldsymbol{\zeta}_\tau$. The series of operators $\mathbf{R}[\varepsilon]$ starts at $k=0$ and acts from $\mathcal{C}^\infty(\overline{\Omega})^3$ into $\mathcal{C}^\infty(\overline{S})^3$. Its first coefficient is the mean-value operator

$$\mathbf{f} \mapsto \mathbf{R}^0\mathbf{f} \quad \text{with} \quad \mathbf{R}^0\mathbf{f}(\mathbf{x}_\tau) = \frac{1}{2}\int_{-1}^{1} \mathbf{f}(\mathbf{x}_\tau, \mathsf{X}_3)\,\mathrm{d}\mathsf{X}_3. \tag{23}$$

Finally, the coefficients of the operator series $\mathbf{d}[\varepsilon]$ are trace operators acting on $\boldsymbol{\zeta}$. The first terms are

$$\mathbf{d}^0\boldsymbol{\zeta} = \begin{pmatrix} \boldsymbol{\zeta}_\tau\cdot\mathbf{n} \\ \boldsymbol{\zeta}_\tau\times\mathbf{n} \\ 0 \\ 0 \end{pmatrix}, \quad \mathbf{d}^1\boldsymbol{\zeta} = \begin{pmatrix} -c^{\mathsf{m}}_{\lambda,\mu}\operatorname{div}\boldsymbol{\zeta}_\tau \\ 0 \\ 0 \\ 0 \end{pmatrix}, \quad \mathbf{d}^2\boldsymbol{\zeta} = \begin{pmatrix} \bullet \\ \bullet \\ \zeta_3 \\ \partial_{\mathbf{n}}\zeta_3 \end{pmatrix}, \quad \mathbf{d}^3\boldsymbol{\zeta} = \begin{pmatrix} \bullet \\ \bullet \\ 0 \\ -c^{\mathsf{b}}_{\lambda,\mu}\Delta_\tau\zeta_3 \end{pmatrix} \tag{24}$$

where $c^{\mathsf{b}}_{\lambda,\mu}$ is the constant in (18), $c^{\mathsf{m}}_{\lambda,\mu}$ is another positive constant and $\bullet$ indicates the presence of higher order operators on $\boldsymbol{\zeta}_\tau$.

Note that the first three equations in (21): $\mathbf{L}^0\boldsymbol{\zeta}^{-2}=0$, $\mathbf{L}^0\boldsymbol{\zeta}^{-1}=0$, $\mathbf{L}^0\boldsymbol{\zeta}^0+\mathbf{L}^2\boldsymbol{\zeta}^{-2}=\mathbf{R}^0\mathbf{f}^0$ on S and $\mathbf{d}^0\boldsymbol{\zeta}^{-2}=0$, $\mathbf{d}^0\boldsymbol{\zeta}^{-1}+\mathbf{d}^1\boldsymbol{\zeta}^{-1}=0$, $\mathbf{d}^0\boldsymbol{\zeta}^0+\mathbf{d}^1\boldsymbol{\zeta}^{-1}+\mathbf{d}^2\boldsymbol{\zeta}^{-2}=0$ on ∂S, give back (15), (18) and (19) together with the fact that $\boldsymbol{\zeta}_\tau^{-2}=\boldsymbol{\zeta}_\tau^{-1}=0$.

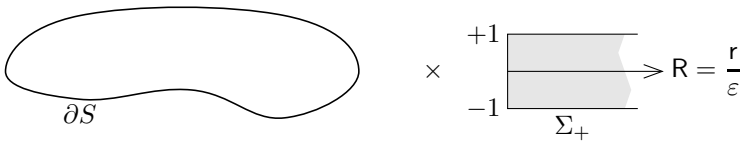

Figure 3. Boundary layer coordinates in $\partial S\times\Sigma_+$.

2.2.5. Boundary layer terms. The terms $\mathbf{w}^k$ have a quite different structure. Their natural variables are $(\mathsf{R},\mathsf{s},\mathsf{X}_3)$, see §2.1, and they are easier to describe in boundary fitted components $(\mathsf{w}_\mathsf{r},\mathsf{w}_\mathsf{s},\mathsf{w}_3)$ corresponding to the local coordinates $(\mathsf{r},\mathsf{s},\mathsf{x}_3)$. The first boundary layer term, $\mathbf{w}^0$ is a bending displacement in the sense of (5) and has a tensor product form: In boundary fitted components it reads

$$\mathsf{w}^0_\mathsf{s}=0 \quad \text{and} \quad (\mathsf{w}^0_\mathsf{r},\mathsf{w}^0_3)(\mathsf{R},\mathsf{s},\mathsf{X}_3)=\varphi(\mathsf{s})\,\overline{\mathbf{w}}^0_*(\mathsf{R},\mathsf{X}_3) \quad \text{with} \quad \varphi=\Delta_\tau\zeta_3^{-2}\big|_{\partial S}$$

and $\overline{\mathbf{w}}^0_*$ is a two component *exponentially decreasing profile* on the semi-strip $\Sigma_+ := \{(\mathsf{R},\mathsf{X}_3), \mathsf{R}>0,\ |\mathsf{X}_3|<1\}$: There exists $\eta>0$ such that

$$|e^{\eta\mathsf{R}}\,\overline{\mathbf{w}}^0_*(\mathsf{R},\mathsf{X}_3)| \quad \text{is bounded as} \quad \mathsf{R}\to\infty.$$

The least upper bound of such η is the smallest exponent η_0 arising from the Papkovich-Fadle eigenfunctions, see Gregory and Wan, 1984. Both components of $\overline{\mathbf{w}}^0_*$ are non-zero.

The next boundary layer terms $\mathbf{w}^k$ are combinations of products of (smooth) traces on ∂S by profiles $\overline{\mathbf{w}}^{k,\ell}$ in $(\mathsf{R},\mathsf{X}_3)$. These profiles have singularities at the corners $(0,\pm1)$ of Σ_+, according to the general theory of Kondrat'ev, 1967. Thus, in contrast with the "regular" terms $\mathbf{v}^k$ which are smooth up to the boundary of Ω, the terms $\mathbf{w}^k$ do have singular parts along the edges $\partial S\times\{\pm1\}$ of the plate. Finally, the edge singularities of the solution $\mathbf{u}^\varepsilon$ of problem (3) are related with the boundary layer terms only, see Dauge and Gruais, 1998 for further details.

Encyclopedia of Computational Mechanics. Edited by Erwin Stein, René de Borst and Thomas J.R. Hughes.

2.3. Properties of the displacement expansion outside the boundary layer

Let S' be a subset of S such that the distance between $\partial S'$ and ∂S is positive. As a consequence of expansion (6) there holds

$$\mathbf{u}^\varepsilon(\mathbf{x}) = \sum_{k=-2}^{K} \varepsilon^k \mathbf{v}^k(\mathbf{x}_\tau, \mathsf{X}_3) + \mathcal{O}(\varepsilon^{K+1}) \quad \text{uniformly for} \quad \mathbf{x} \in \overline{S}' \times (-\varepsilon, \varepsilon).$$

Coming back to physical variables $(\mathbf{x}_\tau, \mathsf{x}_3)$, the expansion terms $\mathbf{v}^k$ being polynomials of degree $k+2$ in X_3 (Lemma 2.2), we find that

$$\mathbf{u}^\varepsilon(\mathbf{x}) = \sum_{k=-2}^{K} \varepsilon^k\, \widehat{\mathbf{v}}^{K,k}(\mathbf{x}_\tau, \mathsf{x}_3) + \mathcal{O}(\varepsilon^{K+1}) \quad \text{uniformly for} \quad \mathbf{x} \in \overline{S}' \times (-\varepsilon, \varepsilon)$$

with fields $\widehat{\mathbf{v}}^{K,k}$ being polynomials in x_3 of degree $K-k$. That means that the expansion (6) can also be seen as a *Taylor expansion* at the mid-surface, provided we are at a fixed positive distance from the lateral boundary.

Let us write the first terms in the expansions of the bending and membrane parts $\mathbf{u}_\mathsf{b}^\varepsilon$ and $\mathbf{u}_\mathsf{m}^\varepsilon$ of $\mathbf{u}^\varepsilon$:

$$\begin{aligned}\mathbf{u}_\mathsf{b}^\varepsilon = \varepsilon^{-2}\big(-\mathsf{x}_3\nabla_\tau\zeta_3^{-2},\ \zeta_3^{-2} + \frac{\lambda\mathsf{x}_3^2}{2\lambda+4\mu}\Delta_\tau\zeta_3^{-2}\big) - \big(\mathbf{0}, \frac{\lambda}{6\lambda+12\mu}\Delta_\tau\zeta_3^{-2}\big)\\ + \varepsilon^{-1}\big(-\mathsf{x}_3\nabla_\tau\zeta_3^{-1},\ \zeta_3^{-1} + \frac{\lambda\mathsf{x}_3^2}{2\lambda+4\mu}\Delta_\tau\zeta_3^{-1}\big) + \dots \quad (25)\end{aligned}$$

From this formula we can deduce the following asymptotics for the strain and stress components

$$\begin{aligned} e_{\alpha\beta}(\mathbf{u}_\mathsf{b}^\varepsilon) &= -\varepsilon^{-2}\mathsf{x}_3\partial_{\alpha\beta}\big(\zeta_3^{-2} + \varepsilon\zeta_3^{-1}\big) + \mathcal{O}(\varepsilon)\\ e_{33}(\mathbf{u}_\mathsf{b}^\varepsilon) &= \varepsilon^{-2}\frac{\lambda\mathsf{x}_3}{\lambda+2\mu}\Delta_\tau\big(\zeta_3^{-2} + \varepsilon\zeta_3^{-1}\big) + \mathcal{O}(\varepsilon) \quad (26)\\ \sigma^{33}(\mathbf{u}_\mathsf{b}^\varepsilon) &= \mathcal{O}(\varepsilon)\end{aligned}$$

Since $\varepsilon^{-2}\mathsf{x}_3 = \mathcal{O}(\varepsilon^{-1})$, we see that $e_{33} = \mathcal{O}(\varepsilon^{-1})$. Thus σ^{33} is two orders of magnitude less than e_{33}, which means a *plane stress limit*. To compute the shear strain (or stress) we use one further term in the asymptotics of $\mathbf{u}_\mathsf{b}^\varepsilon$ and obtain that it is one order of magnitude less than e_{33}:

$$e_{\alpha3}(\mathbf{u}_\mathsf{b}^\varepsilon) = \frac{2\lambda+2\mu}{\lambda+2\mu}(\varepsilon^{-2}\mathsf{x}_3^2 - 1)\partial_\alpha\Delta_\tau\zeta_3^{-2} + \mathcal{O}(\varepsilon). \quad (27)$$

Computations for the membrane part $\mathbf{u}_\mathsf{m}^\varepsilon$ are simpler and yield similar results

$$\begin{aligned}\mathbf{u}_\mathsf{m}^\varepsilon &= \big(\boldsymbol{\zeta}_\tau^0,\ -\frac{\lambda\mathsf{x}_3}{\lambda+2\mu}\operatorname{div}\boldsymbol{\zeta}_\tau^0\big) + \varepsilon\big(\boldsymbol{\zeta}_\tau^1,\ -\frac{\lambda\mathsf{x}_3}{\lambda+2\mu}\operatorname{div}\boldsymbol{\zeta}_\tau^1\big) + \dots\\ e_{\alpha\beta}(\mathbf{u}_\mathsf{m}^\varepsilon) &= \frac{1}{2}(\partial_\alpha\zeta_\beta^0 + \partial_\beta\zeta_\alpha^0) + \frac{\varepsilon}{2}(\partial_\alpha\zeta_\beta^1 + \partial_\beta\zeta_\alpha^1) + \mathcal{O}(\varepsilon^2) \quad (28)\\ e_{33}(\mathbf{u}_\mathsf{m}^\varepsilon) &= -\frac{\lambda}{\lambda+2\mu}\operatorname{div}\big(\boldsymbol{\zeta}_\tau^0 + \varepsilon\boldsymbol{\zeta}_\tau^1\big) + \mathcal{O}(\varepsilon^2),\end{aligned}$$

and $\sigma^{33}(\mathbf{u}_\mathsf{m}^\varepsilon) = \mathcal{O}(\varepsilon^2)$, $e_{\alpha3}(\mathbf{u}_\mathsf{m}^\varepsilon) = \mathcal{O}(\varepsilon)$.

In (26)-(28) the $\mathcal{O}(\varepsilon)$ and $\mathcal{O}(\varepsilon^2)$ are uniform on any region $\overline{S}' \times (-\varepsilon, \varepsilon)$ where the boundary layer terms have no influence. We postpone global energy estimates to the next section.

Encyclopedia of Computational Mechanics. Edited by Erwin Stein, René de Borst and Thomas J.R. Hughes.

2.4. Eigen-mode problem

For each $\varepsilon > 0$ the spectrum of problem (4) is discrete and positive. Let Λ_j^ε, $j = 1, 2, \ldots$ be the increasing sequence of eigenvalues. In Ciarlet and Kesavan, 1981 it is proved that $\varepsilon^{-2}\Lambda_j^\varepsilon$ converges to the j-th eigenvalue $\Lambda_{\mathsf{b},j}^{\mathsf{KL}}$ of the Dirichlet problem for the Kirchhoff operator L_b, *cf* (16). In Nazarov and Zorin, 1989; Nazarov, 1991 a two-term asymptotics is constructed for the $\varepsilon^{-2}\Lambda_j^\varepsilon$. Nazarov (2000b) proves that $|\varepsilon^{-2}\Lambda_j^\varepsilon - \Lambda_{\mathsf{b},j}^{\mathsf{KL}}|$ is bounded by an $\mathcal{O}(\sqrt{\varepsilon})$ for a much more general material matrix A.

In Dauge *et al.*, 1999, full asymptotic expansions for eigenvalues and eigenvectors are proved: For each j there exist

- bending generators $\zeta_3^{-2}, \zeta_3^{-1}, \ldots$ where ζ_3^{-2} is an eigenvector of L_b associated with $\Lambda_{\mathsf{b},j}^{\mathsf{KL}}$
- real numbers $\Lambda_{\mathsf{b},j}^1, \Lambda_{\mathsf{b},j}^2, \ldots$
- eigenvectors $\mathbf{u}_{\mathsf{b},j}^\varepsilon$ associated with Λ_j^ε for any $\varepsilon \in (0, \varepsilon_0)$

so that for any $K \geq 0$

$$\begin{aligned} \Lambda_j^\varepsilon &= \varepsilon^2\Lambda_{\mathsf{b},j}^{\mathsf{KL}} + \varepsilon^3\Lambda_{\mathsf{b},j}^1 + \ldots + \varepsilon^{K+2}\Lambda_{\mathsf{b},j}^K + \mathcal{O}(\varepsilon^{K+3}) \\ \mathbf{u}_{\mathsf{b},j}^\varepsilon &= \varepsilon^{-2}(-\mathsf{x}_3\nabla_\tau\zeta_3^{-2}, \zeta_3^{-2}) + \varepsilon^{-1}(-\mathsf{x}_3\nabla_\tau\zeta_3^{-1}, \zeta_3^{-1}) + \ldots + \varepsilon^K(\mathbf{v}^K + \chi\mathbf{w}^K) + \mathcal{O}(\varepsilon^{K+1}) \end{aligned} \tag{29}$$

where the terms $\mathbf{v}^k$ and $\mathbf{w}^k$ are generated by the ζ_3^k, $k \geq 0$ in a similar way as in §2.2, and $\mathcal{O}(\varepsilon^{K+1})$ is uniform over Ω^ε.

The bending and membrane displacements are the eigenvectors of the symmetry operator $\mathfrak{S}$, see (5). Since $\mathfrak{S}$ commutes with the elasticity operator, both have a joint spectrum, which means that there exists a basis of common eigenvectors. In other words, each elasticity eigenvalue can be identified as a bending or a membrane eigenvalue. The expansion (29) is the expansion of *bending* eigen-pairs.

The expansion of membrane eigen-pairs can be done in a similar way. Let us denote by $\Lambda_{\mathsf{m},j}^\varepsilon$ the j-th membrane eigenvalue on Ω^ε and by $\Lambda_{\mathsf{m},j}^{\mathsf{KL}}$ the j-th eigenvalue of the plane stress operator L_m, *cf* (20) with Dirichlet boundary conditions. Then we have a similar statement as above, with the distinctive feature that the membrane eigenvalues tend to those of the plane stress model:

$$\Lambda_{\mathsf{m},j}^\varepsilon = \Lambda_{\mathsf{m},j}^{\mathsf{KL}} + \varepsilon^1\Lambda_{\mathsf{m},j}^1 + \ldots + \varepsilon^K\Lambda_{\mathsf{m},j}^K + \mathcal{O}(\varepsilon^{K+1}). \tag{30}$$

This fact, compared with (29), explains why the smallest eigenvalues are bending. Note that the eigenvalue formal series $\Lambda[\varepsilon]$ satisfy reduced equations $\mathbf{L}[\varepsilon]\boldsymbol{\zeta}[\varepsilon] = \Lambda[\varepsilon]\boldsymbol{\zeta}[\varepsilon]$ like (21) with the same $\mathbf{L}^0$, $\mathbf{L}^1 = 0$ and $\mathbf{L}^2$ as in (22). In particular, equations

$$\begin{pmatrix} L_\mathsf{m} & 0 \\ 0 & \varepsilon^2 L_\mathsf{b} \end{pmatrix} \begin{pmatrix} \boldsymbol{\zeta}_\tau \\ \zeta_3 \end{pmatrix} = \Lambda \begin{pmatrix} \boldsymbol{\zeta}_\tau \\ \zeta_3 \end{pmatrix} \tag{31}$$

give back the "limiting" eigenvalues $\Lambda_\mathsf{m}^{\mathsf{KL}}$ and $\varepsilon^2\Lambda_\mathsf{b}^{\mathsf{KL}}$. Our last remark is that the second terms $\Lambda_{\mathsf{b},j}^1$ and $\Lambda_{\mathsf{m},j}^1$ are positive, see Dauge and Yosibash, 2002 for a discussion of that fact.

2.5. Extensions.

2.5.1. Traction on the free parts of the boundary. Instead of a volume load or in addition to it, tractions $\mathbf{g}^\pm$ can be imposed on the faces $S \times \{\pm\varepsilon\}$ of the plate. Let us assume that $\mathbf{g}^\pm$ is independent of ε. Then the displacement $\mathbf{u}^\varepsilon$ has a similar expansion as in (6), with the following modifications:

- If the bending part of $\mathbf{g}^\pm$ is non-zero, then the regular part starts with $\varepsilon^{-3}\mathbf{v}^{-3}$ and the boundary layer part with $\varepsilon^{-1}\chi\mathbf{w}^{-1}$;
- If the membrane part of $\mathbf{g}^\pm$ is non-zero, the membrane regular part starts with $\varepsilon^{-1}\mathbf{v}^{-1}$.

Encyclopedia of Computational Mechanics. Edited by Erwin Stein, René de Borst and Thomas J.R. Hughes.

2.5.2. Lateral boundary conditions. A similar analysis holds for each of the seven remaining types of "canonical" boundary conditions: soft clamping, hard simple support, soft simple support, two types of friction, sliding edge, and free boundary. See Dauge *et al.*, 1999/00 for details. It would also be possible to extend such an analysis to more intimately mixed boundary conditions where only moments through the thickness along the lateral boundary are imposed for displacement or traction components, see Schwab, 1996.

If, instead of volume load $\mathbf{f}$ or tractions $\mathbf{g}^{\pm}$, we set $\mathbf{f} \equiv 0$, $\mathbf{g}^{\pm} \equiv 0$, and impose non-zero lateral boundary conditions, $\mathbf{u}^{\varepsilon}$ will have a similar expansion as in (6) with the remarkable feature that the degree of the regular part in the thickness variable is ≤ 3, see Dauge and Schwab, 2002, Rem.5.4. Moreover, in the clamped situation, the expansion starts with $\mathcal{O}(1)$.

2.5.3. Laminated composites. If the material of the plate is homogeneous, but not isotropic, $\mathbf{u}^{\varepsilon}$ will still have a similar expansion, see Dauge and Gruais, 1996; Dauge and Yosibash, 2002 for orthotropic plates. If the plate is laminated, i.e. formed by the union of several plies made of different homogeneous materials, then $\mathbf{u}^{\varepsilon}$ still expands in regular parts $\mathbf{v}^k$ and boundary layer parts $\mathbf{w}^k$, but the $\mathbf{v}^k$ are no more polynomials in the thickness variable, only *piecewise polynomial* in each ply, and continuous, see Actis *et al.*, 1999. Nazarov (2000a, 2000b) addresses more general material laws where the matrix A depends on the variables $\mathbf{x}_{\tau}$ and $\mathsf{X}_3 = \mathbf{x}_3/\varepsilon$.

3. HIERARCHICAL MODELS FOR PLATES

3.1. The concepts of hierarchical models

The idea of hierarchical models is a natural and efficient extension to that of limiting models and dimension reduction. In the finite element framework it has been firstly formulated in Szabó and Sahrmann, 1988 for isotropic domains, mathematically investigated in Babuška and Li, 1991, 1992a, 1992b, and generalized to laminated composites in Babuška *et al.*, 1992; Actis *et al.*, 1999. A hierarchy of models consists of

- a sequence of subspaces $V^{\mathbf{q}}(\Omega^{\varepsilon})$ of $V(\Omega^{\varepsilon})$ with the *orders* $\mathbf{q} = (q_1, q_2, q_3)$ forming a sequence of integer triples, satisfying

$$V^{\mathbf{q}}(\Omega^{\varepsilon}) \subset V^{\mathbf{q}'}(\Omega^{\varepsilon}) \quad \text{if} \quad \mathbf{q} \preceq \mathbf{q}'. \tag{32}$$

- a sequence of related Hooke laws $\boldsymbol{\sigma} = A_{\mathbf{q}}\boldsymbol{e}$, corresponding to a sequence of elastic bilinear forms $a^{\varepsilon,\mathbf{q}}(\mathbf{u}, \mathbf{u}') = \int_{\Omega^{\varepsilon}} A_{\mathbf{q}}\boldsymbol{e}(\mathbf{u}) : \boldsymbol{e}(\mathbf{u}')$.

Let $\mathbf{u}^{\varepsilon,\mathbf{q}}$ be the solution of the problem

$$\textit{Find } \mathbf{u}^{\varepsilon,\mathbf{q}} \in V^{\mathbf{q}}(\Omega^{\varepsilon}) \quad \textit{such that} \quad a^{\varepsilon,\mathbf{q}}(\mathbf{u}^{\varepsilon,\mathbf{q}}, \mathbf{u}') = \int_{\Omega^{\varepsilon}} \mathbf{f}^{\varepsilon} \cdot \mathbf{u}' \, \mathrm{d}\boldsymbol{x}, \quad \forall \mathbf{u}' \in V^{\mathbf{q}}(\Omega^{\varepsilon}). \tag{33}$$

Note that problem (33) is a Galerkin projection of problem (3) if $a^{\varepsilon,\mathbf{q}} = a^{\varepsilon}$.

Any model which belongs to the hierarchical family has to satisfy three requirements, see Szabó and Babuška, 1991, Chap. 14.5:

(a) *Approximability.* At any fixed thickness $\varepsilon > 0$:

$$\lim_{\mathbf{q}\to\infty} \|\mathbf{u}^{\varepsilon} - \mathbf{u}^{\varepsilon,\mathbf{q}}\|_{E(\Omega^{\varepsilon})} = 0. \tag{34}$$

Encyclopedia of Computational Mechanics. Edited by Erwin Stein, René de Borst and Thomas J.R. Hughes.

(b) *Asymptotic consistency.* For any fixed degree $\mathbf{q}$:

$$\lim_{\varepsilon\to 0} \frac{\|\mathbf{u}^\varepsilon - \mathbf{u}^{\varepsilon,\mathbf{q}}\|_{E(\Omega^\varepsilon)}}{\|\mathbf{u}^\varepsilon\|_{E(\Omega^\varepsilon)}} = 0. \tag{35}$$

(c) *Optimality of the convergence rate.* There exists a sequence of positive exponents $\gamma(\mathbf{q})$ with the growth property $\gamma(\mathbf{q}) < \gamma(\mathbf{q}')$ if $\mathbf{q} \prec \mathbf{q}'$, such that "in the absence of boundary layers and edge singularities":

$$\|\mathbf{u}^\varepsilon - \mathbf{u}^{\varepsilon,\mathbf{q}}\|_{E(\Omega^\varepsilon)} \le C\varepsilon^{\gamma(\mathbf{q})}\|\mathbf{u}^\varepsilon\|_{E(\Omega^\varepsilon)}. \tag{36}$$

The substantiation of hierarchical models for plates in general requires the choice of three sequences of finite-dimensional nested *director spaces* $\Psi_j^0 \subset \ldots \Psi_j^N \subset \ldots \subset H^1(-1,1)$ for $j = 1,2,3$ and the definition of the space $V^{\mathbf{q}}(\Omega^\varepsilon)$ for $\mathbf{q} = (q_1, q_2, q_3)$ as

$$V^{\mathbf{q}}(\Omega^\varepsilon) = \Big\{\mathbf{u} \in V(\Omega^\varepsilon), \quad \Big((\mathbf{x}_\tau, \mathsf{X}_3) \mapsto \mathsf{u}_j(\mathbf{x}_\tau, \varepsilon\mathsf{X}_3)\Big) \in H_0^1(S) \otimes \Psi_j^{q_j}, \quad j = 1,2,3\Big\}. \tag{37}$$

We can reformulate (37) with the help of *director functions*: With $d_j(N)$ being the dimension of Ψ_j^N, let $\Phi_j^n = \Phi_j^n(\mathsf{X}_3)$, $0 \le n \le d_j(N)$, be hierarchic bases (the director functions) of Ψ_j^N. There holds

$$V^{\mathbf{q}}(\Omega^\varepsilon) = \Big\{\mathbf{u} \in V(\Omega^\varepsilon),\ \exists \mathsf{z}_j^n \in H_0^1(S),\ 0 \le n \le d_j(q_j),\ \mathsf{u}_j(\mathbf{x}_\tau, \mathsf{x}_3) = \sum_{n=0}^{d_j(q_j)} \mathsf{z}_j^n(\mathbf{x}_\tau)\, \Phi_j^n\Big(\frac{\mathsf{x}_3}{\varepsilon}\Big)\Big\}. \tag{38}$$

The choice of the *best* director functions is addressed in Vogelius and Babuška, 1981a in the case of second order scalar problems with general coefficients (including possible stratifications). For smooth coefficients, the space Ψ_j^N coincides with the space $\mathbb{P}_N$ of polynomial with degree $\le N$. The director functions can be chosen as the Legendre polynomials $L_n(\mathsf{X}_3)$ or, simply, the monomials X_3^n (and then x_3^n can be used equivalently instead $(\mathsf{x}_3/\varepsilon)^n$ in (38)).

We describe in the sequel in more details the convenient hierarchies for plates and discuss the three qualities (34)-(36), see Babuška and Li (1991, 1992a) and Babuška *et al.*, 1992 for early references.

3.2. The limit model (Kirchhoff-Love)

In view of expansion (6), we observe that if the transverse component f_3 of the load is non zero on the mid-surface, $\mathbf{u}^\varepsilon$ is unbounded as $\varepsilon \to 0$. If we multiply by ε^2 we have a convergence to $(0, \zeta_3^{-2})$, which is not kinematically relevant. At that level, a correct notion of limit uses scalings of coordinates: If we define the scaled displacement $\widetilde{\mathbf{u}}^\varepsilon$ by its components on the stretched plate $\Omega = S \times (-1,1)$ by

$$\widetilde{\mathbf{u}}_\tau^\varepsilon := \varepsilon \mathbf{u}_\tau^\varepsilon \quad \text{and} \quad \widetilde{\mathsf{u}}_3^\varepsilon := \varepsilon^2 \mathsf{u}_3^\varepsilon \tag{39}$$

then $\widetilde{\mathbf{u}}^\varepsilon$ *converges to* $(-\mathsf{X}_3\nabla_\tau\zeta_3^{-2},\, \zeta_3^{-2})$ *in* $H^1(\Omega)^3$ *as* $\varepsilon \to 0$. This result, together with the mathematical derivation of the resultant equation (15) is due to Ciarlet and Destuynder, 1979.

The corresponding subspace of $V(\Omega^\varepsilon)$ is that of bending Kirchhoff displacements or, more generally, of Kirchhoff displacements:

$$V^{\mathsf{KL}}(\Omega^\varepsilon) = \{\mathbf{u} \in V(\Omega^\varepsilon),\ \exists \boldsymbol{\zeta} \in H_0^1 \times H_0^1 \times H_0^2(S), \quad \mathbf{u} = (\boldsymbol{\zeta}_\tau - \mathsf{x}_3\nabla_\tau\zeta_3,\, \zeta_3)\}. \tag{40}$$

It follows from (40) that $e_{13} = e_{23} = 0$ for which the physical interpretation is that "normals to S prior to deformation remain straight lines and normals after deformation". Hooke's law has to be

Encyclopedia of Computational Mechanics. Edited by Erwin Stein, René de Borst and Thomas J.R. Hughes.

modified with the help of what we call "the plane stress trick". It is based on the assumption that the component σ^{33} of the stress is negligible[12]. From standard Hooke's law (1), we extract the relation $\sigma^{33} = \lambda(e_{11} + e_{22}) + (\lambda + 2\mu)e_{33}$, then set σ^{33} to zero, which yields

$$e_{33} = -\frac{\lambda}{\lambda + 2\mu}\,(e_{11} + e_{22}). \tag{41}$$

Then, we modify Hooke's law (1) by substituting e_{33} by its expression (41) in σ^{11} and σ^{22}, to obtain

$$\begin{aligned} \sigma^{ii} &= \frac{2\lambda\mu}{\lambda + 2\mu}(e_{11} + e_{22}) + 2\mu e_{ii}, \quad i = 1, 2 \\ \sigma^{ij} &= 2\mu e_{ij} \quad \text{for} \quad i \neq j. \end{aligned} \tag{42}$$

Thus $\sigma^{ii} = \widetilde{\lambda}(e_{11} + e_{22}) + 2\mu e_{ii}$, with $\widetilde{\lambda}$ given by (17). Taking into account that $e_{33} = 0$ for the elements of $V^{\mathsf{KL}}(\Omega^\varepsilon)$, we obtain a new Hooke's law given by the same formulae as (1) when replacing the Lamé coefficient λ by $\widetilde{\lambda}$. This corresponds to a modified material matrix $\widetilde{A}^{ijkl}$

$$\widetilde{A}^{ijkl} = \widetilde{\lambda}\delta^{ij}\delta^{kl} + \mu(\delta^{ik}\delta^{jl} + \delta^{il}\delta^{jk}) \tag{43}$$

and a reduced elastic energy $\widetilde{a}(\mathbf{u}, \mathbf{u}) = \int_{\Omega^\varepsilon} \sigma^{ij}(\mathbf{u})e_{ij}(\mathbf{u})$. Note that for $\mathbf{u} = (\boldsymbol{\zeta}_\tau - \mathsf{x}_3\nabla_\tau\zeta_3,\, \zeta_3)$

$$\widetilde{a}(\mathbf{u}, \mathbf{u}) = 2\varepsilon \int_S \widetilde{A}^{\alpha\beta\sigma\delta} e_{\alpha\beta}(\boldsymbol{\zeta}_\tau) e_{\sigma\delta}(\boldsymbol{\zeta}_\tau)\,\mathrm{d}\mathbf{x}_\tau + \frac{2\varepsilon^3}{3}\int_S \widetilde{A}^{\alpha\beta\sigma\delta}\partial_{\alpha\beta}(\zeta_3)\partial_{\sigma\delta}(\zeta_3)\,\mathrm{d}\mathbf{x}_\tau, \tag{44}$$

exhibiting a *membrane part* in $\mathcal{O}(\varepsilon)$ and a *bending part* in $\mathcal{O}(\varepsilon^3)$. There holds as a consequence of Theorem 2.1

Theorem 3.1. *Let* $\mathbf{u}^{\varepsilon,\mathsf{KL}}$ *be the solution of problem* (33) *with* $V^{\mathsf{q}} = V^{\mathsf{KL}}$ *and* $a^{\mathsf{q}} = \widetilde{a}$. *Then*
(i) *In general* $\mathbf{u}^{\varepsilon,\mathsf{KL}} = \varepsilon^{-2}\big(-\mathsf{x}_3\nabla_\tau\zeta_3^{-2},\, \zeta_3^{-2}\big) + \mathcal{O}(1)$ *with* ζ_3^{-2} *the solution of* (15)*;*
(ii) *If* $\mathbf{f}$ *is membrane,* $\mathbf{u}^{\varepsilon,\mathsf{KL}} = \big(\boldsymbol{\zeta}_\tau^0, 0\big) + \mathcal{O}(\varepsilon^2)$ *with* $\boldsymbol{\zeta}_\tau^0$ *the solution of* (19)*.*

Can we deduce the asymptotic consistency for that model? No! Computing the lower order terms in the expression (35) we find with the help of (25) that, if $\mathsf{f}_3^0 \not\equiv 0$:

$$\|\mathbf{u}^\varepsilon\|_{E(\Omega^\varepsilon)} \simeq \mathcal{O}(\varepsilon^{-1/2}) \quad \text{and} \quad \|\mathbf{u}^\varepsilon - \mathbf{u}^{\varepsilon,\mathsf{KL}}\|_{E(\Omega^\varepsilon)} \geq \|e_{33}(\mathbf{u}^\varepsilon)\|_{L^2(\Omega^\varepsilon)} \simeq \mathcal{O}(\varepsilon^{-1/2}).$$

Another source of difficulty is that, eventually, relation (41) *is not satisfied* by $\mathbf{u}^{\varepsilon,\mathsf{KL}}$. If $\mathsf{f}_3^0 \equiv 0$ and $\mathbf{f}_\tau^0 \not\equiv 0$, we have exactly the same difficulties with the membrane part.

A way to overcome these difficulties is to consider a complementing operator $\mathbf{C}$ defined on the elements of V^{KL} by

$$\mathbf{C}\mathbf{u} = \mathbf{u} + \Big(\mathbf{0}, -\frac{\lambda}{\lambda + 2\mu}\int_0^{\mathsf{x}_3} \operatorname{div}\mathbf{u}_\tau(\cdot, \mathsf{y})\,\mathrm{d}\mathsf{y}\Big). \tag{45}$$

Then (41) is now satisfied by $\mathbf{C}\mathbf{u}$ for any $\mathbf{u} \in V^{\mathsf{KL}}$. Moreover (still assuming $\mathsf{f}_3 \not\equiv 0$) one can show

$$\|\mathbf{u}^\varepsilon - \mathbf{C}\mathbf{u}^{\varepsilon,\mathsf{KL}}\|_{E(\Omega^\varepsilon)} \leq C\sqrt{\varepsilon}\|\mathbf{u}^\varepsilon\|_{E(\Omega^\varepsilon)}. \tag{46}$$

The error factor $\sqrt{\varepsilon}$ is due to the first boundary layer term $\mathbf{w}^0$. The presence of $\mathbf{w}^0$ is a direct consequence of the fact that $\mathbf{C}\mathbf{u}^{\varepsilon,\mathsf{KL}}$ does not satisfy the lateral boundary conditions.

Although the Kirchhoff-Love model is not a member of the hierarchical family, it is the limit of all models for $\varepsilon \to 0$.

[12] Note that the asymptotics (6) of the three-dimensional solution yields that $\sigma^{33} = \mathcal{O}(\varepsilon)$, whereas $e_{\alpha\beta}$, $e_{33} = \mathcal{O}(\varepsilon^{-1})$ outside the boundary layer, *cf* (26), which justifies the plane stress assumption.

Encyclopedia of Computational Mechanics. Edited by Erwin Stein, René de Borst and Thomas J.R. Hughes.

3.3. The Reissner-Mindlin model

This model is obtained by enriching the space of kinematically admissible displacements, allowing normals to S to rotate after deformation. Instead of (40), we set

$$V^{\mathsf{RM}}(\Omega^\varepsilon) = \{\mathbf{u} \in V(\Omega^\varepsilon),\ \exists \mathbf{z} \in H_0^1(S)^3,\ \exists \boldsymbol{\theta}_\tau \in H_0^1(S)^2, \quad \mathbf{u} = (\mathbf{z}_\tau - \mathsf{x}_3\boldsymbol{\theta}_\tau,\, \mathsf{z}_3)\}.$$

With the elasticity tensor A corresponding to 3D elasticity, the displacements and strain-energy limit of the RM model as $d \to 0$ would not coincide with the 3D limit (or the Kirchhoff-Love limit).

We have again to use instead the reduced elastic bilinear form $\widetilde{a}$ to restore the convergence to the correct limit, by virtue of the same plane stress trick. The corresponding elasticity tensor is $\widetilde{A}$ (43). A further correction can be introduced in the shear components of $\widetilde{A}$ to better represent the fully 3D shear stresses σ^{13} and σ^{23} (and also the strain energy) for small yet non-zero thickness ε. The material matrix entries A^{1313}, A^{2323} are changed by introducing the so-called *shear correction factor* κ:

$$\widetilde{A}^{1313} = \kappa A^{1313} \qquad \widetilde{A}^{2323} = \kappa A^{2323}.$$

By properly chosen κ, either the energy of the RM solution, or the deflection u_3 can be optimized with respect to the fully 3-D plate. The smallest the ε, the smallest the influence of κ on the results. For the isotropic case two possible κ's are (see details in Babuška *et al.*, 1991):

$$\kappa_{\text{Energy}} = \frac{5}{6(1-\nu)} \quad \text{or} \quad \kappa_{\text{Deflection}} = \frac{20}{3(8-3\nu)}, \quad \text{with} \quad \nu = \frac{\lambda}{2(\lambda+\mu)} \quad \text{(Poisson ratio)}.$$

A value of $\kappa = 5/6$ is frequently used in engineering practice, but for modal analysis, no optimal value of κ is available.

Note that, by integrating equations of (33) through the thickness, we find that problem (33) is equivalent to a variational problem for $\mathbf{z}$ and $\boldsymbol{\theta}$ only. For the elastic energy we have

$$\begin{aligned} \widetilde{a}(\mathbf{u},\mathbf{u}) = 2\varepsilon \int_S \widetilde{A}^{\alpha\beta\sigma\delta} e_{\alpha\beta}(\mathbf{z}_\tau) e_{\sigma\delta}(\mathbf{z}_\tau)\, \mathrm{d}\mathbf{x}_\tau \qquad & \textit{(membrane energy)} \\ + \varepsilon \int_S \kappa\mu(\partial_\alpha \mathsf{z}_3 - \theta_\alpha)(\partial_\alpha \mathsf{z}_3 - \theta_\alpha)\, \mathrm{d}\mathbf{x}_\tau \qquad & \textit{(shear energy)} \\ + \frac{2\varepsilon^3}{3} \int_S \widetilde{A}^{\alpha\beta\sigma\delta} e_{\alpha\beta}(\boldsymbol{\theta}_\tau) e_{\sigma\delta}(\boldsymbol{\theta}_\tau)\, \mathrm{d}\mathbf{x}_\tau \qquad & \textit{(bending energy)}. \end{aligned} \tag{47}$$

Let $\mathbf{u}^{\varepsilon,\mathsf{RM}}$ be the solution of problem (33) with $V^{\mathbf{q}} = V^{\mathsf{RM}}$ and $a^{\mathbf{q}} = \widetilde{a}$. The singular perturbation character appears clearly. In contrast with the Kirchhoff-Love model, the solution admits a boundary layer part. Arnold and Falk (1990, 1996) have described the two-scale asymptotics of $\mathbf{u}^{\varepsilon,\mathsf{RM}}$. Despite the presence of boundary layer terms, the question of knowing if $\mathbf{u}^{\varepsilon,\mathsf{RM}}$ is closer to $\mathbf{u}^\varepsilon$ than $\mathbf{u}^{\varepsilon,\mathsf{KL}}$ has no clear answer to our knowledge. A careful investigation of the first eigenvalues Λ_1^ε, $\Lambda_1^{\varepsilon,\mathsf{KL}}$ and $\Lambda_1^{\varepsilon,\mathsf{RM}}$ of these three models in the case of lateral Dirichlet conditions shows the following behavior for ε small enough, *cf* Dauge and Yosibash, 2002:

$$\Lambda_1^{\varepsilon,\mathsf{RM}} < \Lambda_1^{\varepsilon,\mathsf{KL}} < \Lambda_1^\varepsilon,$$

which tends to prove that RM model is not generically better than KL for (very) thin plates. Nevertheless an estimate by the same asymptotic bound as in (46) is valid for $\mathbf{u}^\varepsilon - \mathbf{C}\mathbf{u}^{\varepsilon,\mathsf{RM}}$.

Encyclopedia of Computational Mechanics. Edited by Erwin Stein, René de Borst and Thomas J.R. Hughes.

3.4. Higher order models

The RM model is a (1,1,0) model with reduced elastic energy. For any $\mathbf{q} = (q_\tau, q_\tau, q_3)$ we define the space $V^{\mathbf{q}}$ by (compare with (38) for monomial director functions)

$$V^{\mathbf{q}}(\Omega^\varepsilon) = \Big\{ \mathbf{u} \in V(\Omega^\varepsilon), \quad \exists \mathbf{z}_\tau^n \in H_0^1(S)^2,\ 0 \le n \le q_\tau, \ \ \exists \mathsf{z}_3^n \in H_0^1(S),\ 0 \le n \le q_3 \\ \mathbf{u}_\tau = \sum_{n=0}^{q_\tau} \mathsf{x}_3^n\, \mathbf{z}_\tau^n(\mathbf{x}_\tau) \quad \text{and} \quad \mathsf{u}_3 = \sum_{n=0}^{q_3} \mathsf{x}_3^n\, \mathsf{z}_3^n(\mathbf{x}_\tau) \Big\}. \tag{48}$$

The subspaces $V_{\mathsf{b}}^{\mathbf{q}}$ and $V_{\mathsf{m}}^{\mathbf{q}}$ of bending and membrane displacements in $V^{\mathbf{q}}$ can also be used, according to the nature of the data. The standard 3D elastic energy (2) is used with $V^{\mathbf{q}}$ and $V_{\mathsf{b}}^{\mathbf{q}}$ for any $\mathbf{q} \succeq (1,1,2)$ and with $V_{\mathsf{m}}^{\mathbf{q}}$ for any $\mathbf{q} \succeq (0,0,1)$.

Theorem 3.2. (i) *If* $\mathbf{f}$ *satisfies* $\mathsf{f}_3\big|_S \not\equiv 0$*, for any* $\mathbf{q} \succeq (1,1,2)$ *there exists* $C_{\mathbf{q}} = C_{\mathbf{q}}(\mathbf{f}) > 0$ *such that for all* $\varepsilon \in (0, \varepsilon_0)$

$$\|\mathbf{u}^\varepsilon - \mathbf{u}^{\varepsilon,\mathbf{q}}\|_{E(\Omega^\varepsilon)} \le C_{\mathbf{q}} \sqrt{\varepsilon}\, \|\mathbf{u}^\varepsilon\|_{E(\Omega^\varepsilon)}. \tag{49}$$

(ii) *If* $\mathbf{f}$ *is membrane and* $\mathbf{f}_\tau\big|_S \not\equiv 0$*, for any* $\mathbf{q} \succeq (0,0,1)$ *there exists* $C_{\mathbf{q}} = C_{\mathbf{q}}(\mathbf{f}) > 0$ *such that for all* $\varepsilon \in (0, \varepsilon_0)$ (49) *holds.*

PROOF. Since the energy is not altered by the model, $\mathbf{u}^{\varepsilon,\mathbf{q}}$ is a Galerkin projection of $\mathbf{u}^\varepsilon$ on $V^{\mathbf{q}}(\Omega^\varepsilon)$. Since the strain energy is uniformly equivalent to the elastic energy on any Ω^ε, we have by Céa's lemma that there exists $C > 0$

$$\|\mathbf{u}^\varepsilon - \mathbf{u}^{\varepsilon,\mathbf{q}}\|_{E(\Omega^\varepsilon)} \le C \|\mathbf{u}^\varepsilon - \mathbf{v}^{\mathbf{q}}\|_{E(\Omega^\varepsilon)} \quad \forall \mathbf{v}^{\mathbf{q}} \in V^{\mathbf{q}}(\Omega^\varepsilon).$$

(i) We choose, compare with (25),

$$\mathbf{v}^{\mathbf{q}} = \varepsilon^{-2}\big(-\mathsf{x}_3 \nabla_\tau \zeta_3^{-2},\ \zeta_3^{-2} + \frac{\lambda \mathsf{x}_3^2}{2\lambda + 4\mu} \Delta_\tau \zeta_3^{-2} \big) - \frac{\varepsilon^{-2} \lambda \mathsf{x}_3^2}{2\lambda + 4\mu} \varphi(\mathsf{s}) \big(\mathbf{0}, \xi(\mathsf{R})\big)$$

with $\varphi = \Delta_\tau \zeta_3^{-2}\big|_{\partial S}$ and ξ a smooth cut-off function equal to 1 in a neighborhood of $\mathsf{R} = 0$ and 0 for $\mathsf{R} \ge 1$. Then $\mathbf{v}^{\mathbf{q}}$ satisfies the lateral boundary conditions and we can check (49) by combining Theorem 2.1 with the use of Céa's lemma.
(ii) We choose, instead:

$$\mathbf{v}^{\mathbf{q}} = \big(\boldsymbol{\zeta}_\tau^0,\ -\frac{\lambda \mathsf{x}_3}{\lambda + 2\mu} \operatorname{div} \boldsymbol{\zeta}_\tau^0\big) + \frac{\lambda \mathsf{x}_3}{\lambda + 2\mu} \varphi(\mathsf{s}) \big(\mathbf{0}, \xi(\mathsf{R})\big) \quad \text{with} \quad \varphi = \operatorname{div} \boldsymbol{\zeta}_\tau^0\big|_{\partial S}.$$

□

It is worthwhile to mention that for the $(1,1,2)$ model the shear correction factor[13]

$$\kappa_{(1,1,2)} = \frac{12 - 2\nu}{\nu^2} \left(-1 + \sqrt{1 + \frac{20\nu^2}{(12 - 2\nu)^2}} \right),$$

can be used for optimal results in respect with the error in energy norm and deflection for finite thickness plates, see Babuška *et al.*, 1991. For higher plate models, no shear correction factor is furthermore needed.

[13] When $\nu \to 0$, $\kappa_{(1,1,2)}$ tends to $\frac{5}{6}$, just like for the two shear correction factors of the RM model.

Encyclopedia of Computational Mechanics. Edited by Erwin Stein, René de Borst and Thomas J.R. Hughes.

The result in Schwab and Wright, 1995 regarding the approximability of the boundary layers by elements of $V^{\mathbf{q}}$, yields that the constant $C_{\mathbf{q}}$ in (49) should rapidly decrease when $\mathbf{q}$ increases. Nevertheless the factor $\sqrt{\varepsilon}$ is still present, for any $\mathbf{q}$, because of the presence of the boundary layer terms. The numerical experiments in Dauge and Yosibash, 2000 demonstrate that the higher the degree of the hierarchical model, the better the boundary layer terms are approximated.

If one wants to have an approximation at a higher order in ε one should

either consider a problem without boundary layer, as mentioned in requirement (c) (36), i.e. a rectangular plate with symmetry boundary conditions: In this case, the convergence rate $\gamma(\mathbf{q})$ in ε is at least $\min_j q_j - 1$,

or combine a hierarchy of models with a three-dimensional discretization of the boundary layer, see Stein and Ohnimus, 1997; Dauge and Schwab, 2002.

The $(1,1,2)$ is the lowest order model which is asymptotically consistent for bending. See Paumier and Raoult, 1997; Rössle *et al.*, 1999. It is the first model in the bending model hierarchy

$$(1,1,2), \quad (3,3,2), \quad (3,3,4), \ldots \quad (2n-1,2n-1,2n), \quad (2n+1,2n+1,2n), \ldots$$

The exponent $\gamma(\mathbf{q})$ in (36) can be proved to be $2n-1$ if $\mathbf{q} = (2n-1,2n-1,2n)$ and $2n$ if $\mathbf{q} = (2n+1,2n+1,2n)$, thanks to the structure of the operator series $\mathbf{V}[\varepsilon]$ and $\mathbf{Q}[\varepsilon]$ in (11). If the load $\mathbf{f}$ is constant over the whole plate, then the model of degree $(3,3,4)$ captures the *whole* regular part of $\mathbf{u}^\varepsilon$, Dauge and Schwab, 2002, Rem.8.3, and if, moreover $\mathbf{f} \equiv 0$ (in this case only a lateral boundary condition is imposed), the degree $(3,3,2)$ is sufficient.

3.5. Laminated plates

If the plate is laminated, the material matrix $A = A^\varepsilon$ has a sandwich structure, depending on the thickness variable x_3: We assume that $A^\varepsilon(\mathsf{x}_3) = \mathbb{A}(\mathsf{X}_3)$, where the coefficients of $\mathbb{A}$ are piecewise constant. In Nazarov, 2000a the asymptotic analysis is started, including such a situation. We may presume that a full asymptotic expansion like (6) with a similar internal structure, is still valid.

In the homogeneous case, the director functions in (38) are simply the monomials of increasing degrees, see (48). In the laminated case, the first director functions are still 1 and x_3:

$$\Phi_1^0 = \Phi_2^0 = \Phi_3^0 = 1; \quad \Phi_1^1 = \Phi_2^1 = \mathsf{x}_3.$$

In the homogeneous case, we have $\Phi_3^1 = \mathsf{x}_3$ and $\Phi_j^2 = \mathsf{x}_3^2$, $j = 1,2,3$. In Actis *et al.*, 1999 three more piecewise linear director functions and three piecewise quadratic director functions are exhibited for the laminated case.

How many independent director functions are necessary to increase the convergence rate $\gamma(\mathbf{q})$ (36)? In other words, what is the dimension of the spaces $\Psi_j^{q_j}$, *cf* (37)? In our formalism, see (10)-(11), this question is equivalent to knowing the structure of the operators $\mathbf{V}^j$. Comparing with Nazarov, 2000a, we can expect that

$$\begin{aligned}
\mathbf{V}^1\boldsymbol{\zeta} &= \Big(-\mathsf{X}_3\nabla_\tau\zeta_3,\ P_3^{1,1}(\mathsf{X}_3)\partial_1\zeta_1 + P_3^{1,2}(\mathsf{X}_3)(\partial_1\zeta_2+\partial_2\zeta_1) + P_3^{1,3}(\mathsf{X}_3)\partial_2\zeta_2 \Big) \\
\mathbf{V}^2\boldsymbol{\zeta} &= \Big(\sum_{k=1}^{3} P_j^{2,k,1}(\mathsf{X}_3)\partial_1^2\zeta_k + P_j^{2,k,2}(\mathsf{X}_3)\partial_{12}^2\zeta_k + P_j^{2,k,3}(\mathsf{X}_3)\partial_2^2\zeta_k \Big)_{j=1,2,3}.
\end{aligned} \tag{50}$$

As soon as the above functions $P_j^{n,*}$ are *independent*, they should be present in the bases of the director space Ψ_j^n. The dimensions of the spaces generated by the $P_j^{n,*}$ have upper bounds depending only on n. But their actual dimensions depend on the number of plies and their nature.

Encyclopedia of Computational Mechanics. Edited by Erwin Stein, René de Borst and Thomas J.R. Hughes.

4. MULTI-SCALE EXPANSIONS AND LIMITING MODELS FOR SHELLS

Up to now, the only available results concerning multi-scale expansions for "true" shells concern the case of clamped elliptic shells investigated in Faou (2001a, 2001b, 2003). For (physical) shallow shells, which are closer to plates than shells, multi-scale expansions can also be proved, see Nazarov, 2000a; Andreoiu and Faou, 2001.

In this section, we describe the results for clamped elliptic shells, then present the main features of the classification of shells as flexural and membrane. As a matter of fact, multi-scale expansions are known for the most extreme representatives of the two types: *(i)* plates for flexural shells, *(ii)* clamped elliptic shells for membrane shells. Nevertheless, multi-scale expansions in the general case seem out of reach (or, in certain cases, even irrelevant).

4.1. Curvature of a mid-surface and other important tensors

We introduce minimal geometric tools, namely the *metric* and *curvature tensors* of the mid-surface S, the *change of metric tensor* $\gamma_{\alpha\beta}$ and the *change of curvature tensor* $\rho_{\alpha\beta}$. We also address the essential notions of *elliptic*, *hyperbolic* or *parabolic* point in a surface. We make these notions more explicit for *axisymmetric surfaces*. A general introduction to differential geometry on surfaces can be found in Stoker, 1969.

Let us denote by $\langle X, Y\rangle_{\mathbb{R}^3}$ the standard scalar product of two vectors X and Y in $\mathbb{R}^3$. Using the fact that the mid-surface S is embedded in $\mathbb{R}^3$, we naturally define the *metric tensor* $(a_{\alpha\beta})$ as the projection on S of the standard scalar product in $\mathbb{R}^3$: Let $\mathbf{p}_\top$ be a point of S and X, Y two tangent vectors to S in $\mathbf{p}_\top$. In a coordinate system $\mathbf{x}_\top = (\mathsf{x}_\alpha)$ on S, the components of X and Y are (X^α) and (Y^α), respectively. Then the matrix $\big(a_{\alpha\beta}(\mathbf{x}_\top)\big)$ is the only positive definite symmetric 2×2 matrix such that for all such vectors X and Y

$$\big\langle X, Y\big\rangle_{\mathbb{R}^3} = a_{\alpha\beta}(\mathbf{x}_\top)X^\alpha Y^\beta =: \big\langle X, Y\big\rangle_S.$$

The inverse of $a_{\alpha\beta}$ is written $a^{\alpha\beta}$ and thus satisfies $a^{\alpha\beta}a_{\beta\sigma} = \delta^\alpha_\sigma$ where δ^α_σ is the Kronecker symbol and where we used the repeated indices convention for the contraction of tensors.

The *covariant derivative* D is associated with the metric $a_{\alpha\beta}$ as follows: It is the unique differential operator such that $\mathsf{D}\langle X, Y\rangle_S = \langle \mathsf{D}X, Y\rangle_S + \langle X, \mathsf{D}Y\rangle_S$ for all vector fields X and Y. In a local coordinate system, we have

$$\mathsf{D}_\alpha = \partial_\alpha + \text{terms of order } 0$$

where ∂_α is the derivative with respect to the coordinate x_α. The terms of order 0 do depend on the choice of the coordinate system and on the type of the tensor field on which D is applied. They involve the *Christoffel symbols* of S in the coordinate system (x_α).

The *principal curvatures* at a given point $\mathbf{p}_\top \in S$ can be seen as follows: We consider the family $\mathcal{P}$ of planes P containing $\mathbf{p}_\top$ and orthogonal to the tangent plane to S at $\mathbf{p}_\top$. For $P \in \mathcal{P}$, $P \cap S$ defines a curve in P and we denote by κ its signed curvature κ. The sign of κ is determined by the orientation of S. The *principal curvatures* κ_1 and κ_2 are the minimum and maximum of κ when $P \in \mathcal{P}$. The *principal radii of curvature* are $R_i := |\kappa_i|^{-1}$. The *Gaussian curvature* of S in $\mathbf{p}_\top$ is $K(\mathbf{p}_\top) = \kappa_1\kappa_2$.

A point $\mathbf{p}_\top$ is said *elliptic* if $K(\mathbf{p}_\top) > 0$, *hyperbolic* if $K(\mathbf{p}_\top) < 0$, *parabolic* if $K(\mathbf{p}_\top) = 0$ but κ_1 or κ_2 is non zero, and *planar* if $\kappa_1 = \kappa_2 = 0$. An *elliptic shell* is a shell whose mid-surface is everywhere elliptic up to the boundary (similar definitions hold for hyperbolic and parabolic shells... and planar shells which are plates).

Encyclopedia of Computational Mechanics. Edited by Erwin Stein, René de Borst and Thomas J.R. Hughes.

The curvature tensor is defined as follows: Let $\Psi : \mathbf{x}_\tau \mapsto \Psi(\mathbf{x}_\tau)$ be a parametrization of S in a neighborhood of a given point $\mathbf{p}_\tau \in S$ and $\mathbf{n}(\Psi(\mathbf{x}_\tau))$ be the normal to S in $\Psi(\mathbf{x}_\tau)$. The formula

$$b_{\alpha\beta} := \left\langle \mathbf{n}(\Psi(\mathbf{x}_\tau)) \, , \frac{\partial \Psi}{\partial \mathsf{x}_\alpha \partial \mathsf{x}_\beta}(\mathbf{x}_\tau) \right\rangle_{\mathbb{R}^3}$$

defines, in the coordinate system $\mathbf{x}_\tau = (\mathsf{x}_\alpha)$, the components of a covariant tensor field on S, which is called the *curvature tensor*.

The metric tensor yields diffeomorphisms between tensor spaces of different types (covariant and contravariant): We have for example $b_\alpha^\beta = a^{\alpha\sigma} b_{\sigma\beta}$. With these notations, we can show that in any coordinate system, the eigenvalues of b_β^α at a point $\mathbf{p}_\tau$ are the principal curvatures at $\mathbf{p}_\tau$.

In the special case where S is an axisymmetric surface parametrized by

$$\Psi : (\mathsf{x}_1, \mathsf{x}_2) \mapsto (\mathsf{x}_1 \cos \mathsf{x}_2, \mathsf{x}_1 \sin \mathsf{x}_2, f(\mathsf{x}_1)) \in \mathbb{R}^3, \tag{51}$$

where $\mathsf{x}_1 \geq 0$ is the distance to the axis of symmetry, $\mathsf{x}_2 \in [0, 2\pi[$ is the angle around the axis, and $f : \mathbb{R} \mapsto \mathbb{R}$ a smooth function, we compute directly that

$$(b_\beta^\alpha) = \frac{1}{\sqrt{1 + f'(\mathsf{x}_1)^2}} \begin{pmatrix} \frac{f''(\mathsf{x}_1)}{1+f'(\mathsf{x}_1)^2} & 0 \\ 0 & \frac{f'(\mathsf{x}_1)}{\mathsf{x}_1} \end{pmatrix}, \quad \text{whence} \quad K = \frac{f'(\mathsf{x}_1) f''(\mathsf{x}_1)}{\mathsf{x}_1 (1 + f'(\mathsf{x}_1)^2)^2}.$$

A *deformation pattern* is a three-component field $\boldsymbol{\zeta} = (\zeta_\alpha, \zeta_3)$ where ζ_α is a surface displacement on S and ζ_3 a function on S. The *change of metric tensor* $\gamma_{\alpha\beta}(\boldsymbol{\zeta})$ associated with the deformation pattern $\boldsymbol{\zeta}$ has the following expression:

$$\gamma_{\alpha\beta}(\boldsymbol{\zeta}) = \frac{1}{2}(\mathsf{D}_\alpha \zeta_\beta + \mathsf{D}_\beta \zeta_\alpha) - b_{\alpha\beta}\zeta_3. \tag{52}$$

The *change of curvature tensor* associated with $\boldsymbol{\zeta}$ writes

$$\rho_{\alpha\beta}(\boldsymbol{\zeta}) = \mathsf{D}_\alpha \mathsf{D}_\beta \zeta_3 - b_\alpha^\sigma b_{\sigma\beta}\zeta_3 + b_\alpha^\sigma \mathsf{D}_\beta \zeta_\sigma + \mathsf{D}_\alpha b_\beta^\sigma \zeta_\sigma. \tag{53}$$

4.2. Clamped elliptic shells

The generic member Ω^ε of our family of shells is defined as

$$S \times (-\varepsilon, \varepsilon) \ni (\mathbf{p}_\tau, \mathsf{x}_3) \longrightarrow \mathbf{p}_\tau + \mathsf{x}_3 \, \mathbf{n}(\mathbf{p}_\tau) \in \Omega^\varepsilon \subset \mathbb{R}^3, \tag{54}$$

where $\mathbf{n}(\mathbf{p}_\tau)$ is the normal to S at $\mathbf{p}_\tau$. Now three stretched variables are required (*cf* §2.1 for plates):

$$\mathsf{X}_3 = \frac{\mathsf{x}_3}{\varepsilon}, \quad \mathsf{R} = \frac{\mathsf{r}}{\varepsilon} \quad \text{and} \quad \mathsf{T} = \frac{\mathsf{r}}{\sqrt{\varepsilon}},$$

where (r, s) is a system of normal and tangential coordinates to ∂S in S.

4.2.1. Three-dimensional expansion. The solutions of the family of problems (3) have a three-scale asymptotic expansion in powers of $\varepsilon^{1/2}$, with regular terms $\mathbf{v}^{k/2}$, boundary layer terms $\mathbf{w}^{k/2}$ of scale ε like for plates, and new boundary layer terms $\boldsymbol{\varphi}^{k/2}$ of scale $\varepsilon^{1/2}$.

Theorem 4.1. *[Faou, 2003] For the solutions of problems* (3)*, there exist regular terms* $\mathbf{v}^{k/2}(\mathbf{x}_\tau, \mathsf{X}_3)$*,* $k \geq 0$*, boundary layer terms* $\boldsymbol{\varphi}^{k/2}(\mathsf{T}, \mathsf{s}, \mathsf{X}_3)$*,* $k \geq 0$ *and* $\mathbf{w}^{k/2}(\mathsf{R}, \mathsf{s}, \mathsf{X}_3)$*,* $k \geq 2$*, such that*

$$\mathbf{u}^\varepsilon \simeq (\mathbf{v}^0 + \chi\boldsymbol{\varphi}^0) + \varepsilon^{1/2}(\mathbf{v}^{1/2} + \chi\boldsymbol{\varphi}^{1/2}) + \varepsilon(\mathbf{v}^1 + \chi\boldsymbol{\varphi}^1 + \chi\mathbf{w}^1) + \ldots \tag{55}$$

Encyclopedia of Computational Mechanics. Edited by Erwin Stein, René de Borst and Thomas J.R. Hughes.

in the sense of asymptotic expansions: There holds the following estimates

$$\|\mathbf{u}^\varepsilon - \sum_{k=0}^{2K} \varepsilon^{k/2}(\mathbf{v}^{k/2} + \chi\boldsymbol{\varphi}^{k/2} + \chi\mathbf{w}^{k/2})\|_{E(\Omega^\varepsilon)} \leq C_K(\mathbf{f})\,\varepsilon^{K+1/2}, \quad K = 0, 1, \ldots,$$

where we have set $\mathbf{w}^0 = \mathbf{w}^{1/2} = 0$ *and the constant* $C_K(\mathbf{f})$ *is independent of* $\varepsilon \in (0, \varepsilon_0]$.

Like for plates, the terms of the expansion are linked with each other, and are generated by a series of deformation patterns $\boldsymbol{\zeta}^{k/2} = \boldsymbol{\zeta}^{k/2}(\mathsf{x}_\tau)$ of the mid-surface S. They solve a recursive system of equations which can be written in a condensed form as an equality between formal series, like for plates. The distinction from plates is that, now, half-integer powers of ε are involved and we write e.g. $\boldsymbol{\zeta}[\varepsilon^{1/2}]$ for the formal series $\sum_k \varepsilon^{k/2}\boldsymbol{\zeta}^{k/2}$.

4.2.2. Regular terms. The regular terms series $\mathbf{v}[\varepsilon^{1/2}] = \sum_k \varepsilon^{k/2}\mathbf{v}^{k/2}$ is determined by an equation similar to (10):

$$\mathbf{v}[\varepsilon^{1/2}] = \mathbf{V}[\varepsilon^{1/2}]\boldsymbol{\zeta}[\varepsilon^{1/2}] + \mathbf{Q}[\varepsilon^{1/2}]\mathbf{f}[\varepsilon^{1/2}].$$

(i) The formal series of deformation patterns $\boldsymbol{\zeta}[\varepsilon^{1/2}]$ starts with $k = 0$ (instead of degree -2 for plates).
(ii) The first terms of the series $\mathbf{V}[\varepsilon]$ are

$$\mathbf{V}^0\boldsymbol{\zeta} = \boldsymbol{\zeta}, \quad \mathbf{V}^{1/2} \equiv 0, \quad \mathbf{V}^1\boldsymbol{\zeta} = (-\mathsf{X}_3(\mathsf{D}_\alpha\zeta_3 + 2b_\alpha^\beta\zeta_\beta),\ P^1_{\mathsf{m}}(\mathsf{X}_3)\gamma_\alpha^\alpha(\boldsymbol{\zeta})), \tag{56}$$

where P^1_{m} is the polynomial defined in (9), and the tensors D (covariant derivative) b (curvature) and γ (change of metric) are introduced in §4.1: Even if the displacement $\mathbf{V}^1\boldsymbol{\zeta}$ is given through its components in a local coordinate system, it indeed defines an *intrinsic displacement*, since D_α, b_β^α and γ_β^α are well defined independently of the choice of a local parametrization of the surface. Note that $\gamma_\alpha^\alpha(\boldsymbol{\zeta})$ in (56) degenerates to $\operatorname{div}\boldsymbol{\zeta}_\tau$ in the case of plates where $b_{\alpha\beta} = 0$. More generally, for all integer $k \geq 0$, all "odd" terms $\mathbf{V}^{k+1/2}$ are zero and, if $b \equiv 0$, all even terms $\mathbf{V}^k$ degenerate to the operators in (11). In particular, their degrees are the same as in (11).

(iii) The formal series $\mathbf{Q}[\varepsilon^{1/2}]$ appears as a generalization of (13) and $\mathbf{f}[\varepsilon^{1/2}]$ is the formal Taylor expansion of $\mathbf{f}$ around the mid-surface $\mathsf{x}_3 = 0$, which means that for all integer $k \geq 0$, $\mathbf{f}^{k+1/2} \equiv 0$ and $\mathbf{f}^k$ is given by (12).

4.2.3. Membrane deformation patterns. The first term $\boldsymbol{\zeta}^0$ solves the membrane equation

$$\boldsymbol{\zeta}^0 \in H^1_0 \times H^1_0 \times L^2(S), \quad \forall\,\boldsymbol{\zeta}' \in H^1_0 \times H^1_0 \times L^2(S), \quad a_{S,\mathsf{m}}(\boldsymbol{\zeta}^0, \boldsymbol{\zeta}') = 2\int_S \boldsymbol{\zeta}' \cdot \mathbf{f}^0, \tag{57}$$

where $\mathbf{f}^0 = \mathbf{f}|_S$ and $a_{S,\mathsf{m}}$ is the *membrane form*

$$a_{S,\mathsf{m}}(\boldsymbol{\zeta}, \boldsymbol{\zeta}') = 2\int_S \widetilde{A}^{\alpha\beta\sigma\delta}\gamma_{\alpha\beta}(\boldsymbol{\zeta})\gamma_{\sigma\delta}(\boldsymbol{\zeta}')\,\mathrm{d}S, \tag{58}$$

with the reduced energy material tensor on the mid-surface (with $\widetilde{\lambda}$ still given by (17)):

$$\widetilde{A}^{\alpha\beta\sigma\delta} = \widetilde{\lambda}a^{\alpha\beta}a^{\sigma\delta} + \mu(a^{\alpha\sigma}a^{\beta\delta} + a^{\alpha\delta}a^{\beta\sigma}).$$

Problem (57) can be equivalently formulated as $\mathbf{L}^0\boldsymbol{\zeta}^0 = \mathbf{f}^0$ with Dirichlet boundary conditions $\boldsymbol{\zeta}^0_\tau = 0$ on ∂S and is corresponding to the membrane equations on plates (compare with (19) and (22)). The

operator $\mathbf{L}^0$ is called *membrane operator* and, thus, the change of metric $\gamma_{\alpha\beta}(\boldsymbol{\zeta})$ with respect to the deformation pattern $\boldsymbol{\zeta}$ appears to coincide with the *membrane strain tensor* (see Naghdi, 1963; Koiter, 1970a). If $b \equiv 0$ the third component of $\mathbf{L}^0\boldsymbol{\zeta}$ vanishes while the surface part degenerates to the membrane operator (20). In the general case, the properties of $\mathbf{L}^0$ depends on the geometry of S: $\mathbf{L}^0$ is elliptic[(14)] in $\mathbf{x}$ if and only if S is elliptic in $\mathbf{x}$, see Ciarlet, 2000; Genevey, 1996; Sanchez-Hubert and Sanchez-Palencia, 1997.

As in (21), the formal series $\boldsymbol{\zeta}[\varepsilon^{1/2}]$ solves a reduced equation on the mid-surface with formal series $\mathbf{L}[\varepsilon^{1/2}]$, $\mathbf{R}[\varepsilon^{1/2}]$, $\mathbf{f}[\varepsilon^{1/2}]$ and $\mathbf{d}[\varepsilon^{1/2}]$, degenerating to the formal series (21) in the case of plates.

4.2.4. Boundary layer terms. Problem (57) cannot solve for the boundary conditions $\zeta_3^0|_{\partial S} = \partial_{\mathbf{n}}\zeta_3^0|_{\partial S} = 0$ (see the first terms in (24)). The two-dimensional boundary layer terms $\boldsymbol{\varphi}^{k/2}$ compensate these non-zero traces: We have for $k = 0$.

$$\boldsymbol{\varphi}^0 = (\mathbf{0}, \varphi_3^0(\mathsf{T}, \mathsf{s})) \quad \text{with} \quad \varphi_3^0(0, \mathsf{s}) = -\zeta_3^0|_{\partial S} \quad \text{and} \quad \partial_{\mathbf{n}}\varphi_3^0(0, \mathsf{s}) = 0.$$

For $k = 1$, the trace $\partial_{\mathbf{n}}\zeta_3^0|_{\partial S}$ is compensated by $\varphi_3^{1/2}$: The scale $\varepsilon^{1/2}$ arises from these surface boundary layer terms. More generally, the terms $\boldsymbol{\varphi}^{k/2}$ are polynomials of degree $[k/2]$ in X_3 and satisfy

$$|e^{\eta\mathsf{T}}\boldsymbol{\varphi}(\mathsf{T}, \mathsf{s}, \mathsf{X}_3)| \quad \text{bounded as} \quad \mathsf{T} \to \infty$$

for all $\eta < (3\mu(\widetilde{\lambda} + \mu))^{1/4}(\widetilde{\lambda} + 2\mu)^{-1/2} b_{\mathsf{ss}}(0, \mathsf{s})^{1/2}$ where $b_{\mathsf{ss}}(0, \mathsf{s}) > 0$ is the tangential component of the curvature tensor along ∂S.

The three-dimensional boundary layer terms $\mathbf{w}^{k/2}$ have a structure similar to the case of plates. The first non-zero term is $\mathbf{w}^1$.

4.2.5. The Koiter model. Koiter, 1960 proposed the solution $\mathbf{z}^\varepsilon$ of following surface problem

$$\textit{Find } \mathbf{z}^\varepsilon \in V_{\mathsf{K}}(S) \textit{ such that } \quad \varepsilon a_{S,\mathsf{m}}(\mathbf{z}^\varepsilon, \mathbf{z}') + \varepsilon^3 a_{S,\mathsf{b}}(\mathbf{z}^\varepsilon, \mathbf{z}') = 2\varepsilon \int_S \mathbf{z}' \cdot \mathbf{f}^0, \ \ \forall\, \mathbf{z}' \in V_{\mathsf{K}}(S) \tag{59}$$

to be a good candidate for approximating the three-dimensional displacement by a two-dimensional one. Here the variational space is

$$V_{\mathsf{K}}(S) := H_0^1 \times H_0^1 \times H_0^2(S) \tag{60}$$

and the bilinear form $a_{S,\mathsf{b}}$ is the *bending form*:

$$a_{S,\mathsf{b}}(\mathbf{z}, \mathbf{z}') = \frac{2}{3} \int_S \widetilde{A}^{\alpha\beta\sigma\delta} \rho_{\alpha\beta}(\mathbf{z}) \rho_{\sigma\delta}(\mathbf{z}') \, \mathrm{d}S. \tag{61}$$

Note that the operator underlying problem (59) has the form $\mathbf{K}(\varepsilon) = \varepsilon\mathbf{L}^0 + \varepsilon^3\mathbf{B}$ where the membrane operator $\mathbf{L}^0$ is the same as in (57) and the *bending* operator $\mathbf{B}$ is associated with $a_{S,\mathsf{b}}$. Thus the change of curvature tensor $\rho_{\alpha\beta}$ appears to be identified with the *bending strain tensor*. Note that $\mathbf{K}(\varepsilon)$ is associated with the two-dimensional energy, compare with (44)

$$2\varepsilon \int_S \widetilde{A}^{\alpha\beta\sigma\delta} \gamma_{\alpha\beta}(\mathbf{z}) \gamma_{\sigma\delta}(\mathbf{z}) \, \mathrm{d}S + \frac{2\varepsilon^3}{3} \int_S \widetilde{A}^{\alpha\beta\sigma\delta} \rho_{\alpha\beta}(\mathbf{z}) \rho_{\sigma\delta}(\mathbf{z}) \, \mathrm{d}S. \tag{62}$$

[14] Of multi-degree $(2, 2, 0)$ in the sense of Agmon *et al.*, 1964.

Encyclopedia of Computational Mechanics. Edited by Erwin Stein, René de Borst and Thomas J.R. Hughes.

For ε small enough, the operator $\mathsf{K}(\varepsilon)$ is elliptic of multi-degree $(2,2,4)$ and is associated with the Dirichlet conditions $\mathsf{z}=0$ and $\partial_{\mathsf{n}}\mathsf{z}_3=0$ on ∂S. The solution z^ε of the Koiter model for the clamped case solves equivalently the equations

$$(\mathsf{L}^0+\varepsilon^2\mathsf{B})\mathsf{z}^\varepsilon(\mathsf{x}_\tau)=\mathsf{f}^0(\mathsf{x}_\tau)\ \text{ on }\ S\quad\text{and}\quad \mathsf{z}^\varepsilon|_{\partial S}=\mathbf{0},\ \partial_{\mathsf{n}}\mathsf{z}_3^\varepsilon|_{\partial S}=0. \tag{63}$$

This solution has also a multi-scale expansion given by the following theorem.

Theorem 4.2. *[Faou, 2003] For the solutions of problem* (63)*, $\varepsilon\in(0,\varepsilon_0]$, there exist regular terms $\mathsf{z}^{k/2}(\mathsf{x}_\tau)$ and boundary layer terms $\boldsymbol{\psi}^{k/2}(\mathsf{T},\mathsf{s})$, $k\geq 0$, such that*

$$\mathsf{z}^\varepsilon\simeq\mathsf{z}^0+\chi\boldsymbol{\psi}^0+\varepsilon^{1/2}(\mathsf{z}^{1/2}+\chi\boldsymbol{\psi}^{1/2})+\varepsilon^1(\mathsf{z}^1+\chi\boldsymbol{\psi}^1)+\dots \tag{64}$$

in the sense of asymptotic expansions: The following estimates hold

$$\|\mathsf{z}^\varepsilon-\sum_{k=0}^{2K}\varepsilon^{k/2}(\mathsf{z}^{k/2}+\chi\boldsymbol{\psi}^{k/2})\|_{\varepsilon,S}\leq C_K(\mathbf{f})\,\varepsilon^{K+1/4},\quad K=0,1,\dots,$$

where $\|\mathsf{z}\|^2_{\varepsilon,S}=\|\boldsymbol{\gamma}(\mathsf{z})\|^2_{L^2(S)}+\varepsilon^2\|\boldsymbol{\rho}(\mathsf{z})\|^2_{L^2(S)}$ and $C_K(\mathbf{f})$ is independent of $\varepsilon\in(0,\varepsilon_0]$.

The precise comparison between the terms in the expansions (55) and (64) shows that[15] $\boldsymbol{\zeta}^0=\mathsf{z}^0$, $\boldsymbol{\zeta}^{1/2}=\mathsf{z}^{1/2}$, $\boldsymbol{\varphi}^0=\boldsymbol{\psi}^0$, $\boldsymbol{\varphi}_\tau^{1/2}=\boldsymbol{\psi}_\tau^{1/2}$, while $\boldsymbol{\zeta}^1$ and z^1, $\varphi_3^{1/2}$ and $\psi_3^{1/2}$ are generically different, respectively. This allows to obtain optimal estimates in various norms: Considering the scaled domain $\Omega\simeq S\times(-1,1)$, we have

$$\|\mathbf{u}^\varepsilon-\mathsf{z}^\varepsilon\|_{H^1\times H^1\times L^2(\Omega)}\leq\|\mathbf{u}^\varepsilon-\boldsymbol{\zeta}^0\|_{H^1\times H^1\times L^2(\Omega)}+\|\mathsf{z}^\varepsilon-\boldsymbol{\zeta}^0\|_{H^1\times H^1\times L^2(\Omega)}\leq C\varepsilon^{1/4}. \tag{65}$$

This estimate implies the convergence result of Ciarlet and Lods, 1996a and improves the estimate in Mardare, 1998. To obtain an estimate in the energy norm, we need to reconstruct a 3D displacement from z^ε : First, the Kirchhoff-like[16] displacement associated with z^ε writes, *cf* (56)

$$\mathsf{U}^{1,1,0}_{\mathsf{KL}}\mathsf{z}^\varepsilon=\big(\mathsf{z}^\varepsilon_\alpha-\mathsf{x}_3(\mathsf{D}_\alpha\mathsf{z}^\varepsilon_3+2b^\sigma_\alpha\mathsf{z}^\varepsilon_\sigma),\mathsf{z}^\varepsilon_3\big) \tag{66}$$

and next, according to Koiter, 1970a, we define the reconstructed quadratic displacement[17]:

$$\mathsf{U}^{1,1,2}_{\mathsf{K}}\mathsf{z}^\varepsilon=\mathsf{U}^{1,1,0}_{\mathsf{KL}}\mathsf{z}^\varepsilon+\frac{\lambda}{\lambda+2\mu}\left(\mathbf{0},-\mathsf{x}_3\gamma^\alpha_\alpha(\mathsf{z}^\varepsilon)+\frac{\mathsf{x}_3^2}{2}\rho^\alpha_\alpha(\mathsf{z}^\varepsilon)\right). \tag{67}$$

Then there holds (compare with (46) for plates):

$$\|\mathbf{u}^\varepsilon-\mathsf{U}^{1,1,2}_{\mathsf{K}}\mathsf{z}^\varepsilon\|_{E(\Omega^\varepsilon)}\leq C\sqrt{\varepsilon}\|\mathbf{u}^\varepsilon\|_{E(\Omega^\varepsilon)}, \tag{68}$$

and similar to plates, the error factor $\sqrt{\varepsilon}$ is optimal and is due to the first boundary layer term $\mathbf{w}^1$. Moreover expansion (64) allows to prove that the classical models discussed in Budiansky and Sanders, 1967; Naghdi, 1963; Novozhilov, 1959; Koiter, 1970a have all the same convergence rate (68).

---

[15] We have a similar situation with plates, where the solution $\mathbf{u}^{\varepsilon,\mathsf{KL}}$ of the Kirchhoff-Love model gives back the first generating terms on the asymptotics of $\mathbf{u}^\varepsilon$, *cf* Theorem 3.1.

[16] The actual Kirchhoff-Love displacement (satisfying $e_{i3}=0$) is slightly different, containing an extra quadratic surface term.

[17] The complementing operator C defined in (45) for plates satisfies $\mathsf{C}\mathsf{U}^{1,1,0}_{\mathsf{KL}}=\mathsf{U}^{1,1,2}_{\mathsf{K}}$.

Encyclopedia of Computational Mechanics. Edited by Erwin Stein, René de Borst and Thomas J.R. Hughes.

4.3. Convergence results for general shells

We still embed Ω^d in the family (54) with S the mid-surface of Ω^d. The fact that all the classical models are equivalent for clamped elliptic shells may not be true in more general cases, when the shell becomes sensitive (e.g. for a partially clamped elliptic shell with a free portion in its lateral surface) or produces bending effects (case of parabolic or hyperbolic shells with adequate lateral boundary conditions).

4.3.1. Surface membrane and bending energy. Nevertheless the Koiter model seems to keep good approximation properties with respect to the 3D model. The variational space V_{K} of the Koiter model is, in the totally clamped case[18] given by the space $V_{\mathsf{K}}(S)$ (60). As already mentioned (62), the Koiter model is associated with the bilinear form $\varepsilon a_{S,\mathsf{m}} + \varepsilon^3 a_{S,\mathsf{b}}$ with $a_{S,\mathsf{m}}$ and $a_{S,\mathsf{b}}$ the membrane and bending forms defined for $\mathbf{z}$, $\mathbf{z}' \in V_{\mathsf{K}}(S)$ by (58) and (61) respectively.

From the historical point of view, such a decomposition into a membrane (or stretching) energy and a bending energy on the mid-surface was first derived by Love, 1944 in *principal curvature coordinate systems*, i.e. for which the curvature tensor (b^α_β) is diagonalized. The expression of the membrane energy proposed by Love is the same as (61), in contrast with the bending part for which the discussion was very controversial: See Budiansky and Sanders, 1967; Novozhilov, 1959; Koiter, 1960; Naghdi, 1963 and the reference therein. Koiter, 1960 gave the most natural expression, using intrinsic tensor representations: The Koiter bending energy only depends on the change of curvature tensor $\rho_{\alpha\beta}$, in accordance with Bonnet theorem characterizing a surface by its metric and curvature tensors $a_{\alpha\beta}$ and $b_{\alpha\beta}$, see e.g. Stoker, 1969.

For any geometry of the mid-surface S, the Koiter model in its variational form (59) has a unique solution, see Bernadou and Ciarlet, 1976.

4.3.2. Classification of shells. According to that principle each shell, in the zero thickness limit, concentrates its energy either in the bending surface energy $a_{S,\mathsf{b}}$ (*flexural* shells) or in the membrane surface energy $a_{S,\mathsf{m}}$ (*membrane* shells).

The behavior of the shell depends on the *"inextensional displacement" space*

$$V_{\mathsf{F}}(S) := \big\{\boldsymbol{\zeta} \in V_{\mathsf{K}}(S) \,|\, \gamma_{\alpha\beta}(\boldsymbol{\zeta}) = 0\big\}. \tag{69}$$

The key role played by this space is illustrated by the following fundamental result:

Theorem 4.3. (i) *(Sanchez-Hubert and Sanchez-Palencia, 1997; Ciarlet et al., 1996). Let* $\mathbf{u}^\varepsilon$ *be the solution of problem* (3)*. In the scaled domain* $\Omega \simeq S \times (-1,1)$*, the displacement* $\varepsilon^2 \mathbf{u}^\varepsilon(\mathsf{x}_\top, \mathsf{X}_3)$ *converges in* $H^1(\Omega)^3$ *as* $\varepsilon \to 0$*. Its limit is given by the solution* $\boldsymbol{\zeta}^{-2} \in V_{\mathsf{F}}(S)$ *of the bending problem*

$$\forall\, \boldsymbol{\zeta}' \in V_{\mathsf{F}}(S) \quad a_{S,\mathsf{b}}(\boldsymbol{\zeta}^{-2}, \boldsymbol{\zeta}') = 2\int_S \boldsymbol{\zeta}' \cdot \mathbf{f}^0. \tag{70}$$

(ii) *(Ciarlet and Lods, 1996b) Let* $\mathbf{z}^\varepsilon$ *be the solution of problem* (59)*. Then* $\varepsilon^2 \mathbf{z}^\varepsilon$ *converges to* $\boldsymbol{\zeta}^{-2}$ *in* $V_{\mathsf{K}}(S)$ *as* $\varepsilon \to 0$*.*

A shell is said *flexural* (or *non-inhibited*) when $V_{\mathsf{F}}(S)$ is not reduced to $\{\mathbf{0}\}$. Examples are provided by cylindrical shells (or portions of cones) clamped along their generatrices and free elsewhere. Of

[18] If the shell Ω^ε is clamped only on the part $\gamma_0 \times (-\varepsilon, \varepsilon)$ of its boundary (with $\gamma_0 \subset \partial S$), the Dirichlet boundary conditions in the space V_{K} have to be imposed only on γ_0.

Encyclopedia of Computational Mechanics. Edited by Erwin Stein, René de Borst and Thomas J.R. Hughes.

course, plates are flexural shells according to the above definition since in that case $V_{\mathsf{F}}(S)$ is given by $\{\boldsymbol{\zeta} = (\mathbf{0}, \zeta_3) \,|\, \zeta_3 \in H_0^2(S)\}$ and the bending operator (70) coincides with the operator (16).

In the case of clamped elliptic shells, we have $V_{\mathsf{F}}(S) = \{\mathbf{0}\}$. For these shells $\mathbf{u}^\varepsilon$ and $\mathbf{z}^\varepsilon$ converge in $H^1 \times H^1 \times L^2$ to the solution $\boldsymbol{\zeta}^0$ of the membrane equation (57), see Ciarlet and Lods, 1996a and (65): Such shells are called *membrane shells*. The other shells for which $V_{\mathsf{F}}(S)$ reduces to $\{\mathbf{0}\}$ are called *generalized membrane shells* (or *inhibited shells*) and for these also, a delicate functional analysis provides convergence results to a membrane solution in spaces with special norms depending on the geometry of the mid-surface (see Ciarlet and Lods, 1996a and Ciarlet, 2000, Ch.5). It is also proved that the Koiter model converges in the same sense to the same limits, see Ciarlet, 2000, Ch.7.

Thus plates and elliptic shells represent extreme situations: Plates are a pure bending structures with an inextensional displacement space as large as possible while clamped elliptic shells represent a pure membrane situation where $V_{\mathsf{F}}(S)$ reduces to $\{\mathbf{0}\}$ and where the membrane operator is elliptic.

4.4. Shallow shells

We make a distinction between "physical" shallow shells in the sense of Ciarlet and Paumier, 1986 and "mathematical" shallow shells in the sense of Pitkäranta *et al.*, 2001. The former involves shells with a curvature tensor of the same order as the thickness, whereas the latter addresses a boundary value problem obtained by freezing coefficients of the Koiter problem at one point of a standard shell.

4.4.1. Physical shallow shells. Let R denote the smallest principal radius of curvature of the mid-surface S and let D denote the diameter of S. As proved in Andreoiu and Faou, 2001 if there holds

$$R \geq 2D, \tag{71}$$

then there exists a point $\mathbf{p}_\top \in S$, such that the orthogonal projection of S on its tangent plan in $\mathbf{p}_\top$ allows the representation of S as a $\mathcal{C}^\infty$ graph in $\mathbb{R}^3$:

$$\omega \ni (x_1, x_2) \mapsto \big(x_1, x_2, \Theta(x_1, x_2)\big) := \mathbf{x}_\top \in S \subset \mathbb{R}^3, \tag{72}$$

where ω is an immersed[19] domain of the tangent plane in $\mathbf{p}_\top$, and where Θ is a function on this surface. Moreover, we have

$$|\Theta| \leq CR^{-1} \quad \text{and} \quad \|\nabla\Theta\| \leq CR^{-1}, \tag{73}$$

with constants C depending only on D.

We say that Ω^d is a *shallow shell* if S satisfies a condition of the type

$$R^{-1} \leq Cd, \tag{74}$$

where C does not depend on d. Thus, if S is a surface satisfying (74), for d sufficiently small S satisfies (71) whence representation (72). Moreover (73) yields that Θ and $\nabla\Theta$ are $\lesssim d$. In these conditions, we can choose to embed Ω^d into another family of thin domains than (54): We set $\theta = d^{-1}\Theta$ and define for any $\varepsilon \in (0, d]$ the surface S^ε by its parametrization, *cf* (72)

$$\omega \ni (x_1, x_2) \mapsto \big(x_1, x_2, \varepsilon\theta(x_1, x_2)\big) := \mathbf{x}_\top \in S^\varepsilon.$$

[19] In particular ω may have self-intersection.

Encyclopedia of Computational Mechanics. Edited by Erwin Stein, René de Borst and Thomas J.R. Hughes.

It is natural to consider Ω^d as an element of the family Ω^ε given as the image of the application

$$\omega \times (-\varepsilon, \varepsilon) \ni (x_1, x_2, \mathsf{x}_3) \mapsto \big(x_1, x_2, \varepsilon\,\theta(x_1, x_2)\big) + \mathsf{x}_3\,\mathbf{n}^\varepsilon(\mathbf{x}_\top), \tag{75}$$

where $\mathbf{n}^\varepsilon(\mathbf{x}_\top)$ denotes the unit normal vector to the mid-surface S^ε. We are now in the framework of Ciarlet and Paumier, 1986.

A multi-scale expansion for the solution of (3) is given in Andreoiu and Faou, 2001. The expansion is close to that of plates, except that the membrane and bending operators yielding the deformation patterns are linked by lower order terms: The associated membrane and bending strain components $\tilde{\gamma}_{\alpha\beta}$ and $\tilde{\rho}_{\alpha\beta}$ are respectively given by

$$\tilde{\gamma}_{\alpha\beta} := \tfrac{1}{2}(\partial_\alpha \mathsf{z}_\beta + \partial_\beta \mathsf{z}_\alpha) - \varepsilon \partial_{\alpha\beta}\theta\, \mathsf{z}_3 \quad \text{and} \quad \tilde{\rho}_{\alpha\beta} := \partial_{\alpha\beta}\mathsf{z}_3. \tag{76}$$

It is worth noticing that the above strains are asymptotic approximations of the Koiter membrane and bending strains associated with the mid-surface $S = S^\varepsilon$. As a consequence, the Koiter model and the three-dimensional equations converge to the same Kirchhoff-Love limit.

4.4.2. Mathematical shallow shells. These models consist in freezing coefficients of standard two-dimensional models at a given point $\mathbf{p}_\top \in S$ in a principal curvature coordinate system. That procedure yields, with $b_i := \kappa_i(\mathbf{p}_\top)$:

$$\gamma_{11} = \partial_1 \mathsf{z}_1 - b_1 \mathsf{z}_3, \quad \gamma_{22} = \partial_2 \mathsf{z}_2 - b_2 \mathsf{z}_3, \quad \gamma_{12} = \tfrac{1}{2}(\partial_1 \mathsf{z}_2 + \partial_2 \mathsf{z}_1) \tag{77}$$

for the membrane strain tensor, and

$$\kappa_{11} = \partial_1^2 \mathsf{z}_3 + b_1 \partial_1 \mathsf{z}_1, \quad \kappa_{22} = \partial_2^2 \mathsf{z}_3 + b_2 \partial_2 \mathsf{z}_2, \quad \kappa_{12} = \partial_1 \partial_2 \mathsf{z}_3 + b_1 \partial_2 \mathsf{z}_1 + b_2 \partial_1 \mathsf{z}_2 \tag{78}$$

as a simplified version of the bending strain tensor. Such a localization procedure is considered as valid if the diameter D is small compared to R

$$R \gg D \tag{79}$$

and for the case of cylindrical shells where the strains have already the form (77)-(78) in cylindrical coordinates (see equation (80) below). In contrast with the previous one, this notion of shallowness does not refer to the thickness. Here R is not small, but D is. Such objects are definitively shells and are not plate-like.

These simplified models are valuable so to develop numerical approximation methods, Havu and Pitkäranta (2002, 2003) and to find possible boundary layer length scales, Pitkäranta *et al.*, 2001: These length scales (width of transition regions from the boundary into the interior) at a point $\mathbf{p}_\top \in \partial S$ are $\varepsilon^{1/2}$ in the non-degenerate case ($b_{\mathsf{ss}}(\mathbf{p}_\top) \neq 0$), $\varepsilon^{1/3}$ for hyperbolic degeneration ($\mathbf{p}_\top$ hyperbolic and $b_{\mathsf{ss}}(\mathbf{p}_\top) = 0$) and $\varepsilon^{1/4}$ for parabolic degeneration ($\mathbf{p}_\top$ parabolic and $b_{\mathsf{ss}}(\mathbf{p}_\top) = 0$).

To compare with the standard shell equations, note that in the case of an axisymmetric shell whose mid-surface is represented by

$$\Psi : (\mathsf{x}_1, \mathsf{x}_2) \mapsto (f(\mathsf{x}_1)\cos \mathsf{x}_2, f(\mathsf{x}_1)\sin \mathsf{x}_2, \mathsf{x}_1),$$

where $\mathsf{x}_1 \in \mathbb{R}$, $\mathsf{x}_2 \in [0, 2\pi[$ and $f(\mathsf{x}_1) > 0$ is a smooth function, we have

$$\begin{aligned}
\gamma_{11}(\mathbf{z}) &= \partial_1 \mathsf{z}_1 - \tfrac{f'(\mathsf{x}_1) f''(\mathsf{x}_1)}{1+f'(\mathsf{x}_1)^2}\, \mathsf{z}_1 + \tfrac{f''(\mathsf{x}_1)}{\sqrt{1+f'(\mathsf{x}_1)^2}}\, \mathsf{z}_3, \\
\gamma_{22}(\mathbf{z}) &= \partial_2 \mathsf{z}_2 + \tfrac{f(\mathsf{x}_1) f'(\mathsf{x}_1)}{1+f'(\mathsf{x}_1)^2}\, \mathsf{z}_1 - \tfrac{f(\mathsf{x}_1)}{\sqrt{1+f'(\mathsf{x}_1)^2}}\, \mathsf{z}_3, \\
\gamma_{12}(\mathbf{z}) &= \tfrac{1}{2}(\partial_1 \mathsf{z}_2 + \partial_2 \mathsf{z}_1) - \tfrac{f'(\mathsf{x}_1)}{f(\mathsf{x}_1)}\, \mathsf{z}_2.
\end{aligned} \tag{80}$$

Hence the equation (77) is exact for the case of cylindrical shells, where $f(\mathsf{x}_1) \equiv R > 0$, and we can show that the same holds for (78).

4.5. Versatility of Koiter model.

On any mid-surface S the deformation pattern $\mathbf{z}^\varepsilon$ solution of the Koiter model (59) exists. In general, the mean value of the displacement $\mathbf{u}^\varepsilon$ through the thickness converges to the same limit as $\mathbf{z}^\varepsilon$ when $\epsilon \to 0$ in a weak sense depending on the type of the mid-surface and the boundary conditions, see Ciarlet, 2000. Nevertheless, actual convergence results hold in energy norm when considering reconstructed displacement from the deformation pattern $\mathbf{z}^\varepsilon$.

4.5.1. Convergence of the Koiter reconstructed displacement. On any mid-surface S, the three-dimensional Koiter reconstructed displacement $\mathbf{U}_{\mathsf{K}}^{1,1,2}\mathbf{z}^\varepsilon$ is well-defined by (66)-(67). Let us set

$$\mathbf{e}(S,\varepsilon,\mathbf{z}^\varepsilon,\mathbf{u}^\varepsilon) := \frac{\|\mathbf{u}^\varepsilon - \mathbf{U}_{\mathsf{K}}^{1,1,2}\mathbf{z}^\varepsilon\|_{E(\Omega^\varepsilon)}}{\|\mathbf{z}^\varepsilon\|_{E^\varepsilon(S)}} \tag{81}$$

with $\|\mathbf{z}\|_{E^\varepsilon(S)}$ the square root of the Koiter energy (62).

In Koiter (1970a, 1970b), an estimate is given: $\mathbf{e}(S,\varepsilon,\mathbf{z}^\varepsilon,\mathbf{u}^\varepsilon)^2$ would be bounded by $\varepsilon R^{-1}+\varepsilon^2 L^{-2}$, with R the smallest principal radius of curvature of S and L the smallest wavelength of $\mathbf{z}^\varepsilon$. It turns out that in the case of plates, we have $L=\mathcal{O}(1)$, $R^{-1}=0$ and, since (46) is optimal, the estimate fails. In contrast, in the case of clamped elliptic shells, we have $L=\mathcal{O}(\sqrt{\varepsilon})$, $R^{-1}=\mathcal{O}(1)$ and the estimate gives back (68).

Two years after the publications of Koiter (1970a, 1970b), it was already known that the above estimate does not hold as $\varepsilon \to 0$ for plates. We read in Koiter and Simmonds, 1973 *"The somewhat depressing conclusion for most shell problems is, similar to the earlier conclusions of* GOL'DENWEIZER, *that no better accuracy of the solutions can be expected than of order $\varepsilon L^{-1}+\varepsilon R^{-1}$, even if the equations of first-approximation shell theory would permit, in principle, an accuracy of order $\varepsilon^2 L^{-2}+\varepsilon R^{-1}$."*

The reason for this is also explained by John, 1971 in these terms: *"Concentrating on the interior we sidestep all kinds of delicate questions, with an attendant gain in certainty and generality. The information about the interior behavior can be obtained much more cheaply (in the mathematical sense) than that required for the discussion of boundary value problems, which form a more "transcendental" stage."*.

Koiter's tentative estimate comes from formal computations also investigated by John, 1971. The analysis by operator formal series introduced in Faou, 2002 is in the same spirit: For any geometry of the mid-surface, there exist formal series $\mathbf{V}[\varepsilon]$, $\mathbf{R}[\varepsilon]$, $\mathbf{Q}[\varepsilon]$ and $\mathbf{L}[\varepsilon]$ reducing the three-dimensional formal series problem to a two-dimensional problem of the form (21) with $\mathbf{L}[\varepsilon]=\mathbf{L}^0+\varepsilon^2\mathbf{L}^2+\cdots$ where $\mathbf{L}^0$ is the membrane operator associated with the form (58). The bending operator $\mathbf{B}$ associated with $a_{S,\mathsf{b}}$ can be compared to the operator $\mathbf{L}^2$ appearing in the formal series $\mathbf{L}[\varepsilon]$: We have

$$\forall\,\boldsymbol{\zeta},\boldsymbol{\zeta}' \in V_{\mathsf{F}}(S) \quad \langle \mathbf{L}^2\boldsymbol{\zeta},\boldsymbol{\zeta}'\rangle_{L^2(S)^3} = \langle \mathbf{B}\boldsymbol{\zeta},\boldsymbol{\zeta}'\rangle_{L^2(S)^3}. \tag{82}$$

Using this formal series analysis, the first two authors are working on the derivation of a sharp expression of $\mathbf{e}(S,\varepsilon,\mathbf{z}^\varepsilon,\mathbf{u}^\varepsilon)$ including boundary layers effects, and optimal in the case of plates and clamped elliptic shells, see Dauge and Faou, 2004.

In this direction also, Lods and Mardare, 2002 prove the following estimate for totally clamped shells

$$\|\mathbf{u}^\varepsilon - (\mathbf{U}_{\mathsf{K}}^{1,1,2}\mathbf{z}^\varepsilon + \mathbf{w}^\sharp)\|_{E(\Omega^\varepsilon)} \le C\varepsilon^{1/4}\|\mathbf{u}^\varepsilon\|_{E(\Omega^\varepsilon)}, \tag{83}$$

with $\mathbf{w}^\sharp$ an explicit boundary corrector of $\mathbf{U}_{\mathsf{K}}^{1,1,2}\mathbf{z}^\varepsilon$.

Encyclopedia of Computational Mechanics. Edited by Erwin Stein, René de Borst and Thomas J.R. Hughes.

4.5.2. Convergence of Koiter eigenvalues. The operator $\varepsilon^{-1}\mathbf{K}(\varepsilon)$ has a compact inverse, therefore its spectrum is discrete with only an accumulation point at $+\infty$. We agree to call Koiter eigenvalues the eigenvalues of the former operator, i.e. the solutions μ^ε of

$$\exists\, \mathbf{z}^\varepsilon \in V_{\mathsf{K}}(S) \setminus \{0\} \text{ such that } \quad a_{S,\mathsf{m}}(\mathbf{z}^\varepsilon, \mathbf{z}') + \varepsilon^2 a_{S,\mathsf{b}}(\mathbf{z}^\varepsilon, \mathbf{z}') = 2\mu^\varepsilon \int_S \mathbf{z}^\varepsilon \cdot \mathbf{z}', \ \ \forall\, \mathbf{z}' \in V_{\mathsf{K}}(S). \quad (84)$$

As already mentioned in §2.4, *cf* (31), this spectrum provides the limiting behavior of three-dimensional eigenvalues for plates. Apparently very little is known for general shells.

Concerning Koiter eigenvalues, interesting results are provided by Sanchez-Hubert and Sanchez-Palencia, 1997, Ch.X: The μ^ε are attracted by the spectrum of the membrane operator $\mathfrak{S}(\mathbf{M})$ where $\mathbf{M}$ is the self-adjoint unbounded operator associated with the symmetric bilinear form $a_{S,\mathsf{m}}$ defined on the space $H^1 \times H^1 \times L^2(S)$. There holds (we still assume that S is smooth up to its boundary):

Theorem 4.4. *The operator $\mathbf{M} + \mu\,\mathbf{Id}$ is elliptic of multi-degree $(2,2,0)$ for $\mu > 0$ large enough. Moreover its essential spectrum $\mathfrak{S}_{\mathsf{es}}(\mathbf{M})$ satisfies:*
(i) *If S is elliptic and clamped on its whole boundary, $\mathfrak{S}_{\mathsf{es}}(\mathbf{M})$ is a closed interval $[a,b]$, with $a > 0$,*
(ii) *If S is elliptic and not clamped on its whole boundary, $\mathfrak{S}_{\mathsf{es}}(\mathbf{M}) = \{0\} \cup [a,b]$ with $a > 0$,*
(iii) *For any other type of shell (i.e. there exists at least one point where the Gaussian curvature is ≤ 0) $\mathfrak{S}_{\mathsf{es}}(\mathbf{M})$ is a closed interval of the form $[0,b]$, with $b \geq 0$.*

If the shell is of flexural type, the lowest eigenvalues μ_ε tend to 0 like $\mathcal{O}(\varepsilon^2)$, same as for plates, see (29). If the shell is clamped elliptic, the μ_ε are bounded from below by a positive constant independent of ε. In any other situation we expect that the lowest μ_ε still tends to 0 as $\varepsilon \to 0$.

5. HIERARCHICAL MODELS FOR SHELLS

The idea of deriving hierarchical models for shells goes back to Vekua (1955, 1965, 1985) and corresponds to classical techniques in mechanics: Try to find asymptotic expansions in x_3 by use of Taylor expansion around the mid surface S. An alternative approach consists in choosing the coefficients z_j^n in (38) as moments through the thickness against Legendre polynomials $L_n(\mathsf{x}_3/\varepsilon)$.

Vogelius and Babuška (1981a, 1981b, 1981c) laid the foundations of hierarchical models in view of their applications to numerical analysis (for scalar problems).

5.1. Hierarchies of semi-discrete subspaces

The concepts mentioned in Section 3 can be adapted to the case of shells. In contrast with plates for which there exist convenient *Cartesian* system of coordinates fitting with the tangential and normal directions to the mid-surface, more non-equivalent options are left open for shells. They are for example

The *direction of semi-discretization*: The intrinsic choice is of course the normal direction to the mid-surface (variable x_3), nevertheless for shells represented by a single local chart like in (72), any transverse direction could be chosen. In the sequel, we only consider semi-discretizations in the normal direction.

The presence or absence of privileged components for the displacement field in the Ansatz (38). If one privileged component is chosen, it is of course the normal one u_3 and the two other ones are $(\mathsf{u}_\alpha) = \mathbf{u}_\top$. Then the sequence of orders $\mathbf{q}$ is of the form $\mathbf{q} = (q_\top, q_\top, q_3)$, and the space

Encyclopedia of Computational Mechanics. Edited by Erwin Stein, René de Borst and Thomas J.R. Hughes.

$V^{\mathbf{q}}(\Omega^\varepsilon)$ has the form (48). Note that this space is independent of the choice of local coordinates on S. If there is no privileged component, $\mathbf{q}$ has to be of the form (q,q,q) and the space $V^{\mathbf{q}}(\Omega^\varepsilon)$ can be written

$$V^{\mathbf{q}}(\Omega^\varepsilon)=\Big\{\mathbf{u}=(u_1,u_2,u_3)\in V(\Omega^\varepsilon),\quad \exists \boldsymbol{z}^n=(z_1^n,z_2^n,z_3^n)\in H_0^1(S)^3,\ 0\le n\le q,\\ u_j=\sum_{n=0}^{q}\mathsf{x}_3^n\, z_j^n(\mathbf{x}_\tau),\quad j=1,2,3\Big\}. \tag{85}$$

Here, for ease of use we take Cartesian coordinates, but the above definition is independent of any choice of coordinates in $\Omega^\varepsilon\subset\mathbb{R}^3$. In particular, it coincides with the space (48) for $q_\tau=q_3$.

Then the requirements of approximability (34), asymptotic consistency (35) and optimality of the convergence rate (36) make sense.

5.2. Approximability

For any fixed thickness ε, the approximability issue is as in the case of plates. By Céa's lemma, there exists an adimensional constant $C>0$ depending only on the Poisson ratio ν, such that

$$\|\mathbf{u}^\varepsilon-\mathbf{u}^{\varepsilon,\mathbf{q}}\|_{E(\Omega^\varepsilon)}\le C\|\mathbf{u}^\varepsilon-\mathbf{v}^{\mathbf{q}}\|_{E(\Omega^\varepsilon)}\quad\forall\,\mathbf{v}^{\mathbf{q}}\in V^{\mathbf{q}}(\Omega^\varepsilon),$$

and the determination of approximability properties relies on the construction of a best approximation of $\mathbf{u}^\varepsilon$ by functions in $V^{\mathbf{q}}(\Omega^\varepsilon)$.

In Avalishvili and Gordeziani, 2003, approximability is proved using the density of the sequence of spaces $V^{\mathbf{q}}(\Omega^\varepsilon)$ in $H^1(\Omega^\varepsilon)^3$. But the problem of finding a rate for the convergence in (33) is more difficult, since the solution $\mathbf{u}^\varepsilon$ has singularities near the edges and, consequently, does not belong to $H^2(\Omega^\varepsilon)$ in general. For scalar problems Vogelius and Babuška (1981a, 1981b, 1981c) prove best approximation results using weighted Sobolev norms[20]. Up to now, for elasticity systems there are no such results taking the actual regularity of $\mathbf{u}^\varepsilon$ into account.

It is worth noticing that, in order to obtain an equality of the form (36), we must use Korn inequality, since most approximation results are based on Sobolev norms. But due to blow up of the Korn constant[21] when $\varepsilon\to 0$, it seems hard to obtain sharp estimates in the general case.

5.3. Asymptotic consistency

Like for plates, the presence of the non polynomial three-dimensional boundary layers $\mathbf{w}^k$ generically produces a limitation in the convergence rate in (35). As previously mentioned, the only case where a sharp estimate is available, is the case of clamped elliptic shells. Using (68), we indeed obtain the following result (compare with Theorem 3.2):

Theorem 5.1. *If the mid-surface S is elliptic, if the shell is clamped along its whole lateral boundary, and if $\mathbf{f}\big|_S\not\equiv 0$, then for any $\mathbf{q}\succeq(1,1,2)$ with definition* (48)*, and for any $\mathbf{q}\succeq(2,2,2)$ with* (85)*,*

[20] These norms are those of the domains of the fractional powers A^s of the Sturm-Liouville operator $\mathsf{A}:\zeta\mapsto\partial_x((1-x^2)\partial_x\zeta)$ on the interval $(-1,1)$. Such an approach is now a standard tool in the p-version analysis.

[21] Let us recall that it behaves as ε^{-1} in the case of partially clamped shells

Encyclopedia of Computational Mechanics. Edited by Erwin Stein, René de Borst and Thomas J.R. Hughes.

and with the use of the standard 3D elastic energy (2)*, there exists* $C_{\mathbf{q}} = C_{\mathbf{q}}(\mathbf{f}) > 0$ *such that for all* $\varepsilon \in (0, \varepsilon_0)$

$$\|\mathbf{u}^\varepsilon - \mathbf{u}^{\varepsilon,\mathbf{q}}\|_{E(\Omega^\varepsilon)} \leq C_{\mathbf{q}} \sqrt{\varepsilon}\, \|\mathbf{u}^\varepsilon\|_{E(\Omega^\varepsilon)}. \tag{86}$$

Note that in this case, the two-dimensional boundary layers are polynomial in x_3, Therefore they can be captured by the semi-discrete hierarchy of spaces $V^{\mathbf{q}}$.

Using estimate (83) of Lods and Mardare, 2002, together with the fact that the corrector term $\mathbf{w}^\sharp$ is polynomial in x_3 of degree $(0, 0, 2)$ we obtain a proof for the asymptotic consistency for *any (smooth) clamped shell* without assuming that the mid-surface is elliptic:

Theorem 5.2. *If the shell is clamped along its whole lateral boundary, and if* $\mathbf{f}\big|_S \not\equiv 0$*, then for* $\mathbf{q}$ *as in Theorem 5.1 and the standard energy* (2)*, there exists* $C_{\mathbf{q}} = C_{\mathbf{q}}(\mathbf{f}) > 0$ *such that for all* $\varepsilon \in (0, \varepsilon_0)$

$$\|\mathbf{u}^\varepsilon - \mathbf{u}^{\varepsilon,\mathbf{q}}\|_{E(\Omega^\varepsilon)} \leq C_{\mathbf{q}}\, \varepsilon^{1/4}\, \|\mathbf{u}^\varepsilon\|_{E(\Omega^\varepsilon)}. \tag{87}$$

5.4. Examples of hierarchical models

Various models of degree $(1, 1, 0)$, $(1, 1, 2)$ and $(2, 2, 2)$ are introduced and investigated in the literature. Note that the model $(1, 1, 1)$ is *strictly forbidden* for shells, because it cannot be associated with any correct energy, see Chapelle, Ferent and Bathe, 2003.

5.4.1. $(1, 1, 0)$ *models.* One of the counterparts of Reissner-Mindlin model for plates is given by the Naghdi model: see Naghdi (1963, 1972). The space of admissible displacements is

$$V^{\mathsf{N}}(\Omega^\varepsilon) = \{\mathbf{u} \in V(\Omega^\varepsilon),\ \exists \mathbf{z} \in H_0^1(S)^3,\ \exists \theta_\alpha \in H_0^1(S)^2, \quad \mathbf{u} = (\mathsf{z}_\alpha - \mathsf{x}_3(\theta_\alpha + b_\alpha^\beta \mathsf{z}_\beta),\, \mathsf{z}_3)\}. \tag{88}$$

As in (47) the energy splits into three parts (with the shear correction factor κ):

$$\begin{aligned} \widetilde{a}(\mathbf{u}, \mathbf{u}) = {} & 2\varepsilon \int_S \widetilde{A}^{\alpha\beta\sigma\delta} \gamma_{\alpha\beta}(\mathbf{z}_\top) \gamma_{\sigma\delta}(\mathbf{z}_\top)\, \mathrm{d}S && \textit{(membrane energy)} \\ & + \varepsilon\kappa \int_S \mu a^{\alpha\sigma} (\mathsf{D}_\alpha \mathsf{z}_3 + b_\alpha^\delta \mathsf{z}_\delta - \theta_\alpha)(\mathsf{D}_\sigma \mathsf{z}_3 + b_\sigma^\beta \mathsf{z}_\beta - \theta_\sigma)\, \mathrm{d}S && \textit{(shear energy)} \\ & + \frac{2\varepsilon^3}{3} \int_S \widetilde{A}^{\alpha\beta\sigma\delta} \overline{\rho}_{\alpha\beta}(\mathbf{z}, \boldsymbol{\theta}) \overline{\rho}_{\sigma\delta}(\mathbf{z}, \boldsymbol{\theta})\, \mathrm{d}S && \textit{(bending energy)}, \end{aligned} \tag{89}$$

where

$$\overline{\rho}_{\alpha\beta}(\mathbf{z}, \boldsymbol{\theta}) = \tfrac{1}{2}(\mathsf{D}_\alpha \theta_\beta + \mathsf{D}_\beta \theta_\alpha) - c_{\alpha\beta} \mathsf{z}_3 + \tfrac{1}{2} b_\alpha^\sigma \mathsf{D}_\beta z_\sigma + \tfrac{1}{2} b_\beta^\sigma \mathsf{D}_\alpha z_\sigma.$$

Note that when the penalization term in the shear energy goes to zero, we get $\theta_\sigma = \mathsf{D}_\sigma \mathsf{z}_3 + b_\sigma^\beta \mathsf{z}_\beta$ and the displacement $\mathbf{u}$ in (88) coincides with (66). In Lods and Mardare, 2002, an estimate of the error between the solution of the Naghdi model and the solution of the 3D model is provided in a sub-energetic norm.

A more recent $(1, 1, 0)$ model (called *general shell element*, see Chapelle and Bathe, 2000) consists of the reduced energy projection on the space $V^{(1,1,0)}(\Omega^\varepsilon)$. Indeed it does not coincide with the Naghdi model but both models possess similar asymptotic properties and they are preferred to Koiter's for discretization.

Encyclopedia of Computational Mechanics. Edited by Erwin Stein, René de Borst and Thomas J.R. Hughes.

5.4.2. Quadratic kinematics. In accordance with Theorems 5.1 and 5.2, it is relevant to use the standard 3D elastic energy (2) for such kinematics. Quadratic models based on the $(1,1,2)$ model are investigated in Bischoff and Ramm, 2000. The enrichment of the general shell element by the introduction of quadratic terms, – model $(2,2,2)$, is thoroughly studied from both asymptotic and numerical point views in Chapelle, Ferent and Le Tallec, 2003; Chapelle, Ferent and Bathe, 2003.

6. FINITE ELEMENT METHODS IN THIN DOMAINS

We herein address some of the characteristics of finite element methods (FEM), mainly the p-version of the FEM, when applied to the primal weak formulations (3) and (33) for the solution of plate and shell models. We only address isotropic materials, although our analysis could be extended to laminated composites.

As illustrative examples, we present the results of some computations performed with the p-version FE computer program StressCheck[22].

6.1. FEM discretizations

Let us recall that, when conformal, the FEM is a Galerkin projection into finite dimensional subspaces V_N of the variational space associated with the models under consideration. In the p-version of the FEM, subspaces are based on *one partition* of the domain into a finite number of subdomains $K \in \mathcal{T}$ (the *mesh*) in which the unknown displacement is discretized by mapped polynomial functions of increasing degree p. The subdomains K are mapped from reference element(s) $\widehat{K}$.

6.1.1. Meshes. All finite element discretizations we consider here are based on a mesh $\mathcal{T}_S$ of the mid-surface S: We mean that the 3D mesh of Ω^ε has in normal coordinates $(\mathbf{x}_\top, \mathsf{x}_3)$ the tensor product form[23] $\mathcal{T}_S \otimes \mathcal{I}_\varepsilon$ where $\mathcal{I}_\varepsilon$ represents a partition of the interval $(-\varepsilon, \varepsilon)$ in layers, e.g. the two halves $(-\varepsilon, 0)$ and $(0, \varepsilon)$, or – this case is important in the sequel –, the trivial partition by only *one element through the thickness*. We agree to call that latter mesh a *thin element mesh*.

The 3D elements K are thus images by maps ψ_K from reference elements $\widehat{K}$ which are either pentahedral (triangle $\times$ interval) or hexahedral:

$$\psi_K : \widehat{K} = \widehat{T} \times [0,1] \ni (\hat{x}_1, \hat{x}_2, \hat{x}_3) \mapsto \mathbf{x} \in K$$

with $\widehat{T}$ the reference triangle or the reference square. For the 2D FEM, we denote by T the elements in $\mathcal{T}_S$: They are the image of $\widehat{T}$ by maps ψ_T

$$\psi_T : \widehat{T} \ni (\hat{x}_1, \hat{x}_2) \mapsto \mathbf{x}_\top \in T.$$

If Ω_ε is a plate, the mid-surface S is plane but its boundary ∂S is not straight. For some lateral boundary conditions, e.g. the hard simple supported plate, the approximation of ∂S by a polygonal lines produces in general *wrong results*. This effect is known as the *Babuška paradox* Babuška and

[22] StressCheck is a trade mark of Engineering Software Research and Development, Inc., 10845 Olive Blvd., Suite 170, St. Louis, MO 63141, USA

[23] Of course, different mesh designs are possible on thin domains. If one wants to capture boundary layer terms with an exponential rate of convergence, a *h-p* refinement should be implemented near the edges of Ω^ε, Dauge and Schwab, 2002.

Encyclopedia of Computational Mechanics. Edited by Erwin Stein, René de Borst and Thomas J.R. Hughes.

Pitkäranta, 1990. If Ω_ε is a shell, the geometric approximation of S by "plane" elements is also an issue: If the mappings are affine, the shell is approximated by a faceted surface which has quite different rigidity properties than the smooth surface, see Akian and Sanchez-Palencia, 1992 and Chapelle and Bathe, 2003, §6.2.

As a conclusion good mappings have to be used for the design of the elements K (high degree polynomials or other analytic functions).

6.1.2. Polynomial spaces for hierarchical models. For hierarchical models (33), the discretization is indeed two-dimensional: The degree $\mathbf{q}$ of the hierarchy being fixed, the unknowns of (33) are the functions z_j^n defined on S and representing the displacement according to (38), where the director functions Φ_j^n form adequate bases of polynomials in one variable, e.g. Legendre polynomials L_n.

We have already mentioned in §5 that the only *intrinsic* option for the choice of components is taking $j = (\alpha, 3)$, which results into the Ansatz (written here with Legendre polynomials)

$$\mathbf{u}_\top = \sum_{n=0}^{q_\top} \mathbf{z}_\top^n(\mathbf{x}_\top)\, L_n\Big(\frac{\mathsf{x}_3}{\varepsilon}\Big) \quad \text{and} \quad \mathsf{u}_3 = \sum_{n=0}^{q_3} \mathsf{z}_3^n(\mathbf{x}_\top)\, L_n\Big(\frac{\mathsf{x}_3}{\varepsilon}\Big).$$

Now the discretization consists in requiring that $\mathsf{z}_\alpha^n|_T \circ \psi_T$, $\alpha = 1, 2$, and $\mathsf{z}_3^n|_T \circ \psi_T$ belong to the space $\mathbb{P}_p(\widehat{T})$ for some p where $\mathbb{P}_p(\widehat{T})$ is the space of polynomials in two variables

- of degree $\leq p$ if $\widehat{T}$ is the reference triangle,
- of partial degree $\leq p$ if $\widehat{T}$ is the reference square $[0, 1] \times [0, 1]$.

It makes sense to fix different degrees p_j in relation with $j = \alpha, 3$ and we set $\mathbf{p} = (p_1, p_2, p_3)$. When plugged back into formula (38), this discretization of the z_j^n, $j = \alpha, 3$, yields a finite dimensional subspace $V_{\mathbf{p}}^{\mathbf{q}}(\Omega^\varepsilon)$ of $V^{\mathbf{q}}(\Omega^\varepsilon)$. As already mentioned for the transverse degrees $\mathbf{q}$, *cf* (48) and §5, we have to assume for coherence that $p_1 = p_2$ for shells. In the situation of plates, if T is affinely mapped from the reference square, the $\mathsf{z}_j^n|_T$ are simply given by

$$\mathsf{z}_1^n(\mathbf{x}_\top) = \textstyle\sum_{i,k=0}^{p_1} z_{1,ik}^n P_i(x_1)P_k(x_2) \quad \mathsf{z}_2^n(\mathbf{x}_\top) = \sum_{i,k=0}^{p_2} z_{2,ik}^n P_i(x_1)P_k(x_2),$$
$$\mathsf{z}_3^n(\mathbf{x}_\top) = \textstyle\sum_{i,k=0}^{p_3} z_{3,ik}^n P_i(x_1)P_k(x_2)$$

where the $z_{j,ik}^n$ are real coefficients and P_i denotes a polynomial of degree i which is obtained from Legendre polynomials (see e.g. Szabó and Babuška, 1991).

The discretization of hierarchical models (33) can also be done through the h-version or the h-p versions of FEM.

6.1.3. Polynomial spaces for 3D discretization. Case of thin elements. In 3D, on the reference element $\widehat{K} = \widehat{T} \times [0, 1]$ we can consider any of the polynomial spaces $\mathbb{P}_{p,q}(\widehat{K}) = \mathbb{P}_p(\widehat{T}) \otimes \mathbb{P}_q([0, 1])$, $p, q \in \mathbb{N}$, For the discretization of (3), each Cartesian component u_i of the displacement is sought for in the space of functions $v \in H^1(\Omega^\varepsilon)$ such that for any K in the mesh, $v|_K \circ \psi_K$ belongs to $\mathbb{P}_{p,q}(\widehat{K})$. We denote by $V_{p,q}(\Omega^\varepsilon)$ the corresponding space of admissible displacements over Ω^ε.

In the situation where we have only one layer of elements over Ω^ε in the thickness (thin element mesh) with a (p, q) discretization, let us set $\mathbf{q} = (q, q, q)$ and $\mathbf{p} = (p, p, p)$. Then it is easy to see that, *in the framework of semi-discrete spaces* (85), we have the equality between discrete spaces:

$$V_{p,q}(\Omega^\varepsilon) = V_{\mathbf{p}}^{\mathbf{q}}(\Omega^\varepsilon). \tag{90}$$

In other words, thin elements are equivalent to the discretization of underlying hierarchical models. Let us insist on the following fact: For a true shell the correspondence between the Cartesian components

u_j and the tangential and transverse components $(\mathbf{u}_\top, \mathrm{u}_3)$ is non-affine. As a consequence, equality (90) holds only if the space $V_{\mathbf{p}}^{\mathbf{q}}(\Omega^\varepsilon)$ corresponds to the discretization of a hierarchical model in *Cartesian coordinates*.

Conversely, hierarchical models of the type $\mathbf{q} = (q, q, q)$ with the "Cartesian" unknowns z_j^n, $n = 0, \ldots, q$, $j = 1, 2, 3$ can be discretized directly on S, or inherit a 3D discretization, see Chapelle, Ferent and Bathe, 2003. Numerical evidence that the p-version with anisotropic Ansatz spaces allows the analysis of three dimensional shells with high accuracy was firstly presented in Düster *et al.*, 2001.

6.1.4. FEM variational formulations. Let us fix the transverse degree $\mathbf{q}$ of the hierarchical model. Its solution $\mathbf{u}^{\varepsilon,\mathbf{q}}$ solves problem (33). For each $\varepsilon > 0$ and each polynomial degree $\mathbf{p}$, (33) is discretized by its finite dimensional subspace $V_{\mathbf{p}}^{\mathbf{q}}(\Omega^\varepsilon)$. Let $\mathbf{u}_{\mathbf{p}}^{\varepsilon,\mathbf{q}}$ be the solution of

$$\textit{Find } \mathbf{u}_{\mathbf{p}}^{\varepsilon,\mathbf{q}} \in V_{\mathbf{p}}^{\mathbf{q}}(\Omega^\varepsilon) \quad \textit{such that} \quad a^{\varepsilon,\mathbf{q}}(\mathbf{u}_{\mathbf{p}}^{\varepsilon,\mathbf{q}}, \mathbf{u}') = \int_{\Omega^\varepsilon} \mathbf{f}^\varepsilon \cdot \mathbf{u}' \, \mathrm{d}\boldsymbol{x}, \quad \forall \mathbf{u}' \in V_{\mathbf{p}}^{\mathbf{q}}(\Omega^\varepsilon). \tag{91}$$

We can say that (91) is a sort of 3D discretization of (33). But, indeed, the actual unknowns of (91) are the $\mathbf{z}_\alpha^n$, $n = 0, \ldots, q_\top$ and z_3^n, $n = 0, \ldots, q_3$, or the z_j^n for $n = 0, \ldots, q$ and $j = 1, 2, 3$. Thus, (91) can be alternatively formulated as a 2D problem involving spaces $Z_{\mathbf{p}}^{\mathbf{q}}(S)$ independent of ε, and a coercive bilinear form $a_S^{\mathbf{q}}(\varepsilon)$ polynomial in ε. Examples are provided by the Reissner-Mindlin model, *cf* (47), the Koiter model (84), and the Naghdi model, *cf* (89). The variational formulation now takes the form

$$\textit{Find } \mathbf{Z} =: (\mathbf{z}^n)_{0 \le n \le q} \in Z_{\mathbf{p}}^{\mathbf{q}}(S) \quad \textit{such that} \quad a_S^{\mathbf{q}}(\varepsilon)(\mathbf{Z}, \mathbf{Z}') = F(\varepsilon)(\mathbf{f}, \mathbf{Z}'), \quad \forall \mathbf{Z}' \in Z_{\mathbf{p}}^{\mathbf{q}}(S), \tag{92}$$

where $F(\varepsilon)(\mathbf{f}, \mathbf{Z}')$ is the suitable bilinear form coupling loadings and test functions. Let us denote by $\mathbf{Z}_{\mathbf{p}}^{\varepsilon,\mathbf{q}}$ the solution of (92).

6.2. Locking issues

In the framework of the family of discretizations considered above, the *locking* effect is said to appear when a *deterioration* in the resulting approximation of $\mathbf{u}^{\varepsilon,\mathbf{q}}$ by $\mathbf{u}_{\mathbf{p}}^{\varepsilon,\mathbf{q}}$, $\mathbf{p} \to \infty$ tends to ∞, occurs as $\varepsilon \to 0$. Of course, a similar effect is reported in the h-version of FEM: The deterioration of the h-approximation also occurs when the thickness ε approaches zero.

Precise definition of locking may be found in Babuška and Suri, 1992: It involves the locking parameter (the thickness ε in the case of plates), the sequence of finite element spaces $V_{\mathbf{p}}^{\mathbf{q}}$ that comprise the extension procedure (the p-version in our case, but h and h-p versions can also be considered), and the norm in which error is to be measured. Of course, in different error measures different locking phenomena are expected.

6.2.1. Introduction to membrane locking. A locking-free approximation scheme is said to be *robust*. For a bilinear form $a_S(\varepsilon)$ of the form $a_0 + \varepsilon^2 a_1$ like Koiter's, a necessary condition for the robustness of the approximation is that the intersections of the discrete spaces with the kernel of a_0 are a sequence of dense subspaces for the whole kernel of a_0, see Sanchez-Hubert and Sanchez-Palencia, 1997, Ch.XI. In the case of the Koiter model, this means that the whole inextensional space $V_{\mathsf{F}}(S)$ (69) can be approximated by the subspaces of the inextensional elements belonging to FE spaces. For hyperbolic shells the only inextensional elements belonging to FE spaces are zero, see Sanchez-Hubert and Sanchez-Palencia, 1997 and Chapelle and Bathe, 2003, §7.3, which prevents all approximation property of $V_{\mathsf{F}}(S)$ if it is not reduced to $\{0\}$.

This fact is an extreme and general manifestation of the *membrane locking* of shells, also addressed in Pitkaranta, 1992; Gerdes *et al.*, 1998 for cylindrical shells, which are a prototype of shells having a

non-zero inextensional space. Plates do not present membrane locking since all elements $\mathbf{z} = (\mathbf{0}, \mathsf{z}_3)$ are inextensional, thus can be approximated easily by finite element sub-spaces. Nevertheless, as soon as the RM model is used, as can be seen from the structure of the energy (47), a shear locking may appear.

6.2.2. Shear locking of the RM and hierarchical plate models. Shear locking occurs because the FE approximation using $\mathcal{C}^0$ polynomials for the RM family of plates at the limit when $\varepsilon \to 0$ has to converge to the KL model in energy norm Suri, 2001, requiring $\mathcal{C}^1$ continuity. Let us consider the three-field RM model on the subspace of $V^{\mathsf{RM}}(\Omega^\varepsilon)$, *cf* §3.3, of displacements with bending parity: $\{\mathbf{u} \in V(\Omega^\varepsilon),\ \mathbf{u} = (-\mathsf{x}_3\boldsymbol{\theta}_\tau,\ \mathsf{z}_3)\}$. According to Suri *et al.*, 1995 we have the following:

Theorem 6.1. *The p-version of the FEM for the RM plate model without boundary layers, on a mesh of triangles and parallelograms, with polynomial degrees of $p_\tau \geq 1$ for rotations $\boldsymbol{\theta}_\tau$ and $p_3 \geq p_\tau$ for z_3 is free of locking in the energy norm.*

For the h-version over a uniform mesh consisting either of triangles or rectangles, to avoid locking the tangential degree p_τ has to be taken equal to 4 or larger, with the transverse degree p_3 being chosen equal to $p + 1$. A similar phenomenon was earlier found in connection with "Poisson Ratio" locking for the equations of elasticity. (i.e. conforming elements of degree four or higher encounter no locking), see Scott and Vogelius, 1985. In Suri *et al.*, 1995 it is proven that locking effects (and results) for the $(1, 1, 2)$ plate model are similar to the RM model because no additional constraints arise as the thickness $\varepsilon \to 0$. Furthermore, it is stated that locking effects carry over to all hierarchical plate models.

Here we have discussed locking in energy norm. However, if shear stresses are of interest, then locking is significantly worse because these involve an extra power ε^{-1}.

For illustration purposes consider a *clamped* plate with ellipsoidal mid-surface of radii 10 and 5, Young modulus[24] $E = 1$ and Poisson ratio $\nu = 0.3$, see Figure 4. The plate is loaded by a constant pressure of value $(2\varepsilon)^2$.

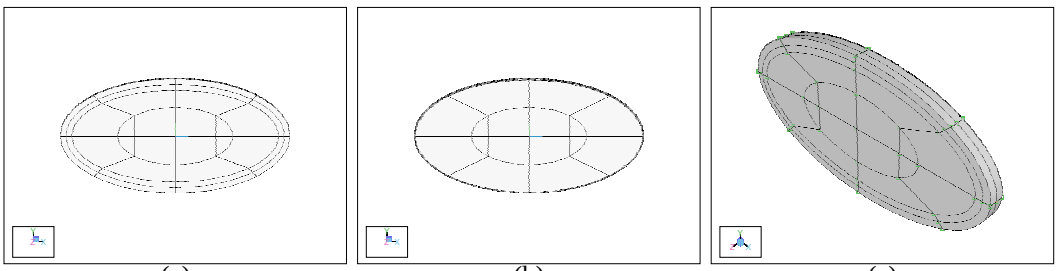

(a) (b) (c)

Figure 4. p-FE mesh for $2\varepsilon = 1, 0.1$ for RM model and $2\varepsilon = 1$ for 3D model.

The discretization is done over a 32 p-element mesh (see Figure 4 (a) and (b) for $2\varepsilon = 1$ and 0.1) using two layers, each of dimension ε in the vicinity of the boundary. The FE space is defined with

[24] We recall that the Young modulus is given by $E = \dfrac{\mu(3\lambda + 2\mu)}{2(\lambda + \mu)}$ and the Poisson ratio by $\nu = \dfrac{\lambda}{2(\lambda + \mu)}$.

$p_3 = p_\tau$ ranging from 1 to 8. We show in Figure 5 the locking effects for the RM model with κ_{Energy}.

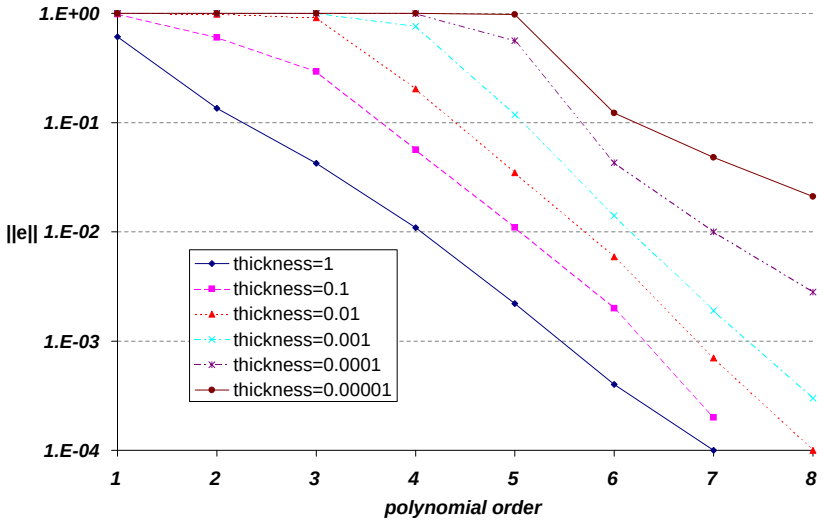

Figure 5. Discretization error vis polynomial degree p for RM plates of various thicknesses ε.

The error plotted in ordinates is the estimated relative *discretization error* in energy norm between the numerical and exact solution of the RM plate model for each fixed thickness ε (it is not the error between the RM numerical solution and the exact 3D plate model). A similar behavior can be observed with the model $\mathbf{q} = (1, 1, 2)$.

To illustrate both the locking effects for the hierarchical family of plates and the modeling errors between the plate models and their 3D counterpart, we have computed for two thicknesses of plates ($2\varepsilon = 1$ or $2\varepsilon = 0.01$), the solution for the first four plate models, see Table I[(25)], and for the fully 3D plate with the degrees $p_\tau = p_3 = 1, 2.., 8$ with the model represented in Figure 4 (c) for $2\varepsilon = 1$.

Model #	1 (RM)	2	3	4
Degrees $\mathbf{q} = (q_1, q_2, q_3)$	(1,1,0)	(1,1,2)	(3,3,2)	(3,3,4)
# independent fields $\mathbf{d} = (d_1, d_2, d_3)$	(1,1,1)	(1,1,2)	(2,2,2)	(2,2,3)

Table I. Hierarchical plate-model definitions for bending symmetry

The relative errors between energy norms of the hierarchical models and the 3D plate model versus the polynomial degree p is shown in Figure 6. As predicted, increasing the order of the plate model

[25] Here, for ease of presentation, we use the numbering system for plate models displayed in Table I, where we also provide the number d_j of fields in each direction for *bending models*, i.e. for which the surface components are odd and the normal component even in x_3.

does not improve the locking ratio, and as the hierarchical model number is increased the relative error decreases. We note that when $2\varepsilon = 1$ the relative error of the four models converges to the modeling error, which is still quite big since ε is not small, whereas when $2\varepsilon = 0.01$ the error stays larger that 15% for all models when $p \leq 4$, and starts converging for $p \geq 5$.

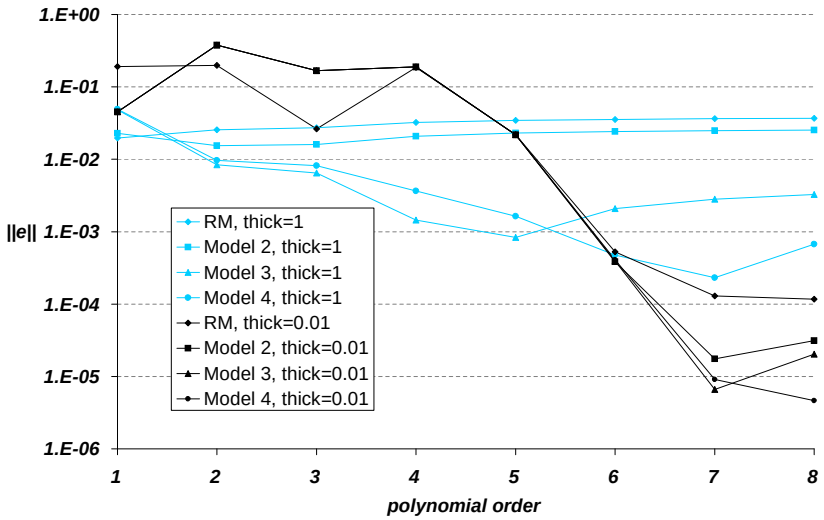

Figure 6. Relative error vis polynomial degree for $2\varepsilon = 1$ and 0.01 for the first 4 hierarchical models

6.3. Optimal mesh layout for hierarchical models with boundary layers

All hierarchical plate models (besides KL model) exhibit boundary layers. These are rapidly varying components which decay exponentially with respect to the stretched distance $\mathsf{R} = \mathsf{r}/\varepsilon$ from the edge, so that at a distance $\mathcal{O}(2\varepsilon)$ these are negligible. Finite element solutions should be able to capture these rapid changes. Using the p-version of the finite element method, one may realize exponential convergence rates if a proper design of meshes and selection of polynomial degrees is applied in the presence of boundary layers.

In a 1D problem with boundary layers, it has been proven in Schwab and Suri, 1996 that the p-version over a refined mesh can achieve exponential convergence for the boundary layers, uniformly in ε. The mesh has to be designed so to consist of one $\mathcal{O}(p(2\varepsilon))$ boundary-layer element at each boundary point. More precisely, the optimal size of the element is $\alpha p(2\varepsilon)$, where, $0 < \alpha < 4/e$.

This result carries over to the heat transfer problem on 2D domains as shown in Schwab *et al.*, 1998, and to the RM plate model, as demonstrated by numerical examples. Typical boundary layer meshes are shown in Figure 4 for $2\varepsilon = 1$ and 0.1: In practice, for ease of computations, two elements in the boundary layer zone are being used, each having the size in the normal direction of ε, independent of the polynomial degree used. This, although not optimal, still captures well the rapid changes in the boundary layer.

In order to realize the influence of the mesh design over the capture of boundary layer effects, we have again solved numerically the RM plate model for a thickness of $2\varepsilon = 0.01$ (and $\kappa_{\text{Deflection}}$ as shear

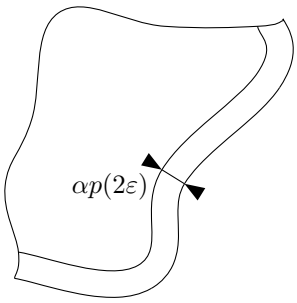

Figure 7. A typical design of the mesh near the boundary for the p-version of the FEM.

correction factor). Three different mesh layouts have been considered, with two layers of elements in the vicinity of the edge of dimension 0.5, 0.05 and 0.005 (the first two ones are represented in Figure 4). For comparison purposes we have computed the 3D solution over a domain having two layers in the thickness direction and two elements in the boundary layer zone of dimension 0.005. We have extracted the vertical displacement u_3 and the shear strain e_{23} along the line starting at $(x_1, x_2) = (9.95, 0)$ and ending at the boundary $(x_1, x_2) = (10, 0)$, i.e. in the boundary layer region. Computations use the degrees $p_\tau = p_3 = 8$. It turns out that the vertical displacement u_3 is rather insensitive to the mesh, whereas the shear strain e_{23} is inadequately computed if the mesh is not properly designed: With the mesh containing fine layers of thickness 0.005, the average relative error is 10%, but this error reaches 100% with mesh layer thickness 0.05 and 400% for the mesh layer thickness 0.5.

Concerning *shells* we have seen in §4.2 that the Koiter model for clamped elliptic shells admits boundary layers of length scale $\sqrt{\varepsilon}$, and in §4.4 that other length scales may appear for different geometries ($\varepsilon^{1/3}$ and $\varepsilon^{1/4}$). Moreover, for Naghdi model, the short length scale ε is also present, see Pitkäranta *et al.*, 2001. Nevertheless, the "long" length scales $\varepsilon^{1/3}$ and $\varepsilon^{1/4}$ appear to be less frequent. We may expect a similar situation for other hierarchical models. As a conclusion the mesh design for shell of small thicknesses should (at least) take into account both length scales ε and $\sqrt{\varepsilon}$. Another phenomenon should also be considered: Hyperbolic and parabolic shells submitted to a concentrated load or a singular data are expected to propagate singularities along their zero curvature lines, with the scale width $\varepsilon^{1/3}$, see Pitkäranta *et al.*, 2001.

6.4. Eigen-frequency computations

Eigen-frequency computations are, in our opinion, a very good indicator of *(i)* the quality of computations, *(ii)* the nature of the shell (or plate) response. In particular, the bottom of the spectrum indicates the maximal possible stress-strain energy to be expected under a load of given potential energy. From Theorem 4.4, we may expect that, except in the case of clamped elliptic shells, the ratio between the energy of the response and the energy of the excitation will behave almost as $\mathcal{O}(\varepsilon^{-2})$.

6.4.1. Eigen-frequency of RM vis 3D for plates Eigen-frequencies obtained by the p-version finite element method for clamped RM plates and their counterpart 3D eigen-frequencies have been compared in Dauge and Yosibash, 2002, where rectangular plates of dimensions $1 \times 2 \times 2\varepsilon$ have been considered. For isotropic materials with Poisson coefficient $\nu = 0.3$, the relative error for the first

three eigen-frequencies was found negligible (less than 0.12%) for thin plates with slender ratio of less than 1%, and still small (0.2%) for moderately thick plates (slander ratio about 5%).

For some orthotropic materials, much larger relative errors between the RM eigen-frequencies and their 3D counterparts have been observed even for relatively thin plates. In one of the orthotropic rectangular plate examples in Dauge and Yosibash, 2002, for which the boundary layer effect on the eigen-frequencies should be the most pronounced, a very large relative error of 25% has been reported for the first eigen-frequency at $\varepsilon = 0.1$. This is a significant deviation whereas the RM model underestimates the "true" 3D by 25%, and is attributed to the boundary layer effect.

6.4.2. 3D eigen-frequency computations for shells We present computations on three families of shells, see Figure 8: (a) clamped spherical shells, (b) sensitive spherical shells, (c) flexural cylindrical shells, all with material parameters $\nu = 0.3$ and $E = 1$. These three families illustrate the three cases *(i)*, *(ii)* and *(iii)* in Theorem 4.4: The shells (a) are elliptic clamped on their whole boundary, (b) are elliptic, but clamped only on a part of their boundaries and (c) are parabolic. *Note that Theorem 4.4 states results relating to Koiter eigenvalues and not for 3D eigenvalues. Nevertheless a similar behavior can be expected for 3D eigenvalues.*

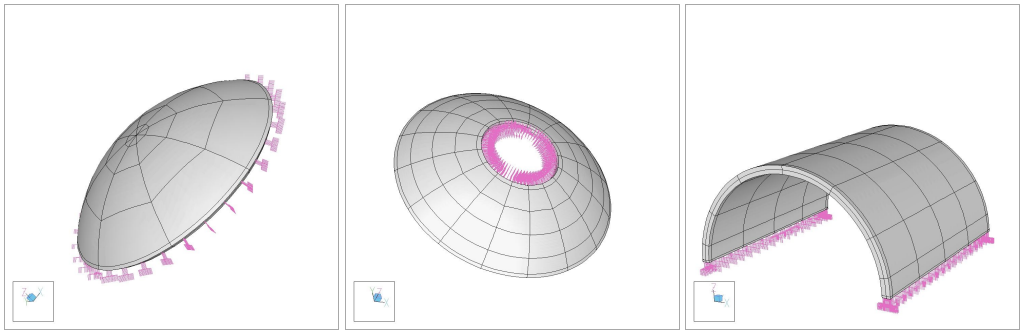

Figure 8. Shell models (a), (b) and (c) for $\varepsilon = 0.04$

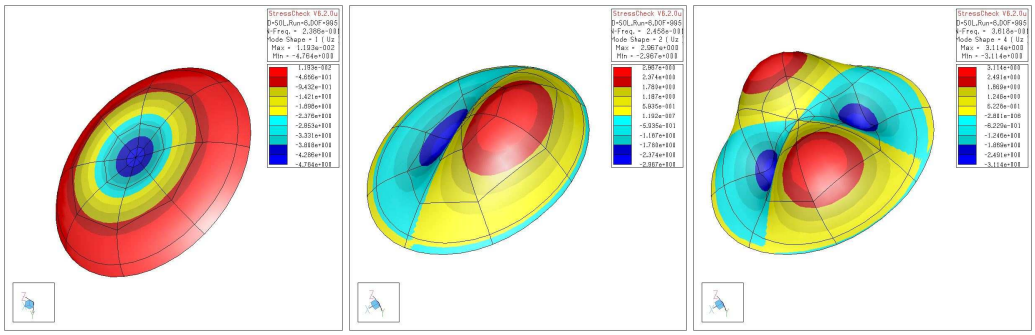

Figure 9. Model (a). vertical components of eigen-modes 1, 2 and 4 for $\varepsilon = 0.16$

Family (a). The mid-surface S is the portion of the unit sphere described in spherical coordinates by $\varphi \in [0, 2\pi)$ and $\theta \in (\frac{\pi}{4}, \frac{\pi}{2}]$. Thus S a spherical cap containing the north pole. The family of shells Ω^ε has its upper and lower surfaces characterized by the same angular conditions, and the radii $\rho = 1 + \varepsilon$ and $\rho = 1 - \varepsilon$, respectively. We clamp Ω^ε along its lateral boundary $\theta = \frac{\pi}{4}$.

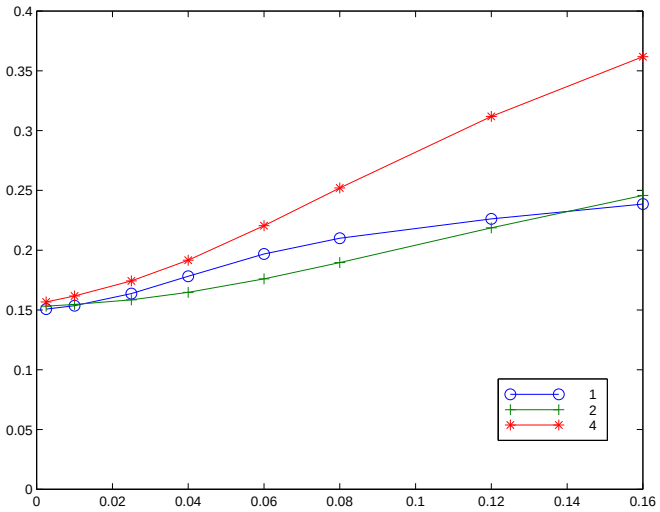

Figure 10. Model (a). Eigen-frequencies versus ε

We have computed the first five eigen-frequencies of the 3D operator (4) by a FE p-discretization based on two layers of elements in the transverse direction and 8×5 elements in the mid-surface, including one thin layer of elements in the boundary layer. The *vertical* (i.e. normal to the tangent plane at the north pole, not transverse to the mid-surface!) component u_3 for three modes are represented in Figure 9 for the (half)-thickness $\varepsilon = 0.16$. Mode 3 is rotated from mode 2, and mode 5 from mode 4 (double eigen-frequencies). The shapes of the eigen-modes for smaller values of the thickness are similar. Figure 10 provides the three first distinct eigen-frequencies as a function of the thickness in natural scales. In accordance with Theorem 4.4 *(i)*, the smallest eigen-frequencies all tend to the same non-zero limit, which should be the (square root of the) bottom of the membrane spectrum.

Family (b). The mid-surface S is the portion of the unit sphere described in spherical coordinates by $\varphi \in [0, 2\pi)$ and $\theta \in (\frac{\pi}{4}, \frac{5\pi}{12}]$. The family of shells Ω^ε has its upper and lower surfaces characterized by the same angular conditions, and the radii $\rho = 1 + \varepsilon$ and $\rho = 1 - \varepsilon$, respectively. We clamp Ω^ε along its lateral boundary $\theta = \frac{5\pi}{12}$ and let it free along the other lateral boundary $\theta = \frac{\pi}{4}$. This shell is a sensitive one in the sense of Pitkäranta and Sanchez-Palencia, 1997, which means that it is sensitive to the thickness and answers differently according to the value of ε.

We have computed the first five (or first ten) eigen-frequencies of the 3D operator (4) by a FE p-discretization similar to that of (a) (two layers in the transverse direction and 8×4 elements in the surface direction – for the "small" thickness, a globally refined mesh of 16×6 elements has been used). In Figure 11 we plot the vertical components of modes number 1, 3, 5, 7, 8 and 9 for $\varepsilon = 0.08$ and in Figure 12, modes number 1, 3, 5 for $\varepsilon = 0.0025$. In both cases, modes 2, 4 and 6 are similar to modes 1, 3 and 5 respectively and associated with the same (double) eigen-frequencies.

Encyclopedia of Computational Mechanics. Edited by Erwin Stein, René de Borst and Thomas J.R. Hughes.

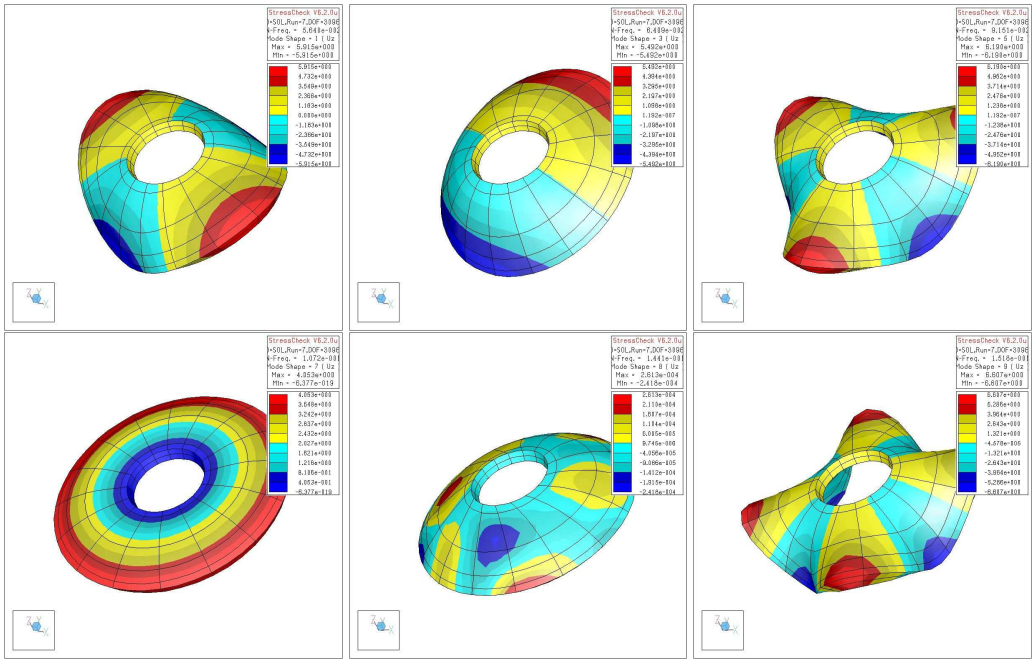

Figure 11. Model (b). Vertical components of modes 1, 3, 5, 7, 8, 9 for $\varepsilon = 0.08$

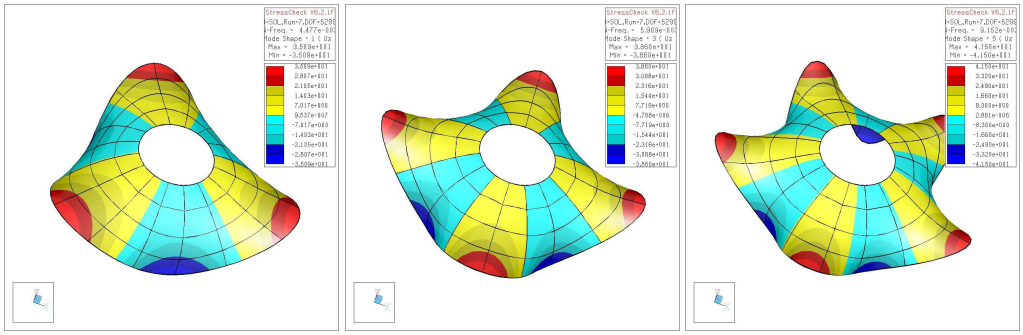

Figure 12. Model (b). Vertical components of modes 1, 3, 5 for $\varepsilon = 0.0025$

For $\varepsilon = 0.08$, we notice the axisymmetric mode at position 7 (it is at position 5 when $\varepsilon = 0.16$, and 9 for $\varepsilon = 0.04$). Mode 8 looks odd. Indeed it is very small (less than 10^{-4}) for normalized eigenvectors in $\mathcal{O}(1)$. This means that this mode is mainly supported in its tangential components (we have checked they have a reasonable size). Mode 8 is in fact a *torsion mode* which means a dominant stretching effect, whereas the other ones have a more pronounced bending character.

Figure 13 provides the first distinct eigen-frequencies classified by the nature of the eigenvector (namely the number of nodal regions of u_3) as a function of the thickness in natural scales. The

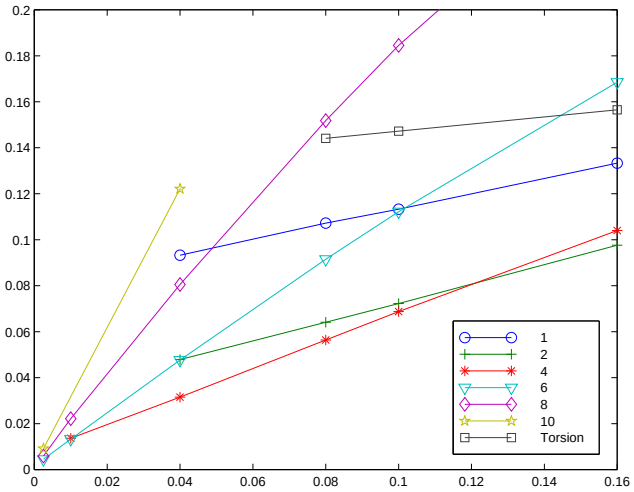

Figure 13. Model (b). Eigen-frequencies versus ε

organization of these eigen-frequencies along affine lines converging to positive limits as $\varepsilon \to 0$ is remarkable. We may expect a convergence as $\varepsilon \to 0$ of the solution $\mathbf{u}^\varepsilon$ of problem (3) *provided the loading has a finite number of angular frequencies in* φ (the displacement will converge to the highest angular frequency of the load). Nevertheless, such a phenomenon is specific to the axisymmetric nature of the shell (b) and could not be generalized to other sensitive shells. Computations with a concentrated load (which, of course, has an infinite number of angular frequencies) display a clearly non-converging behavior Chapelle and Bathe, 2003, §4.5.3.

Family (c). The mid-surface S is a half-cylinder described in cylindrical coordinates (r, θ, y) by $\theta \in (0, \pi)$, $r = 1$ and $y \in (-1, 1)$. The family of shells Ω^ε has its upper and lower surfaces characterized by the same angular and axial condition, and the radii $r = 1 + \varepsilon$ and $r = 1 - \varepsilon$, respectively. We clamp Ω^ε along its lateral boundaries $\theta = 0$ and $\theta = \pi$ and leave it free everywhere else. This is a well known example of flexural shell, where the space of inextensional displacements contains the space, *cf* (80) (note that, below, $\mathsf{z}_r = \mathsf{z}_3$)

$$V_{\mathsf{F},0} := \big\{\mathbf{z} = (\mathsf{z}_r, \mathsf{z}_\theta, \mathsf{z}_y);\ \ \mathsf{z}_y = 0,\ \ \mathsf{z}_r = \mathsf{z}_r(\theta),\ \ \mathsf{z}_\theta = \mathsf{z}_\theta(\theta) \\ \text{with}\quad \partial_\theta \mathsf{z}_\theta = \mathsf{z}_r \quad \text{and} \quad \mathsf{z}_\theta = \mathsf{z}_r = \partial_\theta \mathsf{z}_r = 0 \ \text{ in } \ \theta = 0, \pi\big\}. \quad (93)$$

Besides these patterns independent of the axial variable y, there is another subspace $V_{\mathsf{F},1}$ of inextensional displacements, where z_y is independent on y and z_r, z_θ are linear in y:

$$V_{\mathsf{F},1} := \big\{\mathbf{z} = (\mathsf{z}_r, \mathsf{z}_\theta, \mathsf{z}_y);\ \ \mathsf{z}_y = \mathsf{z}_y(\theta),\ \ \mathsf{z}_\theta = -y\partial_\theta \mathsf{z}_y(\theta),\ \ \mathsf{z}_r = -y\partial_\theta^2 \mathsf{z}_y(\theta) \\ \text{with}\quad \mathsf{z}_y = \mathsf{z}_\theta = \mathsf{z}_r = \partial_\theta \mathsf{z}_r = 0 \ \text{ in } \ \theta = 0, \pi\big\}, \quad (94)$$

and $V_{\mathsf{F}} = V_{\mathsf{F},0} \oplus V_{\mathsf{F},1}$. We agree to call "constant" the displacements associated with $V_{\mathsf{F},0}$ and "linear" those associated with $V_{\mathsf{F},1}$.

We have computed the first ten eigen-frequencies (4) by a FE p-discretization based on two layers of elements in the transverse direction and a mid-surface mesh of 8×6 curved quadrangles. For

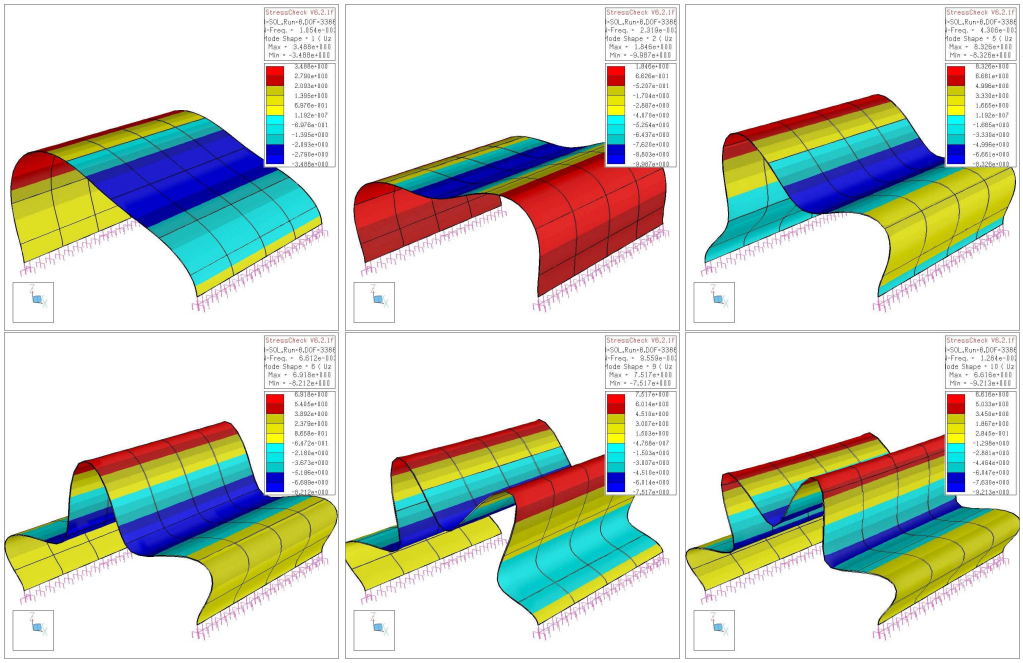

Figure 14. Model (c). Vertical components of modes 1, 2, 5, 6, 9 and 10 for $\varepsilon = 0.0025$

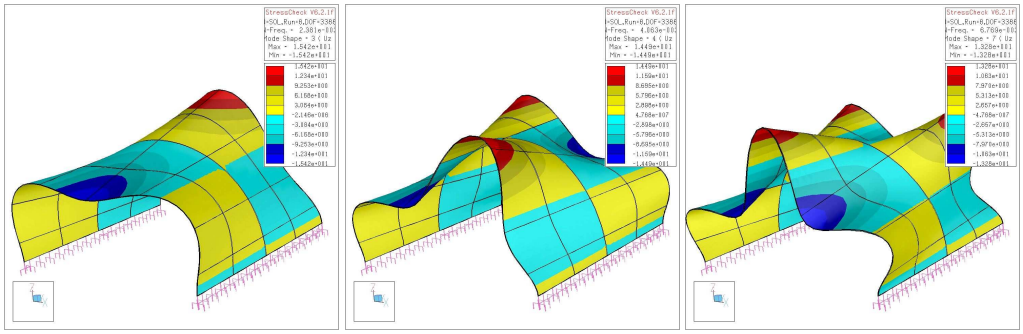

Figure 15. Model (c). Vertical components modes 3, 4 and 7 for $\varepsilon = 0.0025$

the half-thickness $\varepsilon = 0.0025$ we plot the *vertical* component $u_z = \mathrm{u}_r \sin\theta + \mathrm{u}_\theta \cos\theta$ of the eigenmodes **u**: In Figure 14 the first six constant flexural eigenmodes and in Figure 15 the first three linear flexural eigenmodes (their components u_y clearly display a non-zero constant behavior in y). The shapes of the eigen-modes for larger values of the thickness are similar. In Figure 16 we have plotted in logarithmic scale these eigen-frequencies, classified according to the behavior of the flexural eigenmodes ("constant" and "linear"). The black line has the equation $\varepsilon \mapsto \varepsilon/4$: Thus we can see that the slopes of the eigen-frequency lines are close to 1, as expected by the theory (at least for Koiter

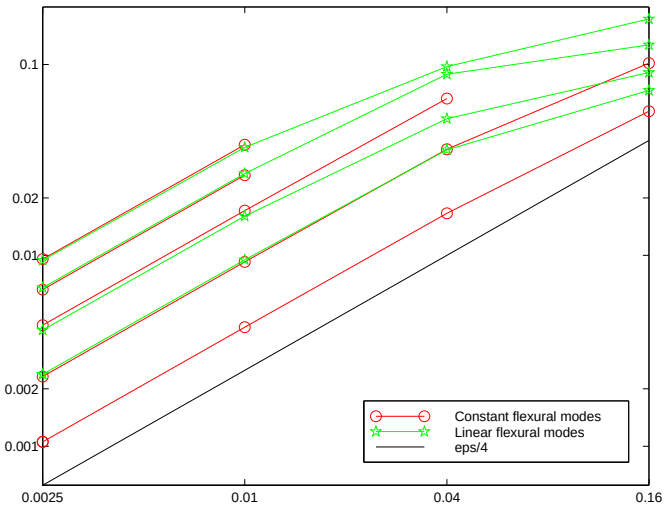

Figure 16. Model (c). Eigen-frequencies versus ε in log-log scale

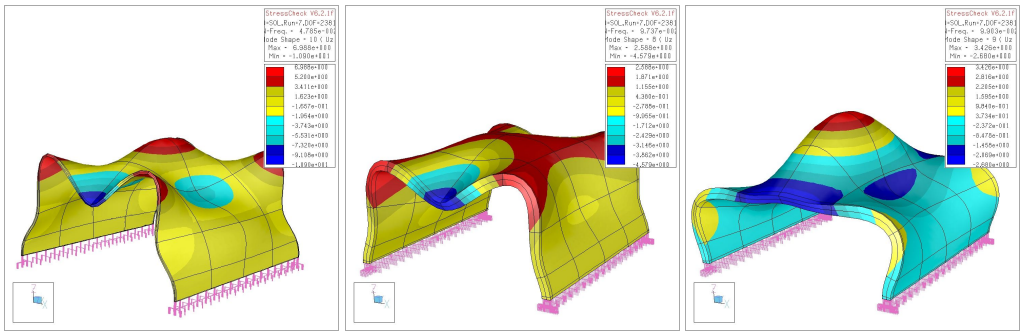

Figure 17. Model (c). First non flexural modes for $\varepsilon = 0.01$ and $\varepsilon = 0.04$

model). In Figure 17 we represent the first non-flexural modes (with rank 10 for $\varepsilon = 0.01$ and rank 8, 9 for $\varepsilon = 0.04$).

6.4.3. Thin element eigen-frequency computations We present in Tables II-IV the computation of the first eigen-frequency of the shell Ω^ε in families (a), (b) and (c), respectively, for a moderate thickness ($\varepsilon = 0.04$) and a small thickness ($\varepsilon = 0.0025$). The degree q is the degree in the transverse direction (according to §6.1.3 there is *one layer of elements*). We notice that, for an accuracy of 0.01% and $\varepsilon = 0.04$, the quadratic kinematics is not sufficient, whereas it is for $\varepsilon = 0.0025$. No locking is visible there. In fact, the convergence of the q-models *to their own limits* is more rapid for $\varepsilon = 0.04$.

	$\varepsilon = 0.04$ and $q = 2$			$\varepsilon = 0.04$ and $q = 3$			$\varepsilon = 0.0025$ and $q = 2$		
p	DOF	e-freq.	% err.	DOF	e-freq.	% err.	DOF	e-freq.	% err.
1	297	0.2271659	37.967	396	0.2264908	37.557	297	0.2055351	36.437
2	729	0.1694894	2.938	828	0.1694269	2.900	729	0.1560694	3.601
3	1209	0.1652870	0.386	1308	0.1652544	0.366	1209	0.1537315	2.049
4	2145	0.1648290	0.108	2244	0.1648001	0.090	2145	0.1517604	0.741
5	3321	0.1646992	0.029	3636	0.1646693	0.011	3321	0.1508741	0.152
6	4737	0.1646859	0.021	5268	0.1646555	0.002	4737	0.1506988	0.036
7	6393	0.1646849	0.020	7140	0.1646544	0.002	6393	0.1506544	0.007
8	8289	0.1646849	0.020	9252	0.1646543	0.002	8289	0.1506447	0.000

Table II. Thin element computations for the first eigen-frequency of model (a).

	$\varepsilon = 0.04$ and $q = 2$			$\varepsilon = 0.04$ and $q = 3$			$\varepsilon = 0.0025$ and $q = 2$		
p	DOF	e-freq.	% err.	DOF	e-freq.	% err.	DOF	e-freq.	% err.
1	864	0.0597700	89.68	1152	0.0595287	88.91	864	0.0462144	932.2
2	2016	0.0326855	3.73	2304	0.0326036	3.46	2016	0.0129819	189.9
3	3168	0.0318094	0.95	3456	0.0317325	0.70	3168	0.0064504	44.06
4	5472	0.0316330	0.39	5760	0.0315684	0.18	5472	0.0047030	5.04
5	8352	0.0316071	0.30	9216	0.0315319	0.06	8352	0.0045085	0.69
6	11808	0.0316011	0.28	13248	0.0315223	0.03	11808	0.0044800	0.06
7	15840	0.0316000	0.28	17856	0.0315200	0.03	15840	0.0044780	0.01
8	20448	0.0315998	0.28	23040	0.0315195	0.03	20448	0.0044779	0.01

Table III. Thin element computations for the first eigen-frequency of model (b).

	$\varepsilon = 0.04$ and $q = 2$			$\varepsilon = 0.04$ and $q = 3$			$\varepsilon = 0.0025$ and $q = 2$		
p	DOF	e-freq.	% err.	DOF	e-freq.	% err.	DOF	e-freq.	% err.
1	567	0.0514951	210.2	756	0.0510683	208.7	567	0.0397025	3666.
2	1311	0.0207290	24.9	1500	0.0206911	24.7	1311	0.0079356	653.1
3	2055	0.0167879	1.2	2244	0.0167596	0.98	2055	0.0011505	9.188
4	3531	0.0166354	0.2	3720	0.0166091	0.08	3531	0.0010578	0.395
5	5367	0.0166293	0.2	5928	0.0166011	0.03	5367	0.0010548	0.108
6	7563	0.0166289	0.2	8496	0.0166004	0.02	7563	0.0010541	0.045
7	10119	0.0166288	0.2	11424	0.0166003	0.02	10119	0.0010538	0.012
8	13035	0.0166288	0.2	14712	0.0166002	0.02	13035	0.0010537	0.002

Table IV. Thin element computations for the first eigen-frequency of model (c).

Encyclopedia of Computational Mechanics. Edited by Erwin Stein, René de Borst and Thomas J.R. Hughes.

6.5. Conclusion

It is worthwhile to point out that the most serious difficulties we have encountered in computing all these models occurred for $\varepsilon = 0.0025$ and model (b) – the sensitive shell: Indeed, in that case, when $\varepsilon \to 0$, the first eigen-mode is more and more oscillating, and the difficulties of approximation are those of a high-frequency analysis. It is also visible from Tables III and IV that the computational effort is lower for the cylinder than for the sensitive shell, for an even better quality of approximation.

It seems that, considering the high performance of the p-version approximation in a smooth mid-surface (for each fixed ε and fixed degree q we have an exponential convergence in p), the locking effects can be equilibrated by slightly increasing the degree p as ε decreases.

Of course, there exist many strategies to overcome locking in different situations: Let us quote here Bathe and Brezzi, 1985; Brezzi *et al.*, 1989; Arnold and Brezzi, 1997 as "early references" on mixed methods which result in a relaxation of the zero-membrane-energy constraint. These methods are addressed in other chapters of the Encyclopedia.

ACKNOWLEDGEMENTS

The authors wish to thank Domique Chapelle (INRIA) for stimulating discussions, Martin Costabel and Yvon Lafranche[26] (University of Rennes) for their valuable technical support.

REFERENCES

Actis RL, Szabo BA and Schwab C. Hierarchic models for laminated plates and shells. *Comput. Methods Appl. Mech. Engrg.* 1999; **172**(1-4): 79–107.

Agmon S, Douglis A and Nirenberg L. Estimates near the boundary for solutions of elliptic partial differential equations satisfying general boundary conditions II. *Comm. Pure Appl. Math.* 1964; **17**: 35–92.

Agratov II and Nazarov SA. Asymptotic analysis of problems in junctions of domains of different limit dimension. An elastic body pierced by thin rods. *J. Math. Sci. (New York)* 2000; **102**(5): 4349–4387. Function theory and applications.

Akian JL and Sanchez-Palencia E. Approximation de coques élastiques minces par facettes planes: Phénomène de blocage membranaire.. *C R. Acad. Sci. Paris, Sér. I.* 1992; **315**: 363–369.

Andreoiu G and Faou E. Complete asymptotics for shallow shells. *Asymptot. Anal.* 2001; **25**(3-4): 239–270.

Anicic S and Léger A. Formulation bidimensionnelle exacte du modèle de coque 3D de Kirchhoff-Love. *C. R. Acad. Sci. Paris Sér. I Math.* 1999; **329**(8): 741–746.

Arnold DN and Brezzi F. Locking-free finite element methods for shells. *Math. Comp.* 1997; **66**(217): 1–14.

Arnold DN and Falk RS. The boundary layer for the Reissner-Mindlin plate model.. *SIAM J. Math. Anal.* 1990; **21 (2)**: 281–312.

Arnold DN and Falk RS. Asymptotic analysis of the boundary layer for the Reissner-Mindlin plate model.. *SIAM J. Math. Anal.* 1996; **27 (2)**: 486–514.

Avalishvili M and Gordeziani D. Investigation of two-dimensional models of elastic prismatic shell. *Georgian Mathematical Journal* 2003; **10**(1): 17–36.

[26] `fig4tex` macro package for drawing figures, see
`http://perso.univ-rennes1.fr/yvon.lafranche/fig4tex/ReferenceGuide.html`

Babuška I, d'Harcourt JM and Schwab C. Optimal shear correction factors in hierarchic plate modelling.. 1991. Technical Note BN-1129, Institute for Physical Science and Technology, University of Maryland, College Park, MD, USA.

Babuška I and Li L. Hierarchic modeling of plates. *Comput. & Structures* 1991; **40**: 419–430.

Babuška I and Li L. The h-p-version of the finite element method in the plate modelling problem. *Comm. Appl. Numer. Meth.* 1992a; **8**: 17–26.

Babuška I and Li L. The problem of plate modelling: Theoretical and computational results.. *Comput. Meth. Appl. Mech. Engrg.* 1992b; **100**: 249–273.

Babuška I and Pitkäranta J. The plate paradox for hard and soft simple support.. *SIAM J. Math. Anal.* 1990; **21**: 551–576.

Babuška I and Suri M. On locking and robustness in the finite element method. *SIAM Jour. Numer. Anal.* 1992; **29**: 1261–1293.

Babuška I, Szabó BA and Actis RL. Hierarchic models for laminated composites. *Internat. J. Numer. Methods Engrg.* 1992; **33**(3): 503–535.

Bathe KJ and Brezzi F. On the convergence of a four node plate bending element based on mindlin-reissner plate theory and a mixed interpolation.. *in* JR. Whiteman (ed.), *The Mathematics of Finite Elements and Applications*. Vol5. Academic Press. London. 1985. pp491–503.

Bernadou M and Ciarlet PG. Sur l'ellipticité du modèle linéaire de coques de W.T.Koiter.. *in* RGlowinski and JLions (eds), *Computing Methods in Applied Sciences and Engineering*. Lecture Notes in Economics and Mathematical Systems, Vol.134. Springer-Verlag. Heidelberg. 1976. pp89–136.

Bischoff M and Ramm E. On the physical significance of higher order kinematic and static variables in a three-dimensional shell formulation. *Internat. J. Solids Structures* 2000; **37**: 6933–6960.

Brezzi F, Bathe K.-J and Fortin M. Mixed-interpolated elements for Reissner-Mindlin plates. *Internat. J. Numer. Methods Engrg.* 1989; **28**(8): 1787–1801.

Budiansky B and Sanders JL. On the "best" first-order linear shell theory.. *W. Prager Anniversary Volume*. Progress in Applied Mechanics. Macmillan. New-York. 1967. pp129–140.

Chapelle D and Bathe K.-J. The mathematical shell model underlying general shell elements. *Internat. J. Numer. Methods Engrg.* 2000; **48**(2): 289–313.

Chapelle D and Bathe K.-J. *The Finite Element Analysis of Shells - Fundamentals*. Computational Fluid and Solid Mechanics. Springer. 2003.

Chapelle D, Ferent A and Bathe K.-J. 3D-shell elements and their underlying mathematical model. 2003. To appear in *Math. Models Methods Appl. Sci.*

Chapelle D, Ferent A and Le Tallec P. The treatment of "pinching locking" in 3D-shell elements. *M2AN Math. Model. Numer. Anal.* 2003; **37**(1): 143–158.

Ciarlet PG. *Mathematical Elasticity. Vol. I, Three-Dimensional Elasticity*. North-Holland. Amsterdam. 1988.

Ciarlet PG. *Mathematical Elasticity. Vol. II, Theory of Plates*. North-Holland. Amsterdam. 1997.

Ciarlet PG. *Mathematical elasticity. Vol. III*. North-Holland Publishing Co.. Amsterdam. 2000. Theory of shells.

Ciarlet PG and Destuynder P. A justification of the two-dimensional plate model. *J. Mécanique* 1979; **18**: 315–344.

Ciarlet PG and Kesavan S. Two-dimensional approximation of three-dimensional eigenvalue problems in plate theory. *Comp. Methods Appl. Mech. Engrg.* 1981; **26**: 149–172.

Ciarlet PG and Lods V. Asymptotic analysis of linearly elastic shells. I. Justification of membrane shell equations. *Arch. Rational Mech. Anal.* 1996a; **136**: 119–161.

Ciarlet PG and Lods V. Asymptotic analysis of linearly elastic shells. III. Justification of Koiter's shell equations. *Arch. Rational Mech. Anal.* 1996b; **136**: 191–200.

Ciarlet PG, Lods V and Miara B. Asymptotic analysis of linearly elastic shells. II. Justification of flexural shell equations. *Arch. Rational Mech. Anal.* 1996; **136**: 163–190.

Encyclopedia of Computational Mechanics. Edited by Erwin Stein, René de Borst and Thomas J.R. Hughes.

Ciarlet PG and Paumier JC. A justification of the marguerre-von- kármán equations. *Computational Mechanics* 1986; **1**: 177–202.

Dauge M, Djurdjevic I, Faou E and Rössle A. Eigenmodes asymptotic in thin elastic plates. *J. Maths. Pures Appl.* 1999; **78**: 925–964.

Dauge M and Faou E. Koiter estimate revisited. *Research report*. INRIA. 2004.

Dauge M and Gruais I. Asymptotics of arbitrary order for a thin elastic clamped plate. I: Optimal error estimates. *Asymptotic Analysis* 1996; **13**: 167–197.

Dauge M and Gruais I. Asymptotics of arbitrary order for a thin elastic clamped plate. II: Analysis of the boundary layer terms. *Asymptotic Analysis* 1998; **16**: 99–124.

Dauge M, Gruais I and Rössle A. The influence of lateral boundary conditions on the asymptotics in thin elastic plates. *SIAM J. Math. Anal.* 1999/00; **31**(2): 305–345 (electronic).

Dauge M and Schwab C. hp-FEM for three-dimensional elastic plates. *M2AN Math. Model. Numer. Anal.* 2002; **36**(4): 597–630.

Dauge M and Yosibash Z. Boundary layer realization in thin elastic 3-d domains and 2-d hierarchic plate models. *Internat. J. Solids Structures* 2000; **37**: 2443–2471.

Dauge M and Yosibash Z. Eigen-frequencies in thin elastic 3-D domains and Reissner-Mindlin plate models. *Math. Methods Appl. Sci.* 2002; **25**(1): 21–48.

Düster A, Bröker H and Rank E. The p-version of the finite element method for three-dimensional curved thin walled structures. *Int. Jour. Num. Meth. Engrg.* 2001; **52**: 673–703.

Faou E. Développements asymptotiques dans les coques elliptiques: équations tridimensionnelles linéarisées. *C. R. Acad. Sci. Paris Sér. I Math.* 2001a; **333**(4): 389–394.

Faou E. Développements asymptotiques dans les coques elliptiques: modèle de Koiter. *C. R. Acad. Sci. Paris Sér. I Math.* 2001b; **333**(2): 139–143.

Faou E. Elasticity on a thin shell: Formal series solution. *Asymptotic Analysis* 2002; **31**: 317–361.

Faou E. Multiscale expansions for linear clamped elliptic shells. *Research Report RR-4956*. INRIA. 2003. To appear in *Comm. Partial Differential Equations*.

Friedrichs KO and Dressler RF. A boundary-layer theory for elastic plates. *Comm. Pure Appl. Math.* 1961; **14**: 1–33.

Genevey K. A regularity result for a linear membrane shell problem. *RAIRO Modél. Math. Anal. Numér.* 1996; **30 (4)**: 467–488.

Gerdes K, Matache AM and Schwab C. Analysis of membrane locking in hp FEM for a cylindrical shell. *ZAMM Z. Angew. Math. Mech.* 1998; **78**(10): 663–686.

Gol'denveizer AL. Derivation of an approximate theory of bending of a plate by the method of asymptotic integration of the equations of the theory of elasticity. *Prikl. Matem. Mekhan.* 1962; **26 (4)**: 668–686. English translation *J. Appl. Maths. Mech.* (1964) 1000–1025.

Gregory RD and Wan FY. Decaying states of plane strain in a semi-infinite strip and boundary conditions for plate theory. *J. Elasticity* 1984; **14**: 27–64.

Havu V and Pitkäranta J. Analysis of a bilinear finite element for shallow shells. I. Approximation of inextensional deformations. *Math. Comp.* 2002; **71**(239): 923–943 (electronic).

Havu V and Pitkäranta J. Analysis of a bilinear finite element for shallow shells. II. Consistency error. *Math. Comp.* 2003; **72**(244): 1635–1653 (electronic).

Il'in AM. *Matching of asymptotic expansions of solutions of boundary value problems*. Vol. 102 of *Translations of Mathematical Monographs*. American Mathematical Society. Providence, R. I.. 1992.

Irago H and Viaño JM. Error estimation in the Bernoulli-Navier model for elastic rods. *Asymptot. Anal.* 1999; **21**(1): 71–87.

John F. Refined interior equations for thin elastic shells.. *Comm. Pure Appl. Math.* 1971; **24**: 583–615.

Encyclopedia of Computational Mechanics. Edited by Erwin Stein, René de Borst and Thomas J.R. Hughes.

Koiter WT. A consistent first approximation in the general theory of thin elastic shells. *Proc. IUTAM Symposium on the Theory on Thin Elastic Shells, August 1959* 1960; pp12–32.

Koiter WT. On the foundations of the linear theory of thin elastic shells: I.. *Proc. Kon. Ned. Akad. Wetensch., Ser.B* 1970a; **73**: 169–182.

Koiter WT. On the foundations of the linear theory of thin elastic shells: II.. *Proc. Kon. Ned. Akad. Wetensch., Ser.B* 1970b; **73**: 183–195.

Koiter WT and Simmonds JG. Foundations of shell theory. *Theoretical and applied mechanics (Proc. Thirteenth Internat. Congr., Moscow Univ., Moscow, 1972)*. Springer. Berlin. 1973. pp150–176.

Kondrat'ev VA. Boundary-value problems for elliptic equations in domains with conical or angular points. *Trans. Moscow Math. Soc.* 1967; **16**: 227–313.

Kozlov V, Maz'ya V and Movchan A. *Asymptotic analysis of fields in multi-structures*. Oxford Mathematical Monographs. The Clarendon Press Oxford University Press. New York. 1999. Oxford Science Publications.

Lods V and Mardare C. A justification of linear Koiter and Naghdi's models for totally clamped shell. *Asymptot. Anal*. 2002; **31**(3-4): 189–210.

Love A. EH. *A treatise on the Mathematical Theory of Elasticity*. Dover Publications, New York. 1944. Fourth Ed.

Mardare C. Asymptotic analysis of linearly elastic shells: error estimates in the membrane case. *Asymptot. Anal.* 1998; **17**: 31–51.

Maz'ya VG, Nazarov SA and Plamenevskii BA. *Asymptotische Theorie elliptischer Randwertaufgaben in singulär gestörten Gebieten II*. Mathematische Monographien, Band 83. Akademie Verlag. Berlin. 1991.

Naghdi PM. Foundations of elastic shell theory. *Progress in Solid Mechanics*. Vol4. North-Holland. Amsterdam. 1963. pp1–90.

Naghdi PM. The theory of shells and plates. *in* SFlügge and CTruesdell (eds), *Handbuch der Physik*. Vol. VI a/2. Springer-Verlag. Berlin. 1972. pp425–640.

Nazarov SA. Two-term asymptotics of solutions of spectral problems with singular perturbation. *Math. USSR Sbornik* 1991; **69 (2)**: 307–340.

Nazarov SA. Justification of the asymptotic theory of thin rods. Integral and pointwise estimates. *J. Math. Sci. (New York)* 1999; **97**(4): 4245–4279. Problems of mathematical physics and function theory.

Nazarov SA. Asymptotic analysis of an arbitrarily anisotropic plate of variable thickness (a shallow shell). *Mat. Sb.* 2000a; **191**(7): 129–159.

Nazarov SA. On the asymptotics of the spectrum of a problem in elasticity theory for a thin plate. *Sibirsk. Mat. Zh.* 2000b; **41**(4): iii, 895–912.

Nazarov SA and Zorin IS. Edge effect in the bending of a thin three-dimensional plate. *Prikl. Matem. Mekhan.* 1989; **53 (4)**: 642–650. English translation *J. Appl. Maths. Mechs.* (1989) 500–507.

Novozhilov VV. *Thin Shell Theory*. Walters-Noordhoff Publishing. Groningen. 1959.

Oleinik OA, Shamaev AS and Yosifian GA. *Mathematical Problems in Elasticity and Homogenization*. Studies in mathematics and its applications. North-Holland. Amsterdam. 1992.

Paumier JC. Existence and convergence of the expansion in the asymptotic theory of elastic thin plates. *Math. Modelling Numer. Anal.* 1990; **25 (3)**: 371–391.

Paumier J.-C and Raoult A. Asymptotic consistency of the polynomial approximation in the linearized plate theory. Application to the Reissner-Mindlin model. *Élasticité, viscoélasticité et contrôle optimal (Lyon, 1995)*. Vol2 of *ESAIM Proc.*. Soc. Math. Appl. Indust.. Paris. 1997. pp203–213 (electronic).

Pitkaranta J. The problem of membrane locking in finite element analysis of cylindrical shells. *Numer. Math.* 1992; **61**: 523–542.

Pitkäranta J, Matache A.-M and Schwab C. Fourier mode analysis of layers in shallow shell deformations. *Comput. Methods Appl. Mech. Engrg.* 2001; **190**: 2943–2975.

Encyclopedia of Computational Mechanics. Edited by Erwin Stein, René de Borst and Thomas J.R. Hughes.

Pitkäranta J and Sanchez-Palencia E. On the asymptotic behaviour of sensitive shells with small thickness.. *C. R. Acad. Sci. Paris, Sér. II* 1997; **325**: 127–134.

Rössle A, Bischoff M, Wendland W and Ramm E. On the mathematical foundation of the $(1, 1, 2)$-plate model. *Internat. J. Solids Structures* 1999; **36**(14): 2143–2168.

Sanchez-Hubert J and Sanchez-Palencia E. *Coques élastiques minces. Propriétés asymptotiques*. Recherches en mathématiques appliquées. Masson. Paris. 1997.

Schwab C. A-posteriori modeling error estimation for hierarchic plate models. *Numer. Math.* 1996; **74 (2)**: 221–259.

Schwab C and Suri M. The p and hp versions of the finite element method for problems with boundary layers. *Math. Comp.* 1996; **65**: 1403–1429.

Schwab C, Suri M and Xenophontos C. The hp finite element method for problems in mechanics with boundary layers. *Comp. Meth. Appl. Mech. Engrg.* 1998; **157**: 311–333.

Schwab C and Wright S. Boundary layer approximation in hierarchical beam and plate models. *Journal of Elasticity* 1995; **38**: 1–40.

Scott LR and Vogelius M. Conforming finite element methods for incompressible and nearly incompressible continua. *Large-scale computations in fluid mechanics, Part 2 (La Jolla, Calif., 1983)*. Vol22 of *Lectures in Appl. Math.*. Amer. Math. Soc.. Providence, RI. 1985. pp221–244.

Stein E and Ohnimus S. Coupled model- and solution-adaptivity in the finite-element method. *Comput. Methods Appl. Mech. Engrg.* 1997; **150**(1-4): 327–350. Symposium on Advances in Computational Mechanics, Vol. 2 (Austin, TX, 1997).

Stoker JJ. *Differential geometry*. Pure and Applied Mathematics, Vol. XX. Interscience Publishers John Wiley & Sons, New York-London-Sydney. 1969.

Suri M. The p and hp finite element method for problems on thin domains. *J. Comput. Appl. Math.* 2001; **128**(1-2): 235–260. Numerical analysis 2000, Vol. VII, Partial differential equations.

Suri M, Babuška I and Schwab C. Locking effects in the finite element approximation of plate models. *Math. Comp.* 1995; **64**: 461–482.

Szabó B and Babuška I. *Finite Element Analysis*. Willey. New-York. 1991.

Szabó B and Sahrmann G. Hierarchic plate and shell models based on p-extension. *Int. Jour. Numer. Meth. Engrg.* 1988; **26**: 1855–1881.

Vekua IN. On a method of computing prismatic shells. *Akad. Nauk Gruzin. SSR. Trudy Tbiliss. Mat. Inst. Razmadze* 1955; **21**: 191–259.

Vekua IN. Theory of thin shallow shells of variable thickness. *Akad. Nauk Gruzin. SSR Trudy Tbiliss. Mat. Inst. Razmadze* 1965; **30**: 3–103.

Vekua IN. *Shell theory: general methods of construction*. Monographs, Advanced Texts and Surveys in Pure and Applied Mathematics, 25. Pitman (Advanced Publishing Program). Boston, MA. 1985.

Vishik MI and Lyusternik LA. Regular degeneration and boundary layers for linear differential equations with small parameter. *Amer. Math. Soc. Transl. (2)* 1962; **20**: 239–364.

Vogelius M and Babuška I. On a dimensional reduction method. I. The optimal selection of basis functions. *Math. Comp.* 1981a; **37**(155): 31–46.

Vogelius M and Babuška I. On a dimensional reduction method. II. Some approximation-theoretic results. *Math. Comp.* 1981b; **37**(155): 47–68.

Vogelius M and Babuška I. On a dimensional reduction method. III. A posteriori error estimation and an adaptive approach. *Math. Comp.* 1981c; **37**(156): 361–384.